CHALMERS
UNIVERSITY OF TECHNOLOGY

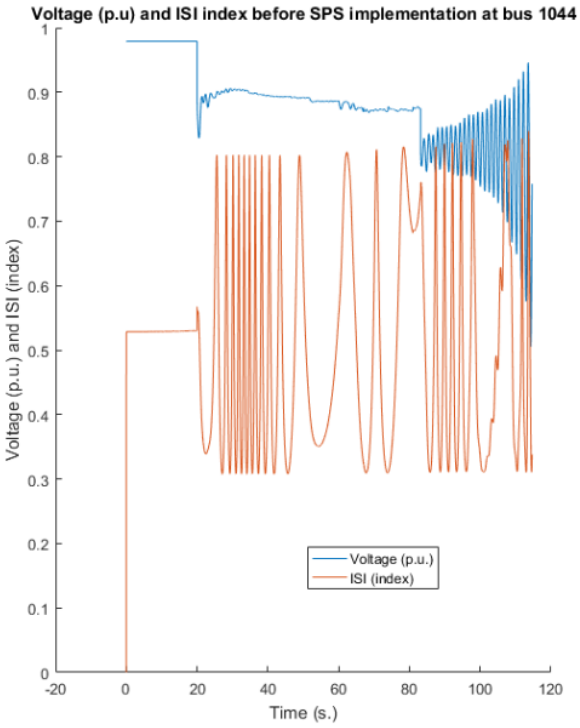

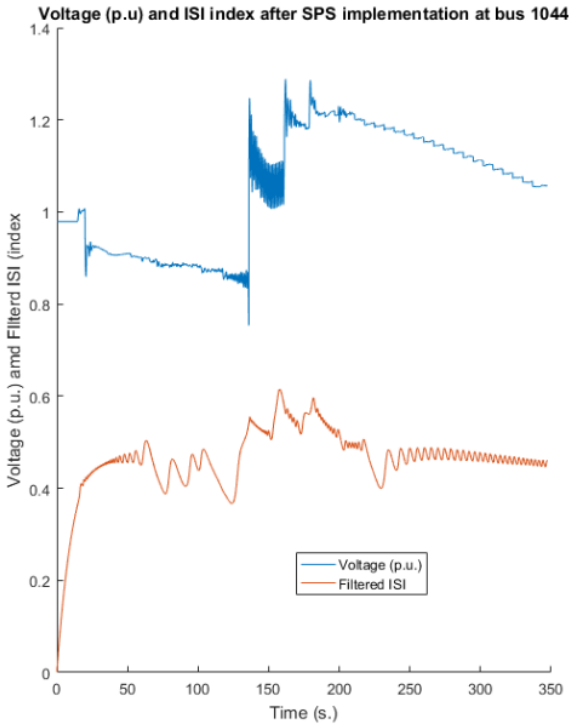

Control methods against voltage collapse based on real-time calculation of voltage stability indicators

Master's thesis in Electric Power Engineering

AHMAD SULTAN ESREB

Department of Electrical Engineering
CHALMERS UNIVERSITY OF TECHNOLOGY
Gothenburg, Sweden 2017

Master's thesis 2017

Control methods against voltage collapse based on real-time calculation of voltage stability indicators

AHMAD SULTAN ESREB

CHALMERS
UNIVERSITY OF TECHNOLOGY

Department of Electrical Engineering
Division of Electric Power Engineering
Chalmers University of Technology
Gothenburg, Sweden 2017

Control methods against voltage collapse based on real-time calculation of voltage stability indicators
AHMAD SULTAN ESREB

Supervisor and Examiner: TUAN A. LE, Department of Electrical Engineering

Master's Thesis 2017
Department of Electrical Engineering
Division of Electric Power Engineering
Chalmers University of Technology
SE-412 96 Gothenburg
Telephone +46 31 772 1000

Typeset in LaTeX
Printed by Chalmers Reproservice
Gothenburg, Sweden 2017

Control methods against voltage collapse based on real-time calculation of voltage stability indicators

AHMAD SULTAN ESREB
Division of Electric Power Engineering
Department of Electrical Engineering
Chalmers University of Technology

Abstract[1]

Power systems always face disturbances, which could lead to voltage collapse or blackout, and weaken with the increase of power demand or load, which is an everyday challenge to Transmission System Operators (TSOs). Nowadays, there aren't specific methods to prevent voltage instability or collapse if a disturbance occurs in a system. The thesis presents a method to prevent voltage collapse occurrence by investigating voltage instability using indicators such as Impedance Stability Index (ISI), Voltage Stability Index based on Short Circuit Capacity (VSCIscc or VCSS or VSCC) and Voltage Collapse Proximity Index (VCPI), i.e. an optimal coordinated control actions for various controllable devices in real-time when disturbance occurs in a system is proposed, and the motivations are as follows :

- obtain good information on the power system conditions,
- act as fast as possible to increase the chances to save the system,
- decrease operation and maintenance costs,
- shed less loads

The indicators were first evaluated in a 10-bus system from [1], in which both ISI and VSCIscc gave good indications of voltage instability and collapse, as opposed to VCPI, which proved to be inefficient. The ISI was selected for the next evaluation only due to the fact that the VSCIscc acted the same way and to limit computational burden. Afterwards, the ISI was tested in the Nordic32 power system with moderate loading [2], in which two different cases were tested to observe voltage collapse, consisting of applying a three-phase balanced fault in the first case, and tripping of a generator in the second one. High oscillations and transients were observed in the ISI indicator, which led to adding simple filter, assumed to be acceptable only for this thesis.

Using the ISI, the model, which is built using a software called Power System Simulator for Engineering (PSS/E) and tested on the Nordic32, consists of control methods of available synchronous generators automatic voltage regulators (AVRs) in the system, taking into account the signals from the Over-excitation limiters (OELs). Consequently, the model identifies the weakest buses, and then increases the AVR set-points of the generators closest to these buses if ISI is greater than 0.5, and then by activating load shedding on loads at or closest to the weakest buses if AVR set-points of all generators were increased or if ISI is greater than 0.6. The voltages, angles, ISIs and OELs are considered to be input signals. The model was successfully verified in both cases, where voltage collapse was prevented. In the first scenario, only the AVR set-points generators closest to the weakest buses were increased. In

the second case, with a more severe event compared to the first one, load-shedding was conducted on loads located at the buses of interest, along with the increase of AVR set-points, due to the fact that the ISI was greater than 0.6. Loads were shedded twice at buses 1044 and 1045 by 35% and a high voltage overshoot was observed at these buses.

Keywords: Monitoring, Voltage stability, Voltage collapse, Impedance Stability Index (ISI), Voltage Collapse Proximity Index (VCPI), Voltage Stability Index based on Short Circuit Capacity (VSCIscc or VSCC or VCSS), Network admittance matrix, PSS/E,Load-Shedding, Over-excitation Limiter (OEL), On-Load Tap Changer (OLTC), Automatic voltage regulator (AVR)

[1]Some of the results from this thesis have been summarized in the paper, which was submitted in the Power System Computation Conference (PSCC) 2018. The paper is found in Appendix D.

Acknowledgements

First, this thesis would not have come to light without the unconditional support of my family. I could not have done it without them.
I would like to thank the supervisor Tuan Anh Le for his patience, help and for all the feedback during the thesis phase, and Mattias Persson for his support in creating the model on PSS/E.
Also, a special thanks to Manh Hung Tran from the Department of Mathematical Sciences and Peiyuan Chen from the Department of Electrical Engineering for their support.
The M.Sc thesis was conducted at the division of Electrical Power Engineering, in the Department of Electrical Engineering at Chalmers University of Technology in Gothenburg, Sweden.

AHMAD SULTAN ESREB, Gothenburg, June 2017

Glossary

Sign	Description	Unit
E_t	Generator Terminal Voltage	[V] or [p.u.]
P	Active Power	[W] or [p.u.]
Q	Reactive Power	[Var] or [p.u.]
Q_c	Reactive Power Compensation	[Var] or [p.u.]
Q_L	Reactive load Power	[Var] or [p.u.]
S	Apparent Power	[VA] or [p.u.]
X_d	Generator Reactance	[Ω] or [p.u.]
X_{Sh}	Shunt Reactance	[Ω] or [p.u.]
Z_{Load}	Load Impedance	[Ω] or [p.u.]
Z_{thv}	Thevenin Impedance	[Ω] or [p.u.]
δ	Voltage Angle	[rad] or [deg]
E	Sending End Voltage	[V] or [p.u.]
I_{ij}	Current between buses i and j	[A] or [p.u.]
I	Current	[A] or [p.u.]
P_r	Active Power at receiving end	[W] or [p.u.]
P_{Load}	Active Load Power	[W] or [p.u.]
R	Resistance	[Ω] or [p.u.]
S_L	Apparent load Power	[VA] or [p.u.]

Sign	Description	Unit
S_j	Apparent Power at bus j	[VA] or [p.u.]
V_i	Voltage at bus i	[V] or [p.u.]
V_j	Voltage at bus j	[V] or [p.u.]
V	Voltage	[V] or [p.u.]
X_T	Transformer Impedance	[Ω] or [p.u.]
X or X_l	Line Impedance	[Ω] or [p.u.]
y_t	Series admittance transfomer	[S] or [p.u.]
Y_{ij}	Series admittance between buses i and j	[S] or [p.u.]
Y_{ii}	Self Admittance at bus i	[S] or [p.u.]
θ_{ij}	Admittance Angle of line between buses i and j	[rad] or [deg]
θ_{ii}	Self Admittance Angle at bus i	[rad] or [deg]

Abbreviations

AVR	Automatic Voltage Regulator
CT	Current Transformer/Transducer
FACTS	Flexible Alternating Current Transmission System
ISI	Impedance Stability Index
OEL	Over-Excitation Limiter
OLTC	On-Load Tap Changer
PMU	Phasor Measurement Unit
PSS/E	Power System Simulator for Engineering
SCADA	Supervisory Control And Data Acquisition
SPS	System Protection Scheme
STATCOM	Static Compensator
SVC	Static Var Compensator
TCSC	Thyristor-controlled series capacitor
TPSI	Transmission Path Stability Index
TSO	Transmission System Operator
VCPI	Voltage Collapse Proximity Index
VSCC or VSCIscc	Voltage Stability Index based on Short Circuit Capacity
VT	Voltage Transformer/Transducer

Contents

List of Figures

List of Tables

1

Introduction

This chapter presents the background, aim and motivations for the thesis. It also shows the structure of the chapters.

1.1 Background and Motivation

Power systems always face disturbances that could occur on the transmission and distribution lines, such as short circuit faults and disconnection of lines, compromising the stability of the systems, and can be divided into three main categories [4]:

- Frequency Stability
- Rotor angle or Transient Stability
- Voltage Stability

Different measures have been presented in the past to avoid any instability, but the main focus in this thesis is to preserve the voltage levels at all buses in system within acceptable boundaries, i.e. preserving voltage stability. The major cause of short or long duration voltage instability is the high voltage drop from the high losses occurring in transmission lines, and from the flow of active and reactive power to the loads, limiting the transmission network capability for voltage support. [1]. Nowadays, there aren't specific methods to prevent voltage instability or collapse if a disturbance occurs in a system, which makes the thesis interesting. Additionally, the integration of renewable energy sources, such as Photovoltaic Panels and Wind Energy, may weaken the grid even more, which pushes towards research of innovative protection scheme to prevent that voltage collapse occurs [5].

Therefore, an optimal coordinated control actions for various controllable devices in real-time when disturbance occurs in a system is proposed. The motivation behind real-time simulation is to:

- obtain good information on the power system conditions,

- act as fast as possible to increase the chances to save the system,
- decrease operation and maintenance costs,
- shed less loads

The main idea is that, when indicators are found to be close to a certain threshold using on-line or real-time simulations, i.e. indicating that the system is close to a voltage collapse, the system protection scheme (SPS) would be activated to send the control signals to various control devices in the system, such as synchronous generators reactive power re-dispatch, set-points of On-Load Tap Changer (OLTC) transformers, controls of HVDC (High Voltage Direct Current)/FACTS(Flexible AC Transmission System) and power-electronic converters of renewable generation, modification of distance-relay settings, under voltage load shedding, and others. The activation of Over-Excitation Limiters (OELs) of synchronous generators, voltage measurements from on-load tap changing (OLTC) transformers can also be used as input signals in SPS.

1.2 Previous Work

A Master's thesis work has been carried out in 2016 by two students from Chalmers University of Technology related to a development of a system protection model against voltage collapse [6]. The goal was to detect voltage instability based on an indicator called Transmission Path System Index (TPSI), and different actions are carried accordingly. Also, different issues arose from the usage of the Impedance Stability Index (ISI) indicator, which will be discussed in Chapter 2. This thesis can be seen as a continuation of their work, focusing extensively on improving the usage of the ISI.

1.3 Task

The main challenge is when, from where, and how many changes that should be made to the controllers of the devices that would be sufficient to save the system and drive the system back to the secure condition from collapse. However, the first challenge is how to identify a voltage collapse, and how to detect if a system is converging towards it. Fortunately, several works presented different aspects regarding the subject.The thesis work at Chalmers University of Technology [6] showed that Transmission Path Stability Index (TPSI) and Impedance Stability Index (ISI) are better voltage stability indicators compared to Fast Voltage Stability Index (FVSI) and S-difference Indicator (SDI). Additionally, TPSI was shown to be more accurate and faster to compute while used in the Nordic 32-bus system, since ISI required a large amount of computational power resulting in long calculation times. However, the latter has

been investigated further since it gives a clear indication based on maximum power transfer to the load. Also, the other main challenge is to analyze if and when an indicator clearly identifies pre-voltage collapse.

The following indicators have been analyzed and taken into account in this thesis:

- Voltage Collapse Index (VCPI) [7]
- Voltage Stability Index based on Short Circuit Capacity (VCIscc or VSCC or VCSS) [3]
- Impedance Stability Index (ISI) [8]

Furthermore, it is important to select the appropriate programs for simulations. In this thesis, PSS/E (Power System Simulator for Engineering) [9][10][11] will be used, with Python script (the interpreter) and Fortran compiler for modeling the coordinate control,i.e. an "algorithm" to coordinately control the devices to prevent voltage collapse can be developed. This will be used in the Nordic 32-Bus systems.

1.4 Aim and Limitations

The aim is to develop an acceptable SPS model for PSS/E to prevent voltage collapse and test on the Nordic 32-bus system. The model would be able to optimally coordinate control actions for various available controllable devices when disturbance occurs in a system. The study focuses on voltage stability only, without taking into account the frequency and transient stability. It will be assumed that voltages, currents and phases are measured in real-time as fast as possible, and the simulations will be considered accurate enough that the control method can be used in real life projects or power systems. Additionally, it will be assumed that the power systems, including generators, transformers, FACTS devices and loads, are accurately modeled on PSS/E, and study of transients and oscillations are out-of-scope.

1.5 Methods

The projects goal is to develop an optimized coordinated control method of different power devices (AVR set-points, on-load tap changing (OLTC) transformers) in order to be able to prevent voltage collapse as fast and as swift as possible based on different characteristics that can be found in a power system, such as Transmission path stability index (TPSI) or Impedance stability index (ISI). The thesis will be carried out with the following tasks:

- Task 1: Literature review of previous relevant work or projects.
- Task 2: Getting familiarized with Python,Fortran, and how to interface both with PSS/E.
- Task 3: Development of combined real-time dynamic simulations and optimization platform using PSS/E and Matlab [12] with data exchange facilitated by Python.
- Task 4: Development control algorithm(s) and user-defined model for PSS/E for voltage collapse protection
- Task 5: Evaluation of indicators and methods using a 10-bus system from [1] and Nordic 32-bus system
- Task 6: Documentation of model implementation and thesis writing

1.6 Thesis Outline

The thesis is divided into six main chapters, excluding the Introduction, as follows:

- Chapter 2 includes the theories used in the thesis, needed to understand the work behind it
- Chapter 3 presents the methodology or algorithm used to prevent voltage collapse in the Nordic32
- Chapter 4 contains the evaluation of the indicators for on the 10-bus system
- Chapter 5 contains the evaluation of the indicators for on the Nordic32 system
- Chapter 6 presents the control method or algorithm implemented in the Nordic32 to prevent voltage collapse
- Chapter 7 is the conclusion drawn from the results and suggestions for future work to improve the results

2

Theory

This chapter presents the theories and information that were used from the literature review for the realization of this thesis. The purpose is to familiarize the reader with basic theories to understand the thesis work.

2.1 Voltage Stability

2.1.1 Definition

With reference to the paper by IEEE/CIGRE Joint Task Force on Stability Terms and Definitions [4], voltage stability is defined as the ability for power systems to maintain steady-state voltage levels within proper limits after the occurrence of any disturbance. With the increase in power demand and the need of reliable and robust power systems, voltage stability is essential for study purpose and monitoring for avoiding blackouts. Therefore, it is needed to explain the power transfer characteristics in power systems in order to understand the voltage stability , and how it can be described.

2.1.2 Bus types

It is critical to differentiate bus types. According to [13], there are 3 main bus types:

- Load buses or PQ buses
- Generation buses or PV buses
- Slack bus

However, it is needed to bear in mind only two different types, categorized as voltage-controllable bus and non-voltage controllable bus [8]. The former category includes power generation and controllable reactive compensation devices, such as the Static-

Var Compensator (SVC), since they can control the bus voltage level. The latter category represents the load and transmission or intermediary buses, in which there are no voltage controllable buses.

2.1.3 PV and VQ Curves

Power transfer and voltage stability can be described from PV and VQ curves in Fig. 2.1 and Fig. 2.2, where P stands for active power, Q for reactive power and V for voltage. Ideal cases, such as no resistances and line charging, and constant power factor are assumed. These curves give a theoretical indication on how robust the transmission lines are and how far or close the power system is from voltage collapse or instability. However, the curves vary dynamically if there is a change in loads or in transmission line impedance, or in reactive power injection [1].

The PV curve is defined based on eq.(2.1), obtained from a two bus equivalent system, where E is the sending voltage, V is the receiving voltage,X is the line equivalent impedance, and δ is the voltage angle difference between E and V [1].

$$Pr = -\frac{EV}{X} sin(\delta) \tag{2.1}$$

Similarly, the QV curve is defined based on eq.(2.2):

$$Qr = \frac{VEcos(\delta) - V^2}{X} \tag{2.2}$$

Eq.(2.3) describes the PV and VQ curves characteristics for reactive power compensation based on eq.(2.1) and eq.(2.2)

$$V = \sqrt{\frac{E^2}{2} - QX \pm \sqrt{\frac{E^4}{4} - X^2P^2 - XE^2Q}} \tag{2.3}$$

The maximum active power transfer can be obtained from Fig.2.1, with its corresponding voltage, such that:

$$P_{max} = \frac{1}{X}\sqrt{\frac{E^2}{4} - XE^2Q} = \frac{E^2}{2X}\frac{cos\phi}{1 + sin\phi} \tag{2.4}$$

$$V_{P,max} = \sqrt{\frac{E^2}{2} - XQ} = \frac{E}{\sqrt{2}}\frac{1}{\sqrt{1 + sin\phi}} \tag{2.5}$$

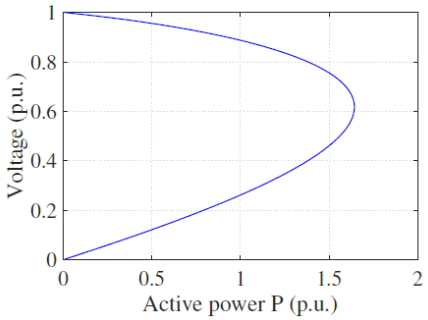

Figure 2.1: PV Curve

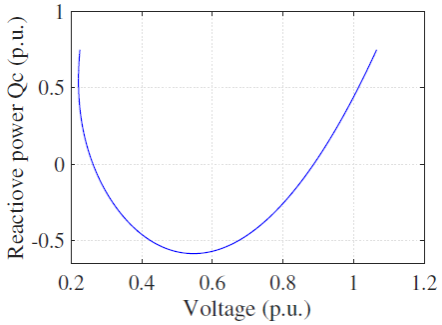

Figure 2.2: QV Curve

Similarly, the minimum reactive power transfer can be obtained from Fig. 2.1, with its corresponding voltage,

$$Q_{C,min} = Q_L - \frac{E^2}{4X} + \frac{XP^2}{E^2} \tag{2.6}$$

$$V_{Qc,min} = \sqrt{\frac{E^2}{4} + \frac{X^2P^2}{E^2}} \tag{2.7}$$

From Fig. 2.1 and 2.2, voltage instability occurs when active power starts to decrease after reaching the maximum active power and when reactive power is positive.

2.1.4 Voltage Instability and Voltage Collapse

With reference to CIGRE and IEEE definition [4], voltage collapse can be defined as a sequence of events caused by voltage instability leading to an unacceptable voltage profile in a power system. Also, voltage instability can be due to the load dynamics to restore power consumption, with transmission and generation systems at their limits. In this section, the different causes of voltage instability will be discussed briefly.

2.1.4.1 Load Increase

Instability is mainly due to an increase in load relative to the capacity of transmission and generation system,which increases the voltage drop across the branches. An increase in load will lead to a decrease in power transfer to the load if we refer to Fig. 2.1. Additionally, it could cause a power unbalance for a short period time if load power is bigger than generated power, which could lead to a decrease in frequency [1]. However, frequency instability, primary and secondary frequency control will not be discussed in this thesis. Also, it is essential to distinguish between different kinds of loads as follows:

$$P = zP_o(\frac{V}{V_o})^{\alpha} \tag{2.8}$$

$$Q = zQ_o(\frac{V}{V_o})^{\beta} \tag{2.9}$$

where z is the dimensionless demand variable, V_o is the reference voltage, α and β are the exponential characteristic of the loads such that:

- if α and $\beta = 1$, load is known as constant current load
- if α and $\beta = 2$, load is a constant admittance load
- if α and $\beta = 0$, load is know as constant power load

The critical characteristic of loads is the dependence on voltage. In case of an increase in constant admittance loads, voltage instability would hardly occur, but low steady voltages would be experienced in severe cases [1]. In this thesis, the emphasis will be on the first two load types since constant power loads are too severe due to their independence on voltages and their increase will lead to a high probability voltage collapse as explained in [1]. Finally, the total equivalent load seen from a load or non-voltage controllable bus is computed in p.u. as follows:

At any bus k,

$$I_k = \sum_{j=1}^{N} Y_{kj} V_j \tag{2.10}$$

then, the total equivalent load is:

$$S_k = V_k I_k^* = V_k [\sum_{j=1}^{N} Y_{kj} V_j]^* \tag{2.11}$$

2.1.4.2 Line and Generator Tripping

A disturbance such as the tripping of a line will lead to a change in the transmission characteristic. However, this can be reflected also as an increase in load as well with respect to the line capacity. It is clear how the load characteristic plays a vital role in voltage instability as shown in eq. 2.8 and 2.9. For a constant power load, the voltage collapse is inevitable. Load-shedding in that case is practically a must. On the other hand, if the load is voltage dependent at some extent,, the voltage instability ban be considered to be less severe and can be avoided with the injection of reactive power to increase the voltage level instead of load shedding. Additionally, a generator tripping will lead to a power unbalance in the system, which can also be seen as a relative increase in load.[1]

2.1.4.3 OLTC

OLTCs are used to maintain a voltage level within an acceptable range depending on the system by regulation the reactive power flow. They are mainly used in distribution systems close to the loads or consumers and have an important role in voltage stability during tap changing operations by changing the series admittance y_t [13]. OLTC transformers can be represented by a π model as shown in Fig. 2.3. The operation of the tap changer is based on varying the value of the tap ratio, consequently the voltage ratio or difference between the primary and secondary sides of the transformer. However, during voltage instability, they act as voltage collapse 'catalysts'.

In fact, during voltage instability and when the voltage level on the non-tapped primary side is below an acceptable value (usually 0.9 p.u), the OLTC varies the series admittance to keep the voltage on the secondary side within a pre-determined range. If it is assumed that the load is not increasing, the power flow across the transformer will stay the same, but since the voltage on the primary side decreases, the current on the same side will increase for a constant power, which therefore increases the losses in the branches, consequently increasing the voltage drop, leading to a voltage collapse if no action is taken.

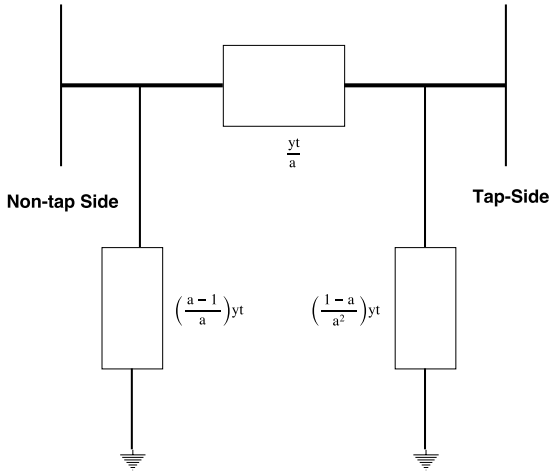

Figure 2.3: π-model of an OLTC transformer with series admittance y_t and tap ratio a

Assuming that the transformers are lossless, the power transfer across them can be written as follows:

$$P = \frac{V_i V_j sin\delta}{a} y_t \tag{2.12}$$

2.1.4.4 OEL

Generators, with an equivalent circuit as in Fig. 2.4 possess AVRs (Automatic Voltage Regulators) to increase the voltage across the terminal by increasing the reactive power production by increasing the field current winding.

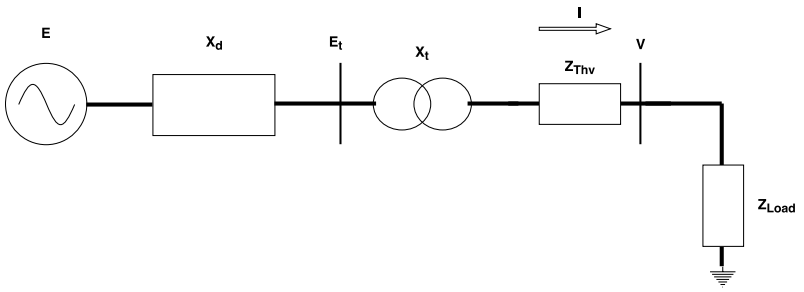

Figure 2.4: Equivalent circuit of a typical generator

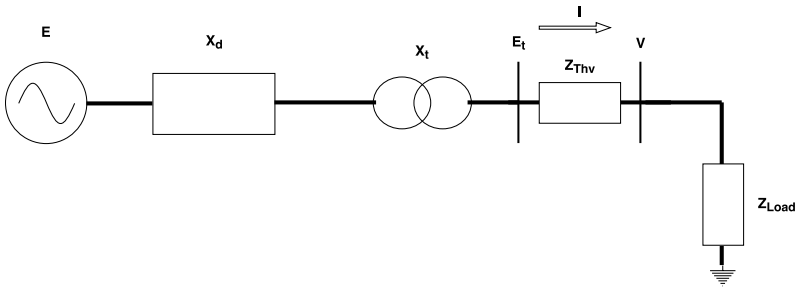

Figure 2.5: Equivalent circuit of a generator when the OEL is activated. The generator impedance X_d is added in series with the transformer impedance X_T and Z_Thv

However, the field winding can overheat if the machine produces reactive power above the limit it is designed for. In order to avoid this, the OEL of the generator activates, which disables the field current control, .i.e preventing reactive power production. This means that the generator isn't able to control the terminal voltage E_t anymore and a constant voltage is then found at E as seen in Fig. 2.5. The total impedance of the generator seen from the receiving end bus will be different, meaning X_d will thus be added to X_t and Z_Thv. This will lead to a weakening of a network and the maximum power transfer is reached, tending the bus voltage to decrease. The signal from the OEL is essential in determining or updating the voltage stability limit or margin, and critical in obtaining the correct thevenin impedance at different buses from the network admittance matrix, which will be discussed i the following section. Basically, the generator bus is a voltage-controllable before activation of the OEL, and non-voltage controllable after the activation.

2.2 Voltage Instability and Collapse Indicators

Lots of studies were made regarding the study and implementation voltage collapse indicators [14][15]. For example, a master 's thesis at NTNU [16] compared different voltage collapse indicators , showing their advantages and disadvantages. More recently, in the master's thesis at Chalmers University and Technology [6], two different indicators were tested in simulations : $TPSI$ (Transmission Path Stability Index) and ISI (Impedance Stability Index). However, the ISI wasn't used in big systems due to the high computational burden of the thevenin impedances caused by the inversion of large matrices. In this thesis, the ISI will be analyzed, with the explanation on how thevenin impedances can be computed more efficiently. Also, two additional indicators were investigated, which are the $VSCIscc$ and $VCPI$.

2.2.1 Indicators

In this subsection, the different indicators investigated for this thesis will be presented. The first one is the ISI, which was presented before [6], but not implemented due to the complexity of obtaining the thevenin impedance at that time.

2.2.1.1 Impedance Stability Index (ISI)

This indicator is based on the maximum power transfer in a circuit. Fig. 2.6 shows the thevenin equivalent circuit.

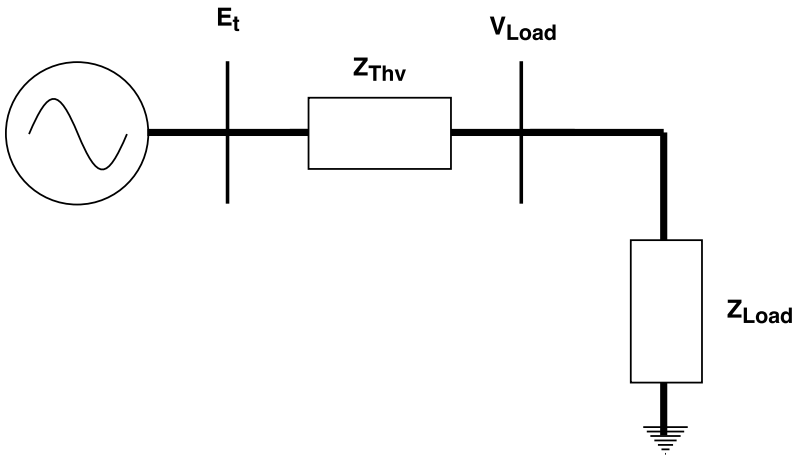

Figure 2.6: Thevenin equivalent circuit

From Fig. 2.6, using voltage divider rule and ohm's law:

$$V = E_t \frac{Z_{Load}}{Z_{Load} + Z_{Thv}} \tag{2.13}$$

$$I = \frac{E_t}{Z_{Load} + Z_{Thv}} \tag{2.14}$$

From eq.(2.13) and eq.(2.14), the power dissipated by the load is determined as follows:

$$P_{Load} = VI\cos\delta = E_t^2 \frac{Z_{Load}}{(Z_{Load} + Z_{Thv})^2}\cos\delta \tag{2.15}$$

The maximum power transfer occurs when $\frac{dP_{Load}}{Z_{Thv}} = 0$. The solution will be Z_{Load} $=Z_{Thv}$ [17], which implies that voltage instability critical point is reached when ISI=1

$$ISI = \frac{|Z_{Thv}|}{|Z_{Load}|} = 1 \tag{2.16}$$

If ISI $\leqslant 1$, the voltage is considered stable, and critically stable or unstable otherwise.

2.2.1.2 VCPI

The Voltage Collapse Proximity Index is a fast indicator that signals also how far is the system from collapse. It uses the admittance matrix elements, the voltage magnitudes and angles.

With reference to [13], for an n-bus system, the injected current into the kth bus can be written as follows:

$$I_k = V_k \sum_{\substack{m=1 \\ m\neq k}}^{n} Y_{km} - \sum_{\substack{m=1 \\ m\neq k}}^{n} V_m Y_{km} \tag{2.17}$$

where:

- Y_{km} is the mutual admittance between the kth bus and the mth bus
- Y_{kk} represents the self admittance of bus k
- V_k represents the voltage at the kth bus

- V_m represents the voltage at the mth bus
- m is a real number

The complex power injected at the kth bus is determined as follows:

$$S_k = V_k I_k^* \tag{2.18}$$

By substituting eq.(2.17) in eq.(2.18), it follows that:

$$S_k^* = |V_k|^2 \sum_{\substack{m=1 \\ m\neq k}}^{n} Y_{km} - V_k^* \sum_{\substack{m=1 \\ m\neq k}}^{n} V_m Y_{km} \tag{2.19}$$

Letting Y_{km}=$\sum_{\substack{m=1 \\ m\neq k}}^{n} Y_{km}$:

$$S_k^* = |V_k|^2 Y_{kk} - V_k^* \sum_{\substack{m=1 \\ m\neq k}}^{n} V_m^{'} Y_{kk} \tag{2.20}$$

where

$$V_m^{'} = \frac{Y_{km}}{\sum_{\substack{j=1 \\ j\neq k}}^{n} Y_{kj}} V_m = |V_m^{'}|\delta_m^{'} \tag{2.21}$$

where δ_m is the voltage angle at mth bus

Consequently from eq.(2.20):

$$\frac{S_k^*}{Y_{kk}} = |V_k|^2 - V_k^* \sum_{\substack{m=1 \\ m\neq k}}^{n} V_m^{'} \tag{2.22}$$

From eq.(2.22), the right hand side can be re-written as a complex number in the form of a+jb where:

$$a = |V_k|^2 - \sum_{\substack{m=1 \\ m\neq k}}^{n} |V_m^{'}||V_k| \cos(\delta_k - \delta_m^{'}) \tag{2.23}$$

$$b = \sum_{\substack{m=1 \\ m\neq k}}^{n} |V_m^{'}||V_k| \sin(\delta_k - \delta_m^{'}) \tag{2.24}$$

Letting $\delta_k - \delta_m^{'} = \delta$, eq.(2.23) and eq.(2.24) can be represented as two equations with two unknowns V_k and δ,which can be solved using partial derivatives and build a Jocabian matrix. Therefore, if $f_1(|V_k|, \delta)$=a and $f_2(|V_k|, \delta)$=b, the partial derivatives of these equations with respect to V_k and δ can be evaluated and the matrix can be provided such that:

$$J = \begin{bmatrix} 2|V_k| - \sum_{\substack{m=1 \\ m\neq k}}^{n} |V_m^{'}| \cos\delta & |V_k| \sum_{\substack{m=1 \\ m\neq k}}^{n} \sin\delta \\ \sum_{\substack{m=1 \\ m\neq k}}^{n} |V_m^{'}| \sin\delta & |V_k| \sum_{\substack{m=1 \\ m\neq k}}^{n} |V_m^{'}| \cos\delta \end{bmatrix} \tag{2.25}$$

Solving the matrix in eq.(2.25) such that it is equal to zero, since the collapse at the kth bus occurs when there is no solution to eq.(2.25), i.e. the matrix is singular at voltage collapse.

Solving, the solution will be:

$$|1 - \frac{\sum_{\substack{m=1 \\ m\neq k}}^{n} V_m^{'}}{V_k}| = 1 \tag{2.26}$$

If eq.(2.26), known as VCPI, equals or is greater than 1, the voltage collapse occurs. The voltage is stable at kth bus when VCPI $\leqslant 1$.

2.2.1.3 VSIscc

The voltage stability index based on short circuit capacity,VSIscc, shows the relationship between the voltage stability and the short circuit capacity. With reference to [3] and from Fig. 2.7, the index at node i can be defined as follows:

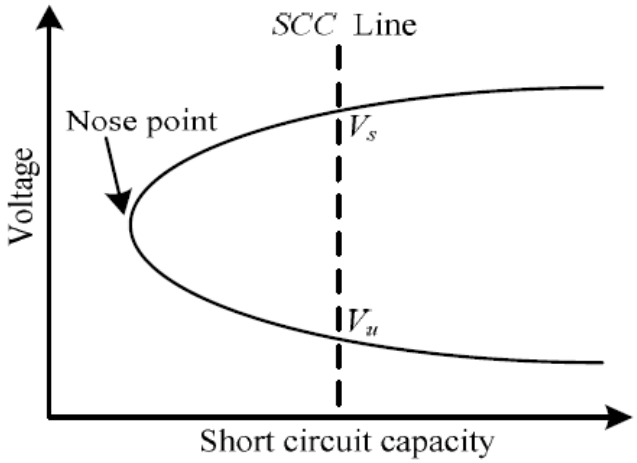

Figure 2.7: Typical SCC-V Curve [3]

$$VSIscc = \frac{SCC_{p_i}}{SCC_{min_i}} \tag{2.27}$$

where SCC_{p_i} is the short circuit capacity at node i supplied by the system. Assuming that R(resistance) «< X(impedance), then SCC_{p_i} can be written as:

$$SCC_{p_i} = \frac{E_{thv}}{X_{Thv}} \tag{2.28}$$

and SCC_{min_i} is the minimum short circuit capacity to provide voltage stability at node i, corresponding to the nose point of the SCC-V curve on Fig.(REFERENCE), and can be computed as follows:

$$SCC_{min_i} = \frac{2S_L(1+\sin\phi)}{E_{Thv}} \tag{2.29}$$

Using eq.(2.27),(2.28) and (2.29),the indicator can be determined as follows:

$$VCIscc = \frac{2S_L(1+\sin\phi)X}{E_{Thv}^2} \tag{2.30}$$

2.3 Prevention

2.3.1 Reactive Power Support

Reactive power support, can be associated with shunt or series fixed capacitor banks to increase the voltage level at a bus or improve the maximum power transfer in order to increase the margin of the voltage instability. The amount of injected reactive power is square-proportional to the bus voltage if it is a shunt capacitor bank, or square-proportional to the current if it is a series capacitor bank. It is obvious from eq.2.31 that the available shunt compensation becomes less when the voltage is lower and vice-versa, where V is the bus voltage, X_{shunt} is the shunt reactance, X_{series} is the series reactance and I is the current flow.

$$Q_C = \frac{V^2}{X_{shunt}} \tag{2.31}$$

$$Q_C = I^2 X_{series} \tag{2.32}$$

2.3.2 AVR Set-Point

Operating Synchronous machines AVRs can be seen as the main action of a voltage control to avoid voltage instability or collapse. They can prevent voltage instability by increasing reactive power production from generators. Additionally, it helps delaying the activation of the OEL, and has the advantage of buying more time that can be used to take further preventive measures, like activating reactive compensating devices or FACTS devices [1]. The idea behind using the AVR is to regulate the voltage set-point in a power system and increase the reactive power generation. The reactive power production is re-dispatched to other units in the system when one or more AVRs looses their controlling capability. When increasing set-points, great caution needs to be taken due to that an excessive increase can result in a too high field current, resulting in the activation of the OEL and loss of voltage control at the terminal as in Fig. 2.5. Increases should preferably be performed in small steps at several generator instead of larger steps on fewer generators [1].

2.3.3 OLTC Blocking

As already mentioned in 2.1.4.3, OLTC transformers act like voltage collapse catalysts. One solution is to delay or block the operation of the tap-changer, or even reverse the operation of the tap changer in the evnt of voltage instability. However, it is essential to mention blocking the operation OLTC must be done for a short

period of time until the system becomes voltage stable again by operating other devices, such as the AVRs setpoint of synchronous generators [18].

2.3.4 FACTS

Flexible alternating current transmission systems (FACTS) devices in the power system have become more abundant in coordination with the development of power electronics devices [19]. They help controlling the reactive power generation, flow and consumption in a power system in a way which wasn't possible before [19]. Being able to control the reactive power balance allows the TSOs to control voltage stability, prevent and anticipate voltage collapse. The use of FACTS devices is advantageous for mainly two reasons:

- operate the power system in accordance with its power flow control capability;
- improve the systems steady-state and transient stability.

2.3.5 Load Shedding

Shedding loads is essential to prevent severe voltage instability and collapse, specifically when it is critical, since it decreases the stress on the system through decrease in both the generated and consumed active and reactive power. The goal is to find a balance between generated power and power consumed or lost. In fact, load shedding is considered as a final resort to avoid a power system collapse. The main challenge is to identify which loads to be shed, when and how much. Additionally, it is imperative to propose a method to obtain the smallest load shedding level that has the most impact on the system health, but still enough to save it from further instability. In this thesis, the concept that will be used will be similar to [6].

2.4 Simulation Models

In PSS/E , built-in models [11] are used to simulate voltage instability or collapse, and have an important role in modeling realistic events. Models for field current excitation, governors and OLTCs were originally added to the Nordic32 test system and 10-bus system, but models for OEL, under voltage tripping of generators as well as distance relays had to be added in the Nordic32. The following models in Table 2.1 are used in the simulations and are found in Appendix A and B.

Models	Descriptions
SEXS	SEXS is a field excitation current model, regulating the field current of generators in PSS/E, i.e. it acts as an AVR. The voltage reference for the model can be changed by increasing and decreasing the AVR set points and therefore be used to prevent voltage instability
MAXEX2	The OEL model of a generator field current. It provides a three point characteristic current limit with corresponding time delays and uses the rated field current as base reference for the three current limits. It has a shorter activation timer for higher field current and vice verse for lower field current. When the OEL is activated, it reduces the field current to 1.05 pu of rated field current. Adding an OEL model is critical since it can have a significant effect on voltage stability due to the decrease in reactive power production. When the MAXEX2 limiter model is applied, it reduces the field current below the lowest field current limit. A signal of whether the OEL is activated or not is also important for determining the systems margin to instability. The decrease in voltage caused by an OEL can result in activation of timers for under-voltage tripping of generators.
VTGTPAT	The VTGTPAT model uses an over and under voltage threshold with a breaker timer and a breaker time delay,tripping a generator for a certain period of time after a generator voltage is below its threshold. VTGTPAT is a miscellaneous model which is applied to generators in the system. Under-voltage tripping is a contributor to a voltage collapse due to that a systems becomes greatly weakened when a generator is tripped due to under voltage.
OLTC1T	The OLTC1T is a two-winding transformer on load tap changer model which was originally added to several loads in the Nordic32 test system. The model is a branch model which is applied to branches which are equipped with transformers in PSS/E. The model uses a time delay for each tap changing operation between the detection of under/over voltage and tap change as well as a time constant for the tap changer.
STAB2A	STAB2A Stabilizer model applied to generators in Nordic32, uses machine electric power as input. Output is used for SEXS field current model.
DISTR1	The DISTR1 model was used for 3 zone protection for branches in the Nordic32 test system. This was mainly for applying three phase faults to branches.
LDFRAL	LDFRAL is a load frequency model which was originally applied to all loads in the Nordic32 test system which causes the frequency to affect the constant current and constant power parts of the loads.
HYGOV	A hydropower plant governor model applied to the Nordic32 test system.
GENROU	The GENROU is a round or cylindrical rotor generator model, used in the 10-bus system and Nordic32
GENCLS	A simple generator model used in the 10-bus system, representing an infinite bus. This model contains only the iertia and damping constant, which are set to 0 in combination with a small generator reactance.
GENSAL	It is a generator model representing a salient pole generator and is used in Nordic32 system

Table 2.1: Table of the different models used for simulating voltage instability and collapse in the 10-bus system and Nordic32

3

Methodology

In this chapter, the methodology and algorithm used in computing the thevenin impedances and the control method on preventing voltage instability and collapse are presented.

3.1 Thevenin Impedance from Network Admittance Matrix

The method presented in this thesis to obtain the thevenin impedance is by inverting the admittance matrix. For any n-bus system, the network admittance matrix can be represented by an $n \times n$ matrix as follows:

$$\mathrm{Y} = \begin{bmatrix} y_{11} & y_{12} & y_{13} & \cdots & y_{1n} \\ y_{21} & y_{22} & y_{23} & \cdots & y_{2n} \\ \cdots & \cdots & \cdots & \cdots & \cdots \\ y_{n1} & y_{n2} & y_{n3} & \cdots & y_{nn} \end{bmatrix}$$

The thevenin impedances for all buses are the diagonal elements of the matrix $\mathrm{Z} = \mathrm{Y}^{-1}$. it is important to note that the network admittance matrix must be updated based on different changes that occur in a power system, such as adding the impedance of the generator X_d in case an OEL is activated, or the turn ratio of an OLTC transformer changes.

The matrix can be inverted by computing the determinants [20]. If Y is a 2×2 matrix such that

$$\mathrm{Y} = \begin{bmatrix} y_{11} & y_{12} \\ y_{21} & y_{22} \end{bmatrix}$$

$$\text{Then } \mathrm{Z} = \mathrm{Y}^{-1} = \frac{1}{\det(\mathrm{A})} \begin{bmatrix} y_{22} & -y_{12} \\ -y_{21} & y_{11} \end{bmatrix}$$

where A = y_{11} y_{22} - y_{21} y_{12} However, this method becomes too exhaustive as the size of matrix increases. There is a better and much faster way, based on simple

'solving' algorithm and factorization, also called 'LU' decomposition.[21] The motivation behind the factorization is due to the sparsity of the admittance matrix in any power systems , i.e. the matrix will contain many zero elements. Furthermore, for any n-bus system, the matrix will always be a square one with non-zero diagonal elements.

3.1.1 LU Decomposition

The first step in obtaining the inverse of the admittance matrix is to decompose into a lower and upper triangular matrix, such that:

[Y]=[L][U], where L is the lower triangular matrix and U is the upper triangular matrix, where:

$$\text{L}= \begin{bmatrix} 1 & 0 & 0 & \dots & 0 \\ l_{21} & 1 & 0 & \dots & 0 \\ l_{31} & l_{32} & 1 & \dots & 0 \\ \dots & \dots & \dots & \dots & \dots \\ l_{n1} & l_{n2} & l_{n3} & \dots & 1 \end{bmatrix}$$

$$\text{U}= \begin{bmatrix} u_{11} & u_{12} & u_{13} & \dots & u_{1n} \\ 0 & u_{22} & u_{23} & \dots & u_{2n} \\ 0 & 0 & u_{33} & \dots & u_{2n} \\ \dots & \dots & \dots & \dots & \dots \\ 0 & 0 & 0 & \dots & u_{nn} \end{bmatrix}$$

It is important to notice that the diagonal elements of [L] are equal to 1 and the LU decomposition is feasible only for square invertible matrices with non-zero diagonal elements. Fortunately, in any real-life n-bus system, the admittance matrix will always be square, invertible or non-singular, with non-zero diagonal elements.

Since [L][U]=[Y], and using matrix multiplication, it is clear that the first row elements of [U] can be determined straight forwardly, such that: u_{11}=y_{11}, u_{12}=y_{12},..., u_{1n}=y_{1n} because only the first element in the first row of matrix [L] is non-zero and equals to 1. Furthermore, the elements of [L] and [U] can easily be determined using the same concept by iteration and by solving. For example, $l_{21} \times u_{11} = y_{21}$, but $u_{11} = y_{11}$, then $l_{21} = \frac{y_{21}}{y_{11}}$. It is good to notice that the equation has only one unknown in it, and other quantities that were already found in the previous equations. This pattern continues until the last row. Similar factorization techniques exist, but the LU decomposition is acceptable for the thesis.

3.1.2 Solve

After obtaining L and U, the next step is to solve the a set of equations [Y][X]=[C], where [X] is the a matrix of unknowns to be determined.

Since [Y] = [L][U], then: [L][U][X]=[C].

Multiplying both sides by $[L]^{-1}$, we get: $[L]^{-1}[L][U][X]=[L]^{-1}[C]$ Since $[L]^{-1}[L]$ = [I], where [I] is the identity matrix or

$$I=\begin{bmatrix} 1 & 0 & 0 & \dots & 0 \\ 0 & 1 & 0 & \dots & 0 \\ 0 & 0 & 1 & \dots & 0 \\ \dots & \dots & \dots & \dots & \dots \\ 0 & 0 & 0 & \dots & 1 \end{bmatrix}$$

then $[I][U][X]=[L]^{-1}[C]$ and $[U][X]=[L]^{-1}[C]$. Let $=[L]^{-1}[C]=[T]$,we get:

$$[L][T] = [C] \tag{3.1}$$

and

$$[U][X] = [T]. \tag{3.2}$$

Therefore, we can solve first eq.(3.1) or [T], and then use eq.(3.2) to calculate [X].

3.2 Control Method

Initially, the network admittance matrix is assumed to be known and updated by monitoring the power system. The voltage magnitudes and angles are measured at all buses, the OELs are being monitored, the OLTC tap-changer positions are observed by measuring the active power flow through the transformers, as already shown in eq.2.12. The control method of different devices to prevent voltage collapse can be initiated after determining the indicator at non-voltage controllable buses. With ISI taken into account, if it reaches a certain value signaling voltage instability at any non-controllable voltage bus, the AVR-setpoints are increased. However, if ISI is greater than a value signaling voltage instability close to collapse,and AVR-setpoints are not enough to counter it, load-shedding is then activated at or close to buses of interest. The applied algorithm is summarized in Fig. 3.1 in a simplified way, which indicates that the prevention of voltage collapse is initiated when ISI is greater than 0.5. This value is not random, but is taken into account after analyzing the ISI in the Nordic32 before implementing the model. The reasons are explained in chapter 5.

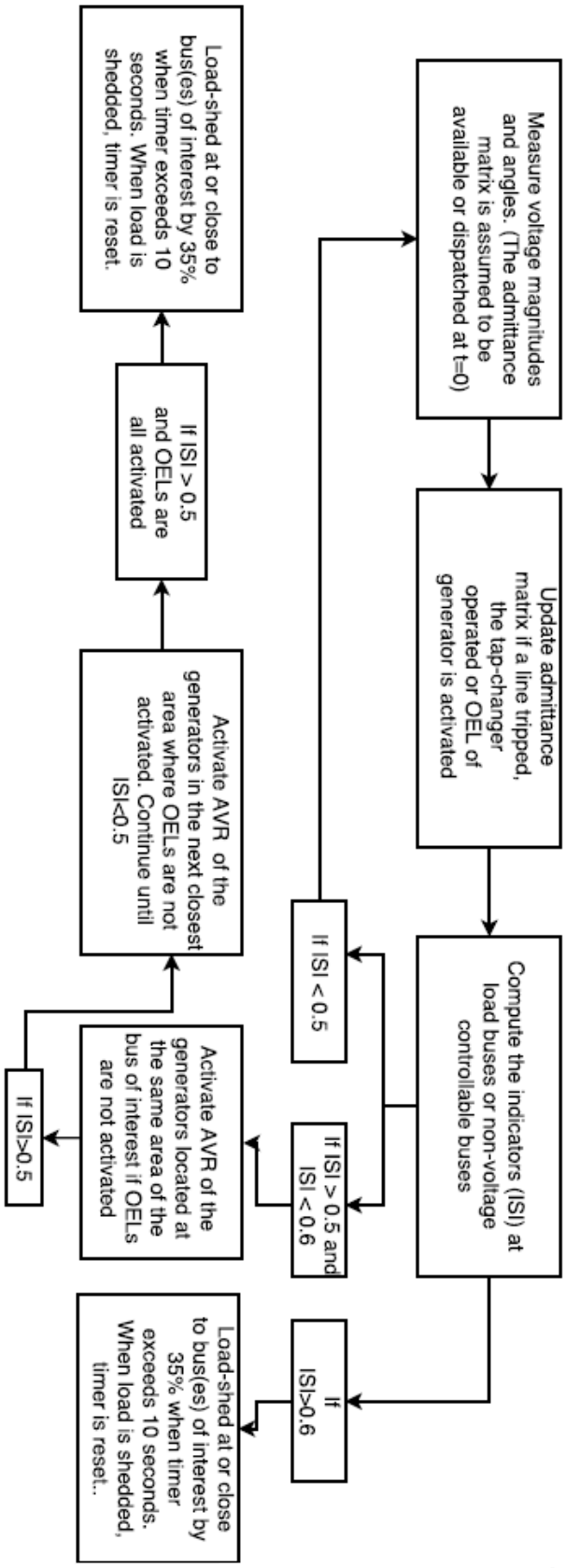

Figure 3.1: Methodology used in preventing voltage collapse

4

Evaluation of indicators in a 10-bus system

This chapter includes the evaluation of the different indicators that were investigated in this thesis in a simple 10-bus system taken from [1], which is also presented as an exercise in PSS/E for voltage instability study, by simulating two different cases with different loads.

4.1 Simulation set-up

The single line diagram of the system can be seen in Fig. 4.1, and the models can be found in Appendix A.

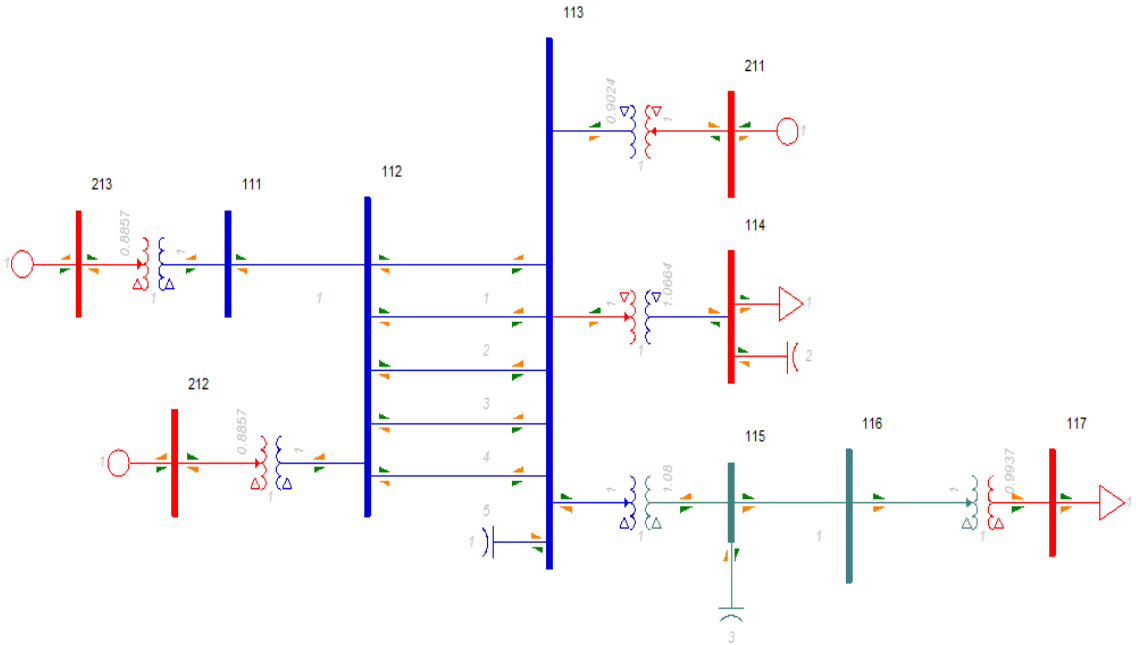

Figure 4.1: 10-Bus system single line diagram

In this chapter, four different cases are presented:

- in the first case, one line will be tripped between bus 112 and 113, and load will increase by 3% every 20 seconds, keeping the load conversions as they are (i.e. 50% constant admittance load and 50% constant current load). in the second case, one line will be tripped,but the OEL and OLTC will be omitted
- In the third and fourth cases, case one and two will be repeated, but with two lines tripped instead of one between bus 112 and bus 113.

4.2 Tripping of one line

4.2.1 OLTC and OEL activated

The dynamic simulations are done using PSS/E, automated by Python scripts. By tripping a line between buses 112 and 113, and increasing the loads in both buses 114 and 117 by 3% every 20 seconds by keeping the same load conversion ratio and power factor, the voltage collapse occurs at 460 sec.

Fig. 4.2 and 4.3 show how the VCIscc increases during load increase. It is important to notice how the indicator suddenly increases when a line is tripped. Also, it looks like bus 114 is weaker than bus 117 due to the a higher value in the indication. The intersection between VCIscc and the bus voltage in Fig. 4.2 is irrelevant when it comes to voltage instability.

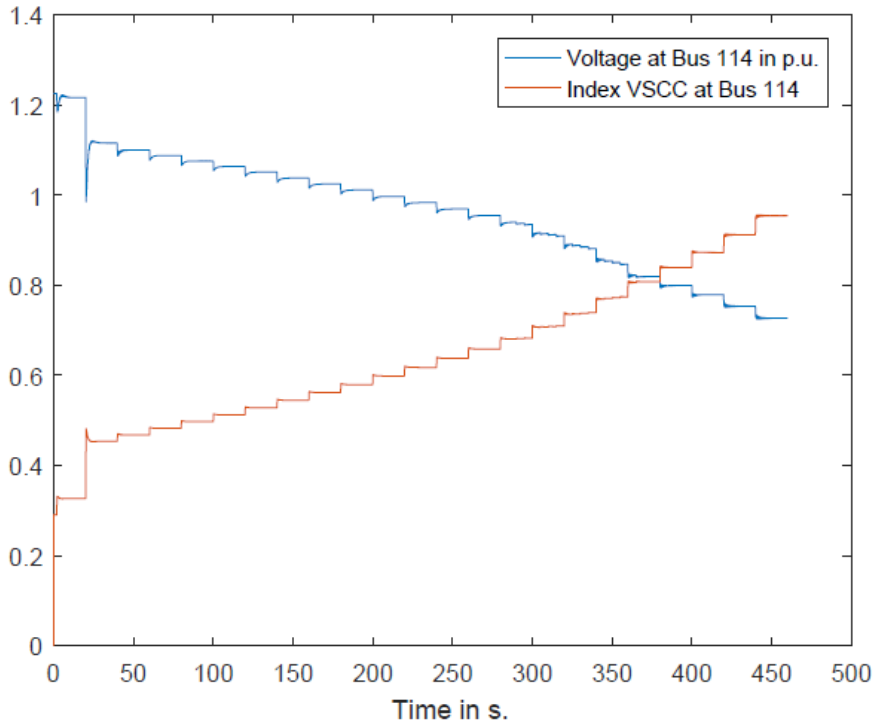

Figure 4.2: VCIscc or VCSS and Voltage (p.u.) plots with respect to Time (s.) at bus 114 with one tripped line, OLTC and OEL activated

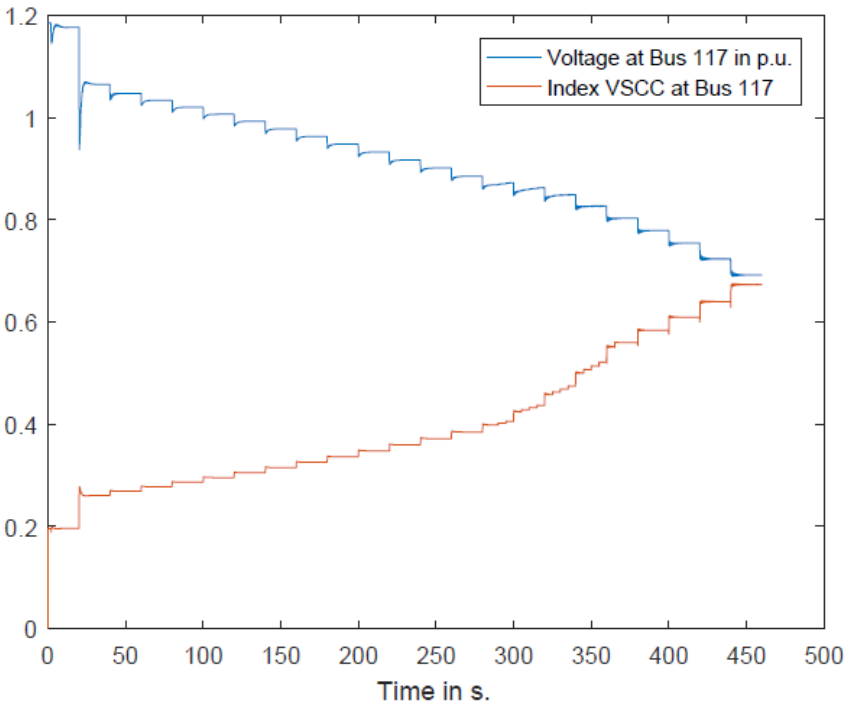

Figure 4.3: VCIscc or VCSS and Voltage (p.u.) plots with respect to Time (s.) at bus 117 with one tripped line, OLTC and OEL activated

In Fig. 4.4 and 4.5, the ISIs of buses 114 and 117 are plotted. It is observable that they are increasing, and bus 114 is again shown to be weaker than bus 117. Also, the sudden increase in the indicator is evident at 20s. However, the highest value that the indicator reached is around 0.58 at collapse, as opposed to the previous one, which reaches 1.

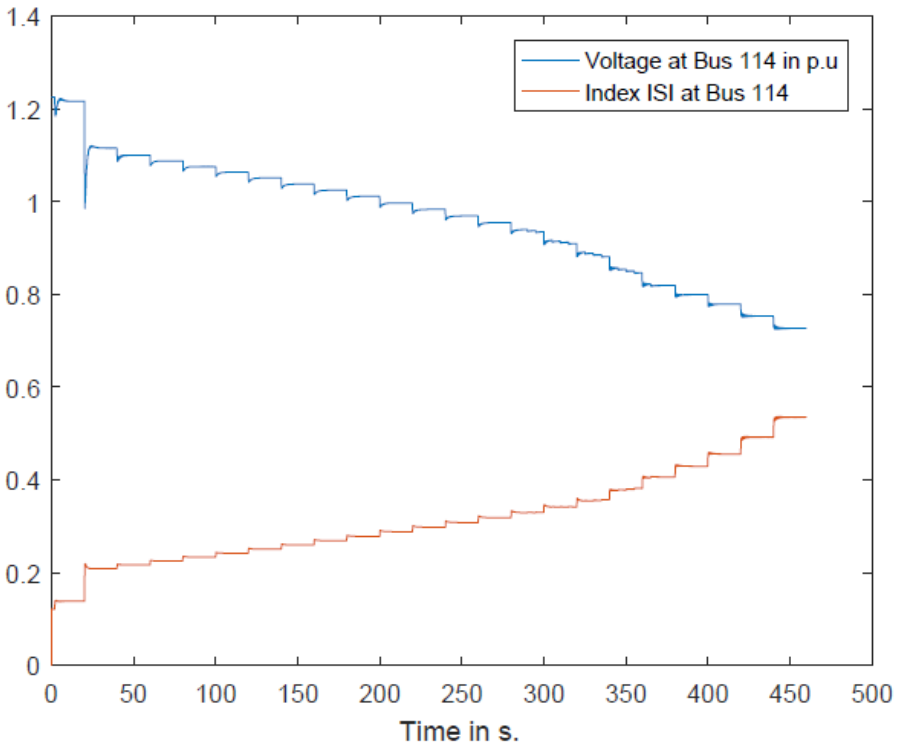

Figure 4.4: ISI and Voltage (p.u.) plots with respect to Time (s.) at bus 114 with one tripped line, OLTC and OEL activated

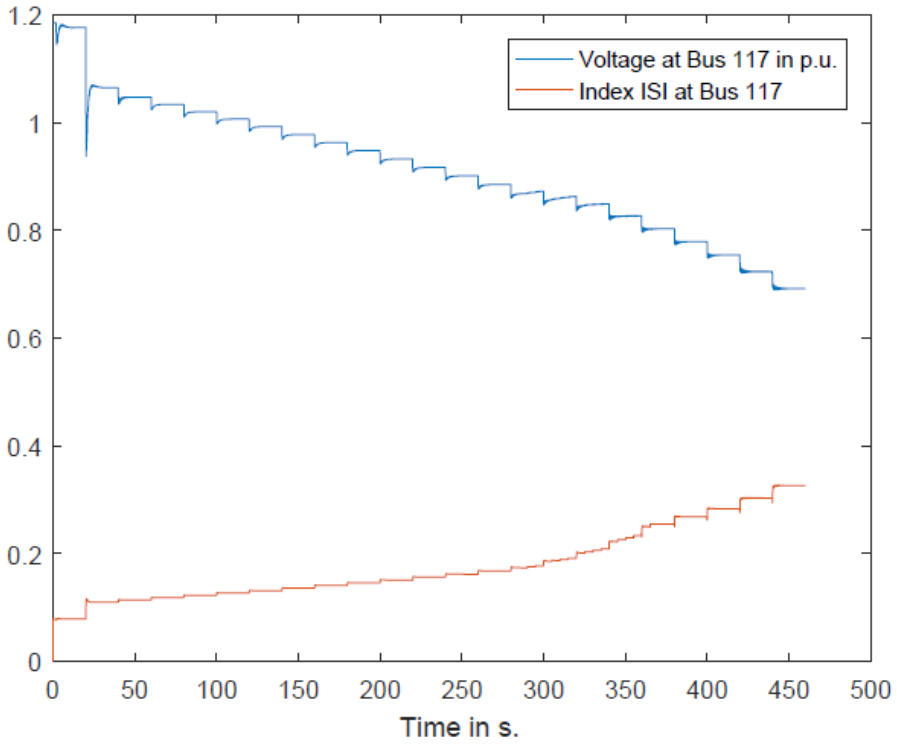

Figure 4.5: ISI and Voltage (p.u.) plots with respect to Time (s.) at bus 117 with one tripped line, OLTC and OEL activated

Fig. 4.6 and 4.7 show the plots of the VCPI, which indicate no clear changes and seem quasi constant during the whole simulation. The VCPI slightly increases when the line is tripped at 20s.

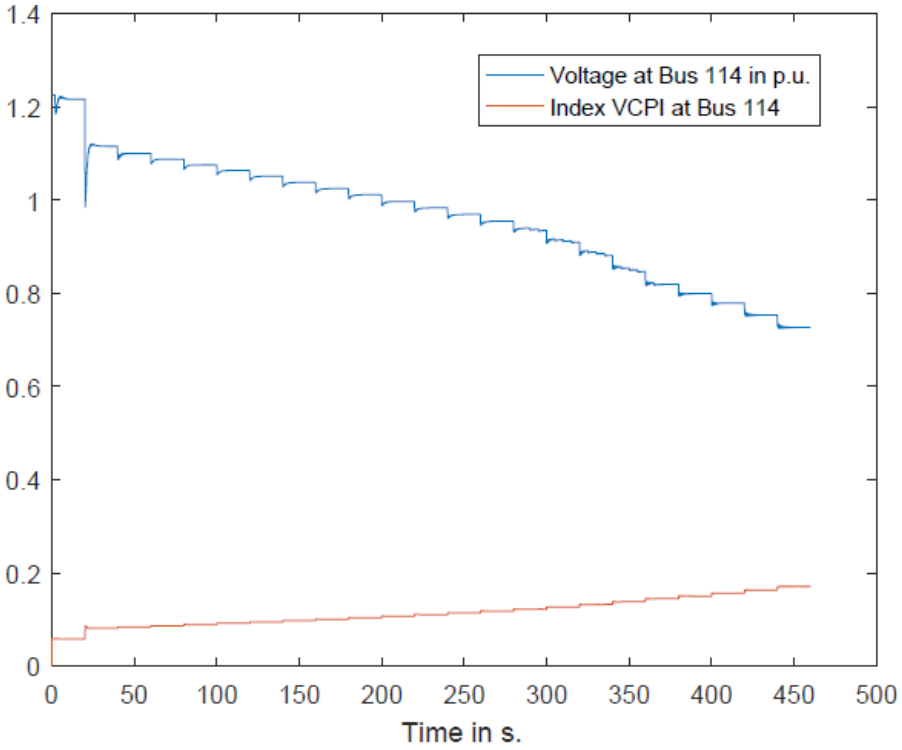

Figure 4.6: VCPI and Voltage (p.u.) plots with respect to Time (s.) at bus 114 with one tripped line, OLTC and OEL activated

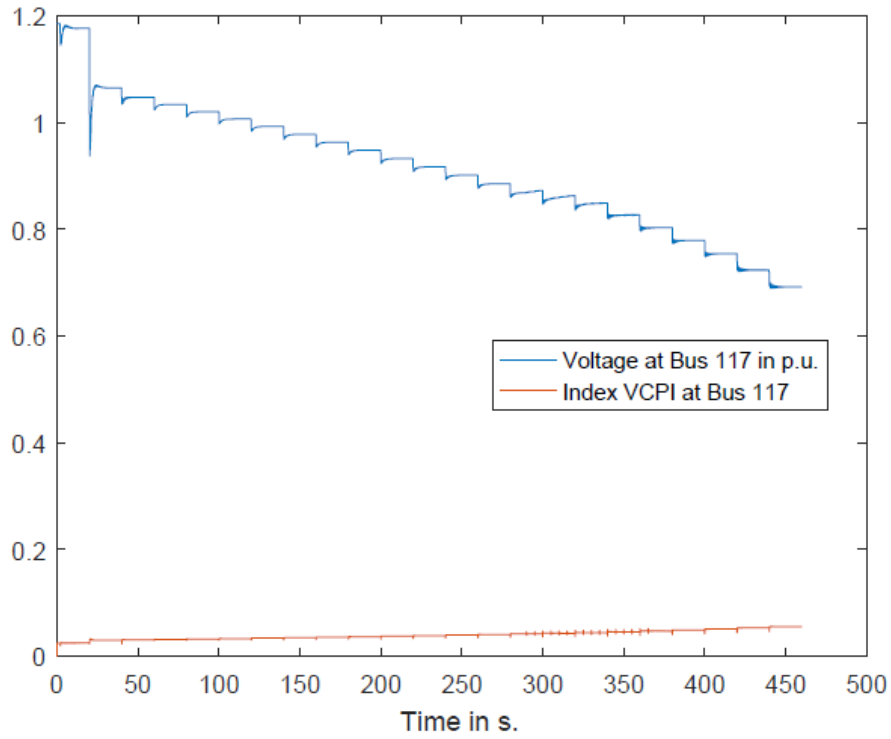

Figure 4.7: VCPI and Voltage (p.u.) plots with respect to Time (s.) at bus 117 with one tripped line, OLTC and OEL activated

The VCIscc indicates a voltage collapse would occur after it reaches 1 at bus 114 in Fig. 4.2. Although the tap changer is connected to bus 117, bus 114 seems to be weaker instead. Similarly, ISI shows similar figures when voltage collapse occurs, but the value is lower than expected. i.e. 0.58. Regarding the VCPI, the indicator doesn't vary much as shown in Fig. 4.6 and 4.7.

4.2.2 OLTC and OEL disabled

The simulation was repeated, but with the deactivation of both OEL and OLTC. The motivation is to observe what would happen if the latter devices are not available and how they would affect the indicators.

It is interesting to observe that all of the indicators are behaving in the same manner as in the previous simulation, with values that are slightly smaller as shown in Fig. 4.8, 4.9, 4.10, 4.11, 4.12 and 4.13.

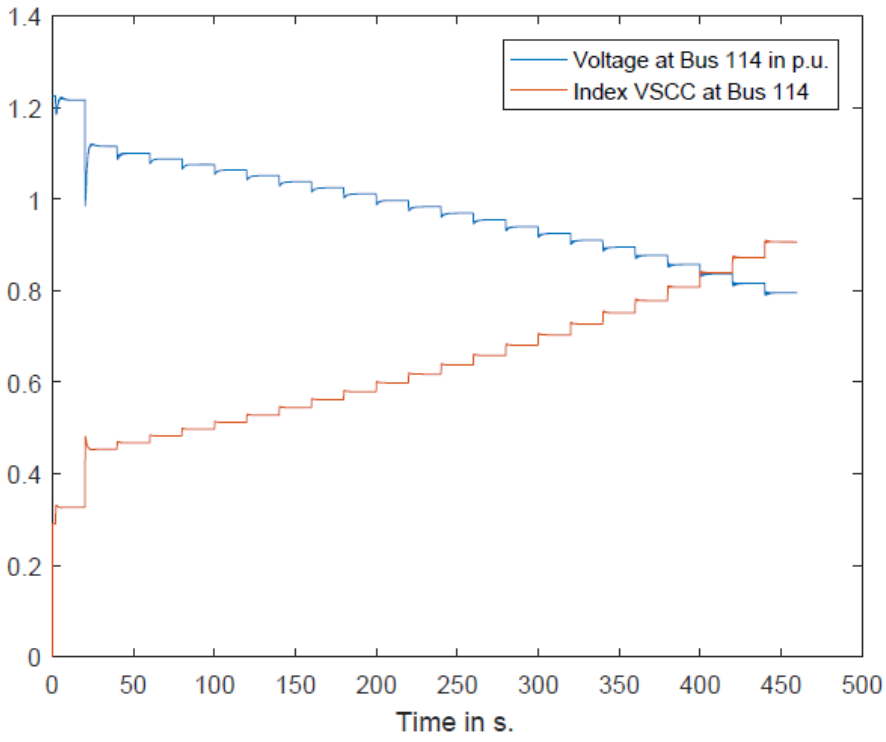

Figure 4.8: VCIscc or VCSS and Voltage (p.u.) plots with respect to Time (s.) at bus 114 with one tripped line, OLTC and OEL disabled

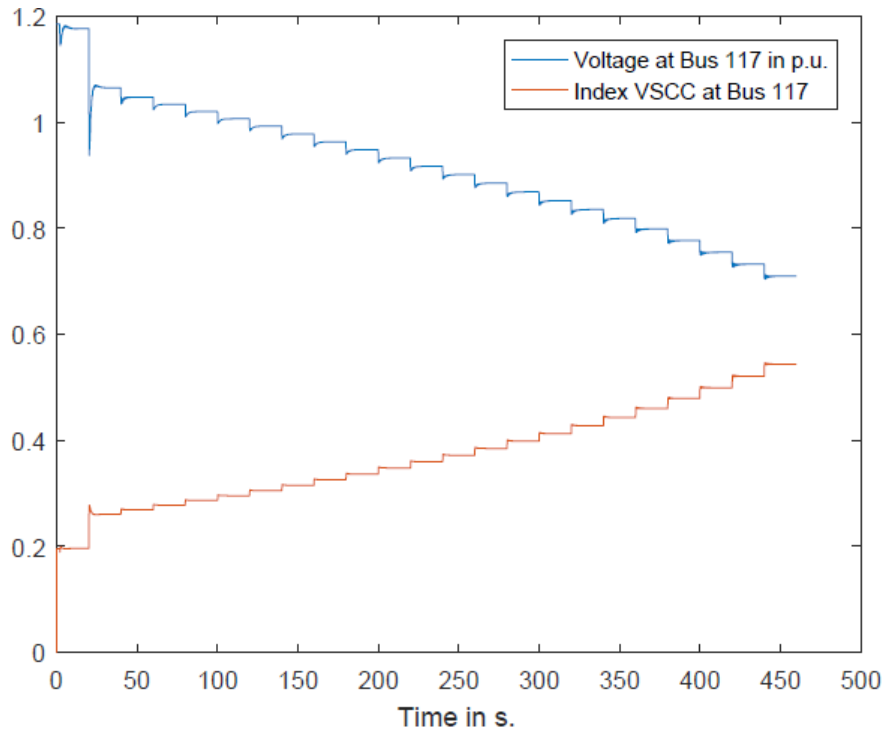

Figure 4.9: VCIscc or VCSS and Voltage (p.u.) plots with respect to Time (s.) at bus 117 with one tripped line, OLTC and OEL disabled

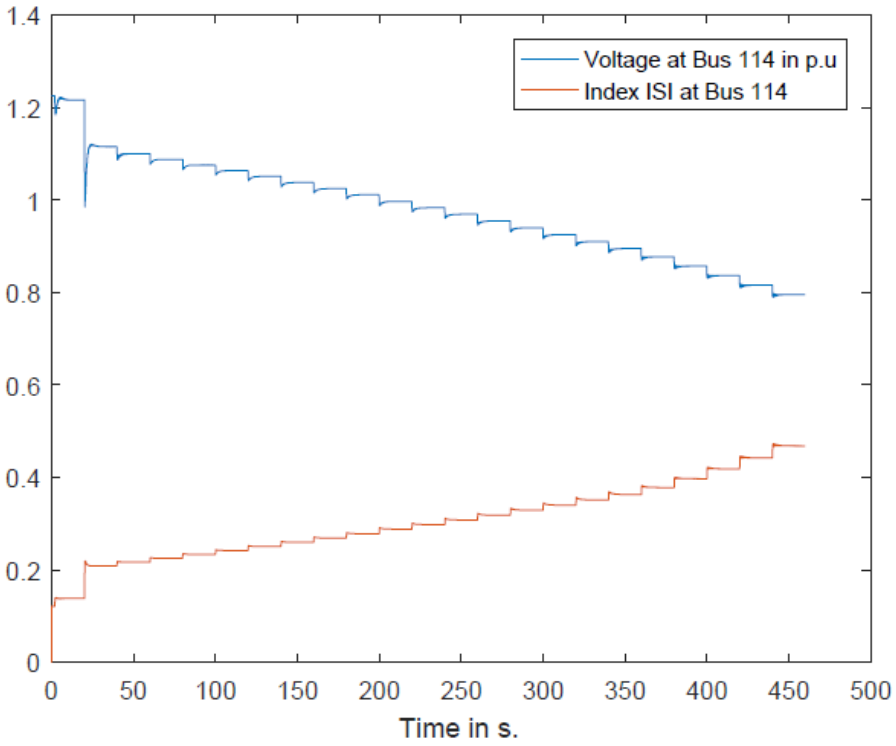

Figure 4.10: ISI and Voltage (p.u.) plots with respect to Time (s.) at bus 114 with one tripped line, OLTC and OEL disabled

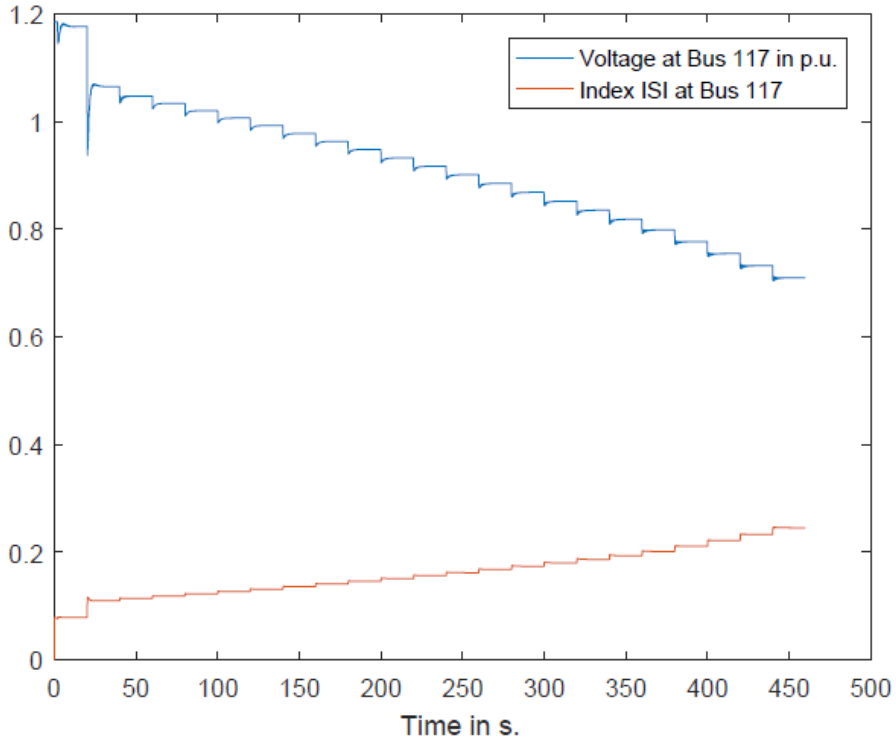

Figure 4.11: ISI and Voltage (p.u.) plots with respect to Time (s.) at bus 117 with one tripped line, OLTC and OEL disabled

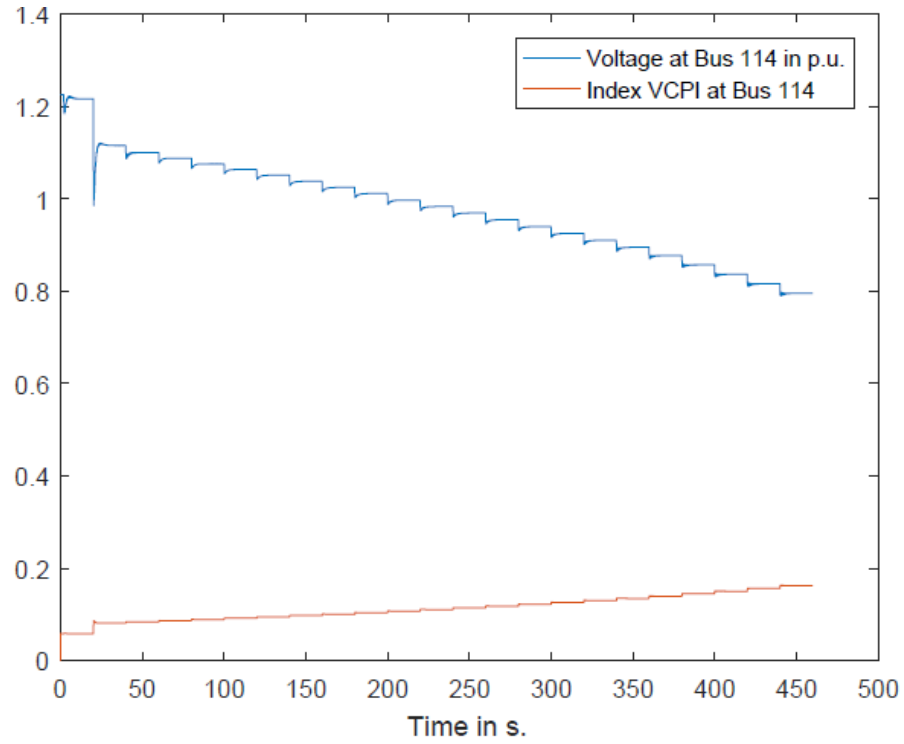

Figure 4.12: VCPI and Voltage (p.u.) plots with respect to Time (s.) at bus 114 with one tripped line, OLTC and OEL disabled

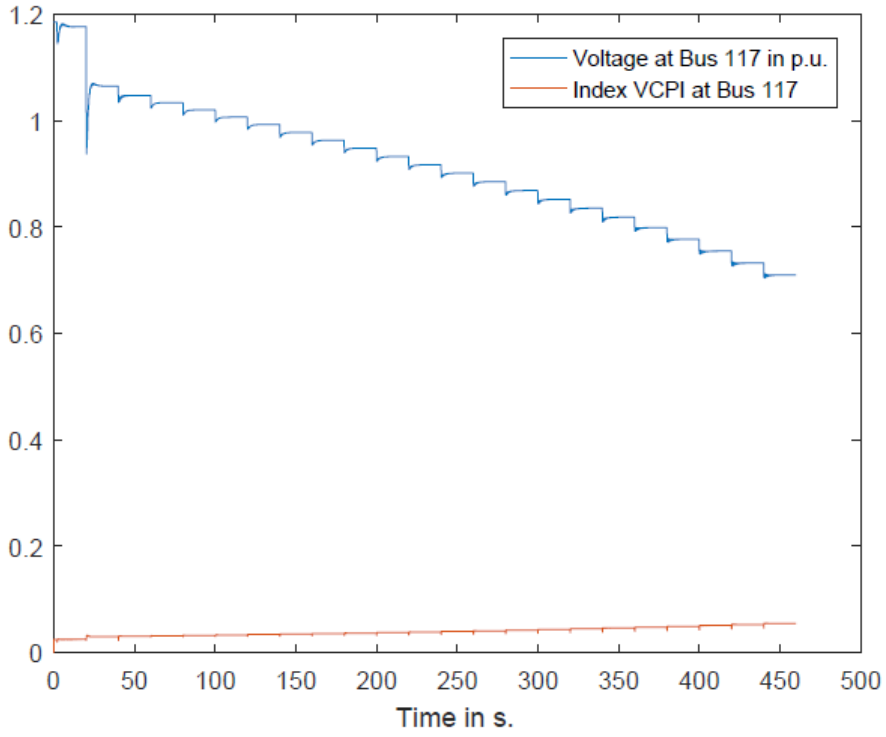

Figure 4.13: VCPI and Voltage (p.u.) plots with respect to Time (s.) at bus 117 with one tripped line, OLTC and OEL disabled

Moreover, PSS/E didn't signal that a voltage collapse occurred, although the voltages are below 0.8 p.u. This is mainly due to the deactivation of the OEL of the generator at bus 211, generating reactive power depending on the load increase, which doesn't illustrate reality at all. This illustrates that OELs and OLTCs have to be at least taken into account to reflect reality, including distance and undervoltage relays, and others.

4.3 Tripping of two lines

In this section, two lines are tripped instead of one between buses 112 and 113 at 2 and 10 s. respectively.

4.3.1 OLTC and OEL activated

Fig. 4.14, 4.15, 4.16 and 4.17 indicate higher values of ISI and VSCIscc compared to the previous simulation,and voltage collapse occurs at around 380 s. instead of 460 s., which is logical since the system is weaker and the maximum power transfer decreases. Additionally, it is shown in those plots that bus 114 is still the weakest and the sudden increase in the indicators is much more noticeable at bus 114. However,

the VSCIscc crosses the value of 1 before voltage collapse occurs. It can be seen that it reaches a value greater than 1.2 when it happens, as opposed to the ISI, which reaches a value of 0.9 approximately.

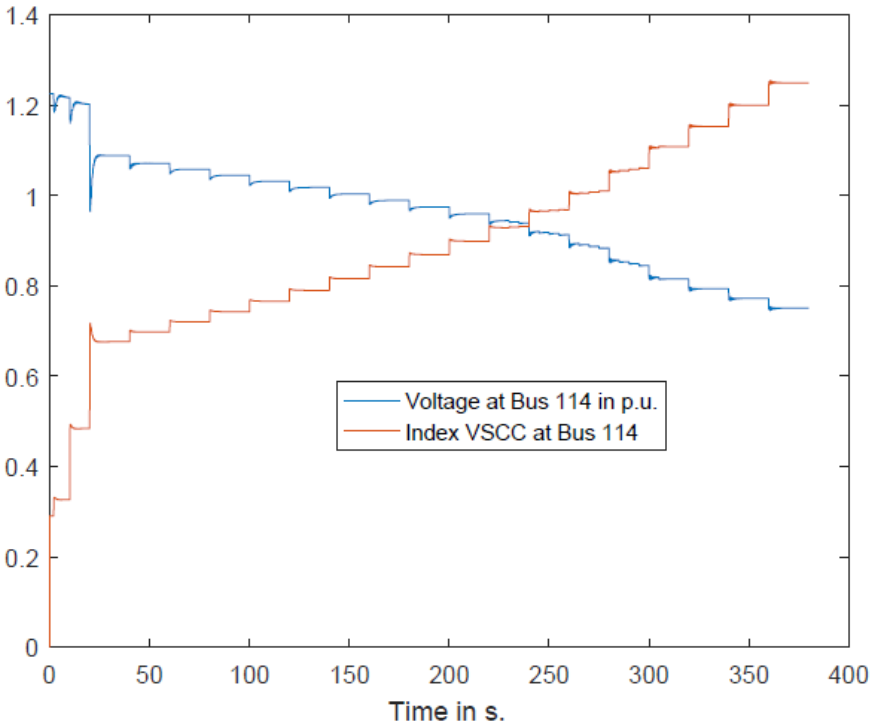

Figure 4.14: VCIscc or VCSS and Voltage (p.u.) plots with respect to Time (s.) at bus 114 with two tripped lines, OLTC and OEL activated

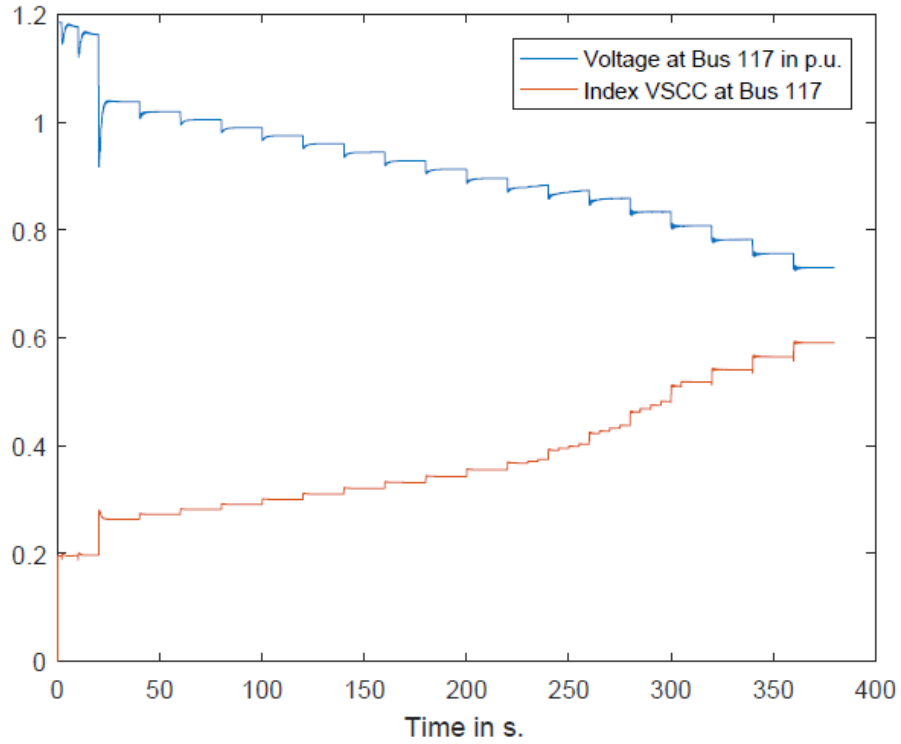

Figure 4.15: VCIscc or VCSS and Voltage (p.u.) plots with respect to Time (s.) at bus 117 with two tripped lines, OLTC and OEL activated

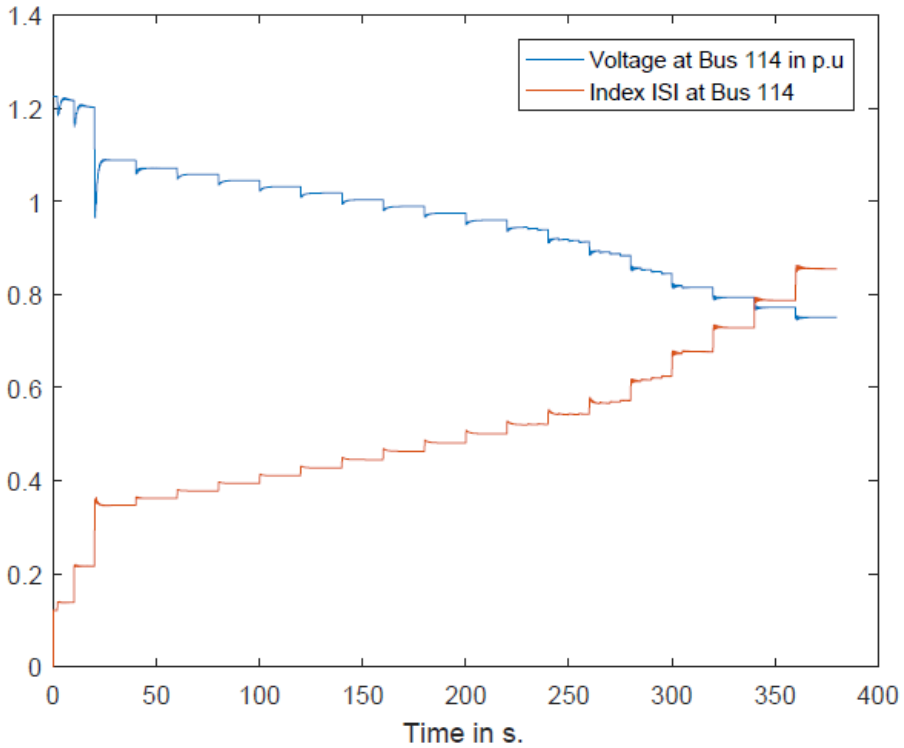

Figure 4.16: ISI and Voltage (p.u.) plots with respect to Time (s.) at bus 114 with two tripped lines, OLTC and OEL activated

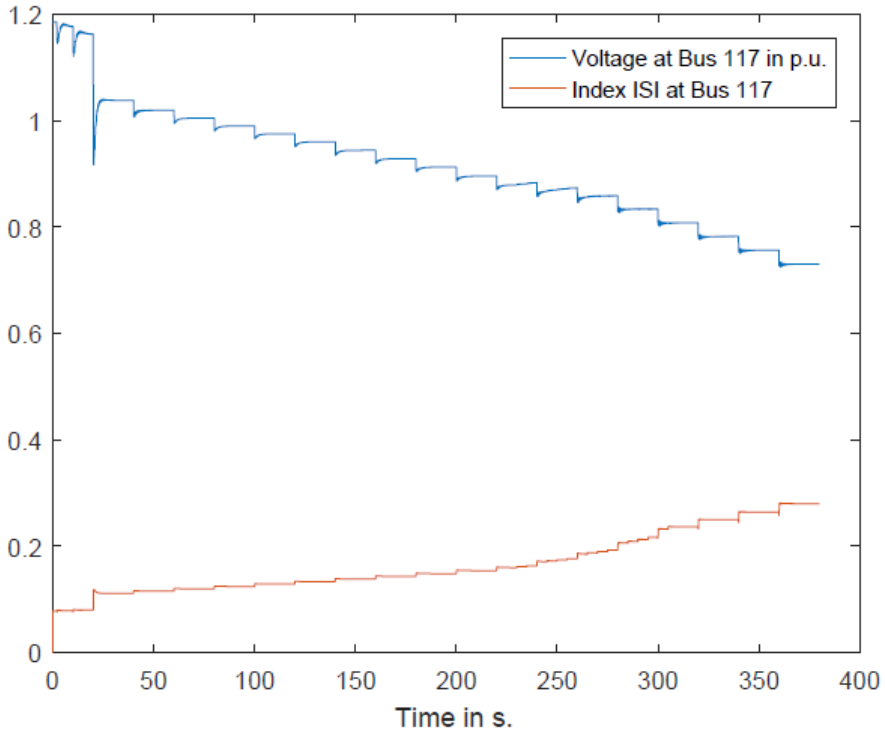

Figure 4.17: ISI and Voltage (p.u.) plots with respect to Time (s.) at bus 117 with two tripped lines, OLTC and OEL activated

In Fig. 4.18 and 4.19,the VCPI showed no signs of change. This could be explained by the fact this indicator depends only on voltages and admittance, without taking into account the power transfer or load power.

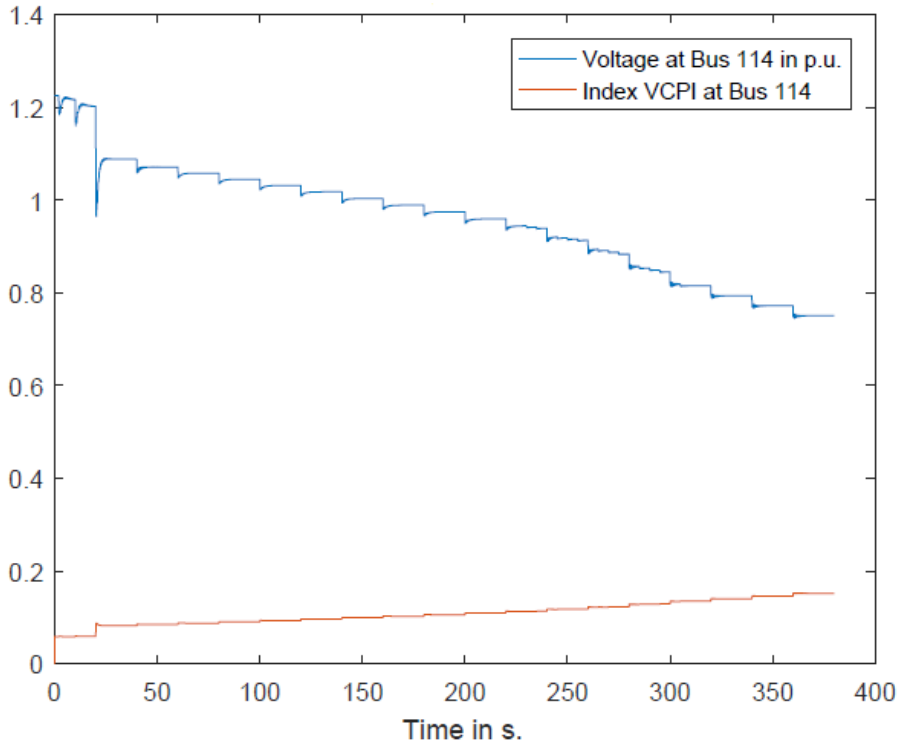

Figure 4.18: VCPI and Voltage (p.u.) plots with respect to Time (s.) at bus 114 with two tripped lines, OLTC and OEL activated

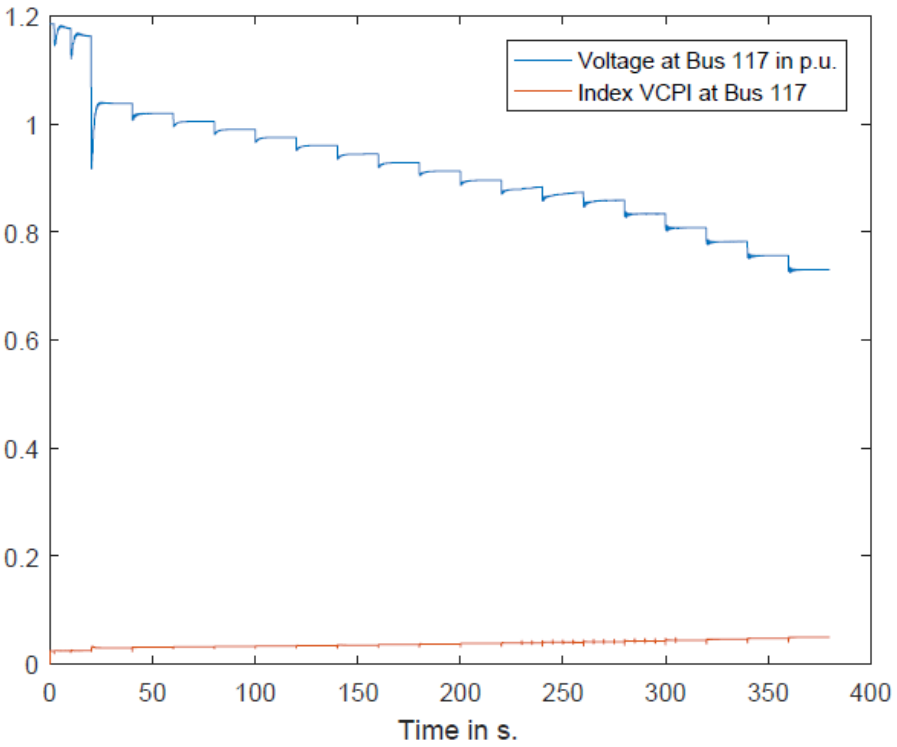

Figure 4.19: VCPI and Voltage (p.u.) plots with respect to Time (s.) at bus 117 with two tripped lines, OLTC and OEL activated

Furthermore, the VCPI is showing that bus 115 is the weakest, as shown in Fig. 4.20

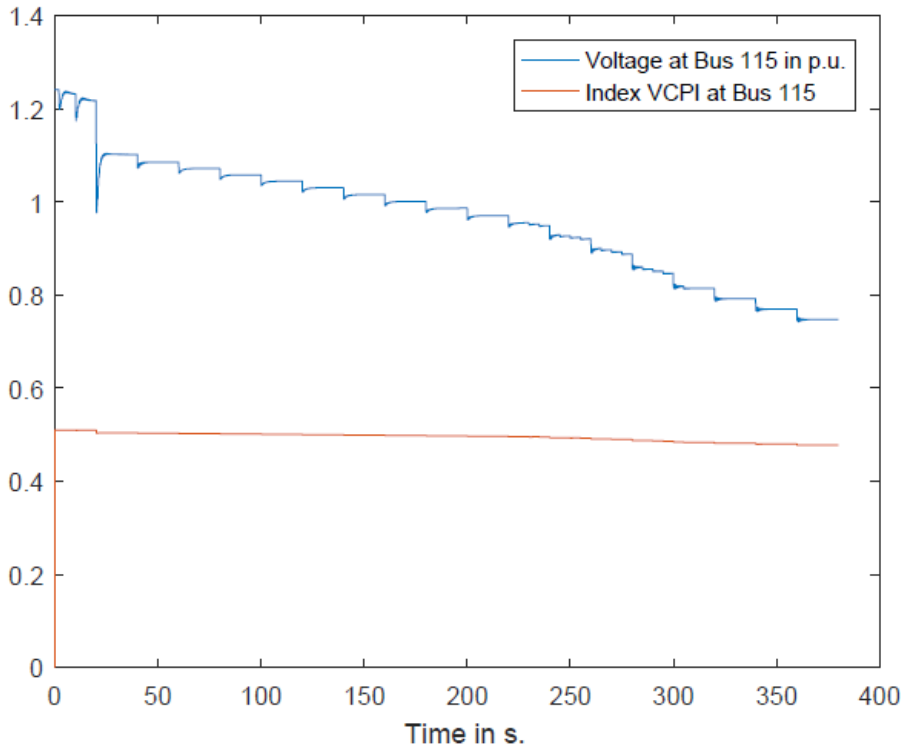

Figure 4.20: VCPI and Voltage (p.u.) plots with respect to Time (s.) at bus 115 with two tripped lines, OLTC and OEL activated

4.3.2 OLTC and OEL disabled

The last simulation for the 10-bus system is to trip two lines between buses 112 and 113 after 2 s. and 10 s. of the start of the simulation, while the OEL and OLTC are disabled. It is noticeable that in Fig. 4.21, 4.22, 4.23, 4.24 ,4.25 and 4.26, the indicators are behaving the same way when the OEL and OLTC are activated, with slightly lower values. The voltage collapse was not shown due to the lack of OEL, OLTC, distance and under-voltage relays, and so on.

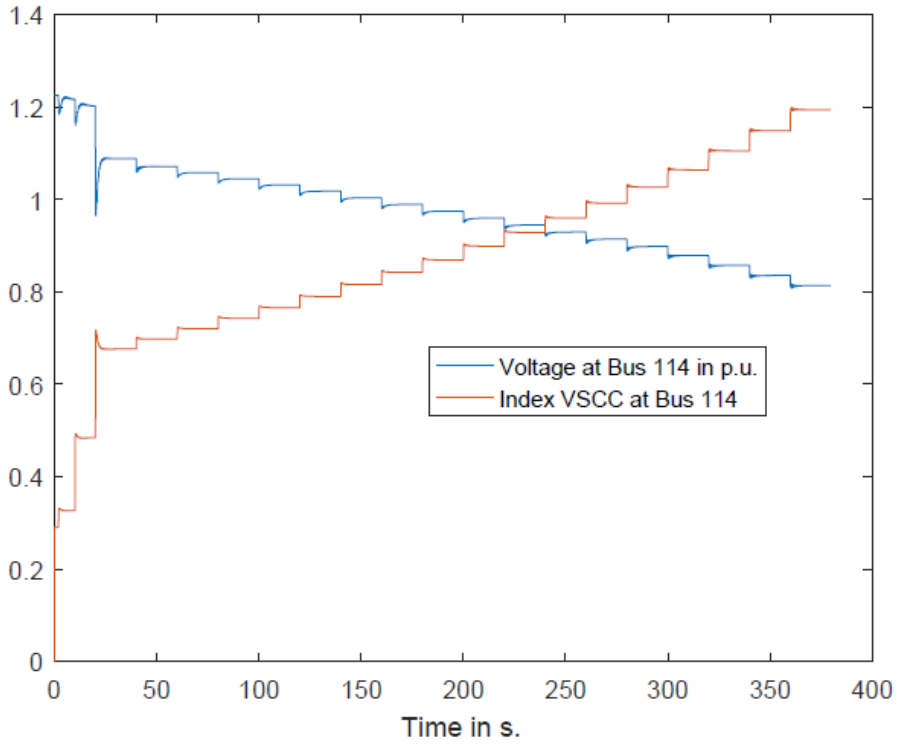

Figure 4.21: VCIscc or VCSS and Voltage (p.u.) plots with respect to Time (s.) at bus 114 with two tripped lines, OLTC and OEL disabled

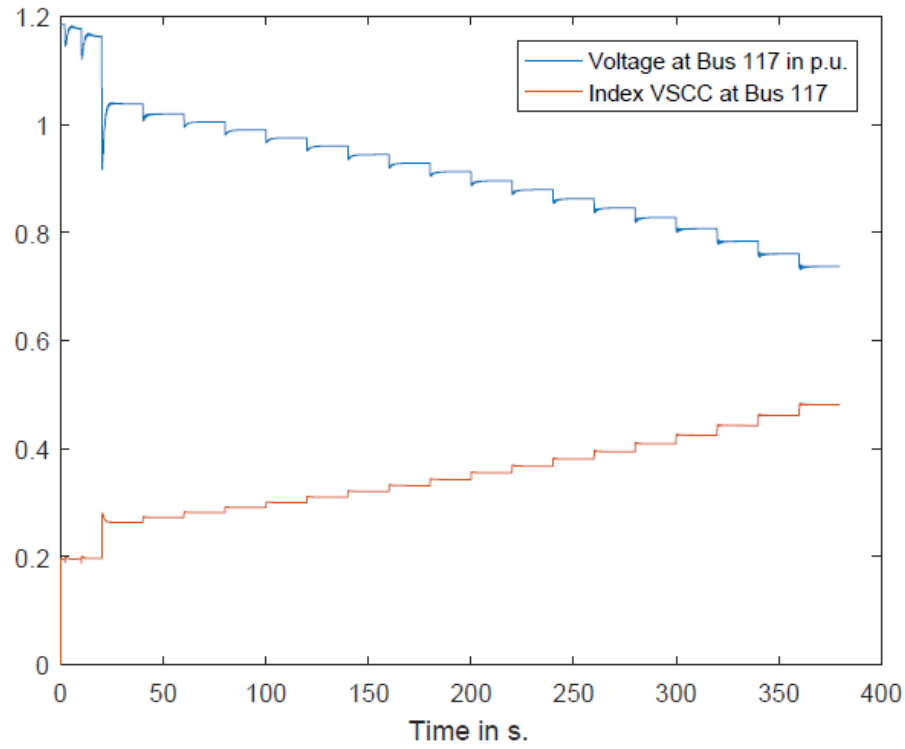

Figure 4.22: VCIscc or VCSS and Voltage (p.u.) plots with respect to Time (s.) at bus 117 with two tripped lines, OLTC and OEL disabled

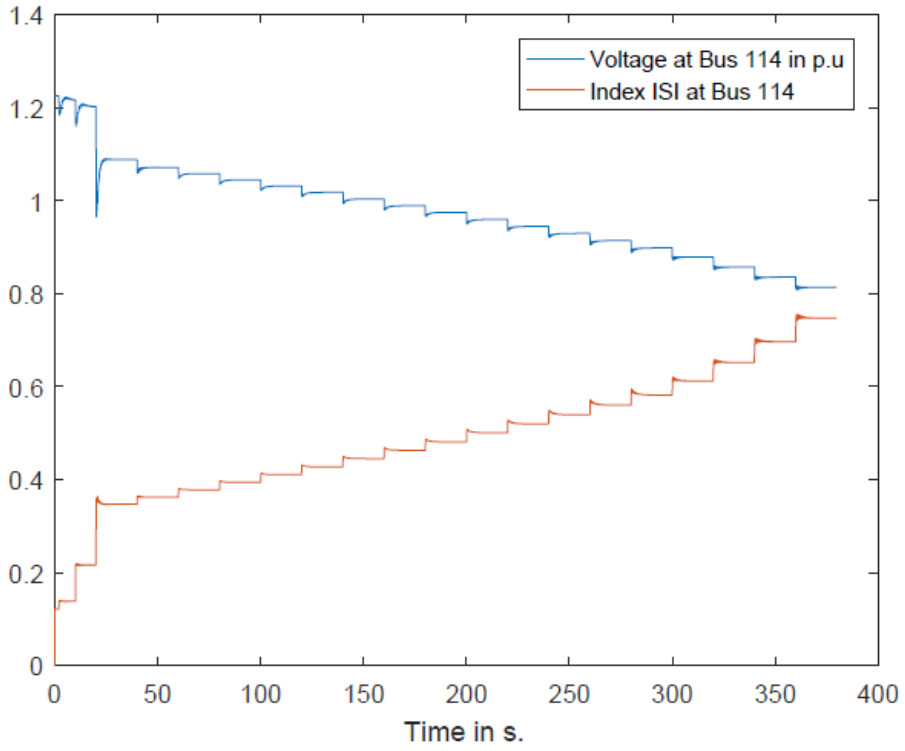

Figure 4.23: ISI and Voltage (p.u.) plots with respect to Time (s.) at bus 114 with two tripped lines, OLTC and OEL disabled

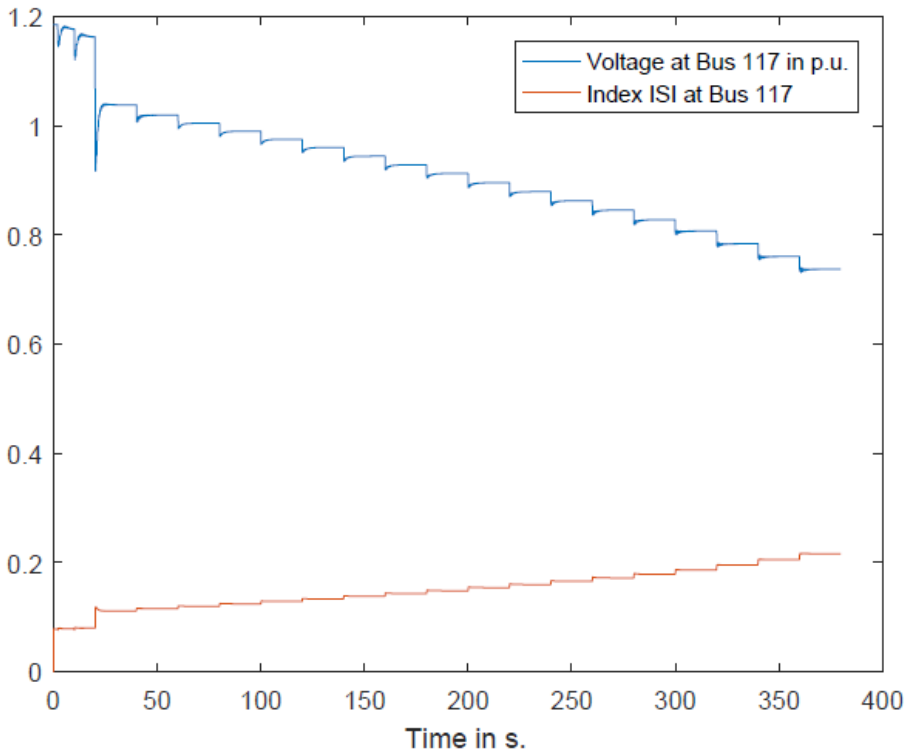

Figure 4.24: ISI and Voltage (p.u.) plots with respect to Time (s.) at bus 117 with two tripped lines, OLTC and OEL disabled

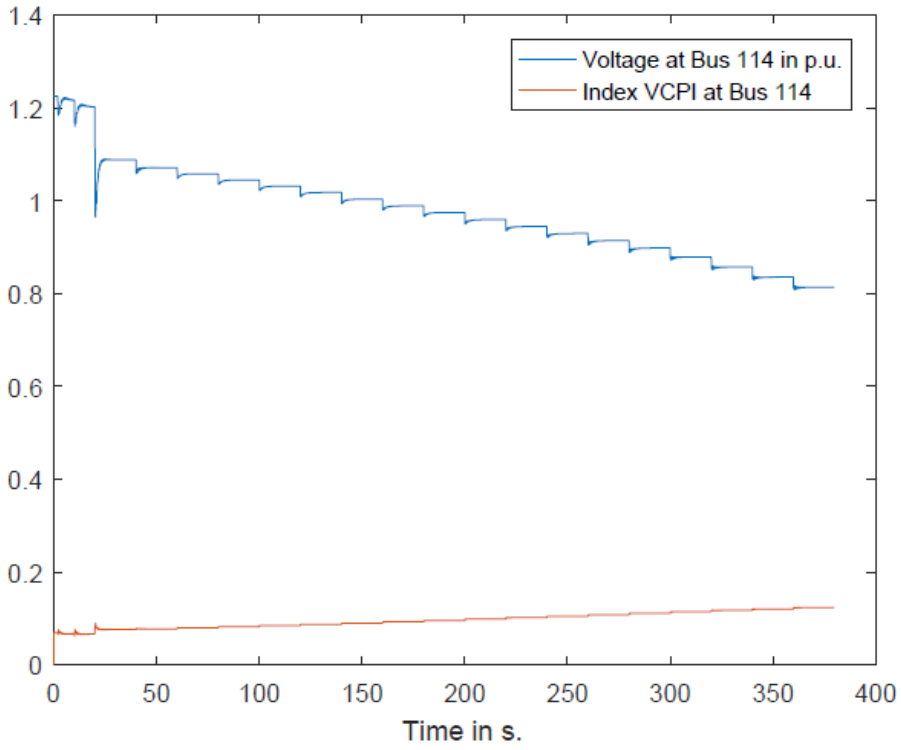

Figure 4.25: VCPI and Voltage (p.u.) plots with respect to Time (s.) at bus 114 with two tripped lines, OLTC and OEL disabled

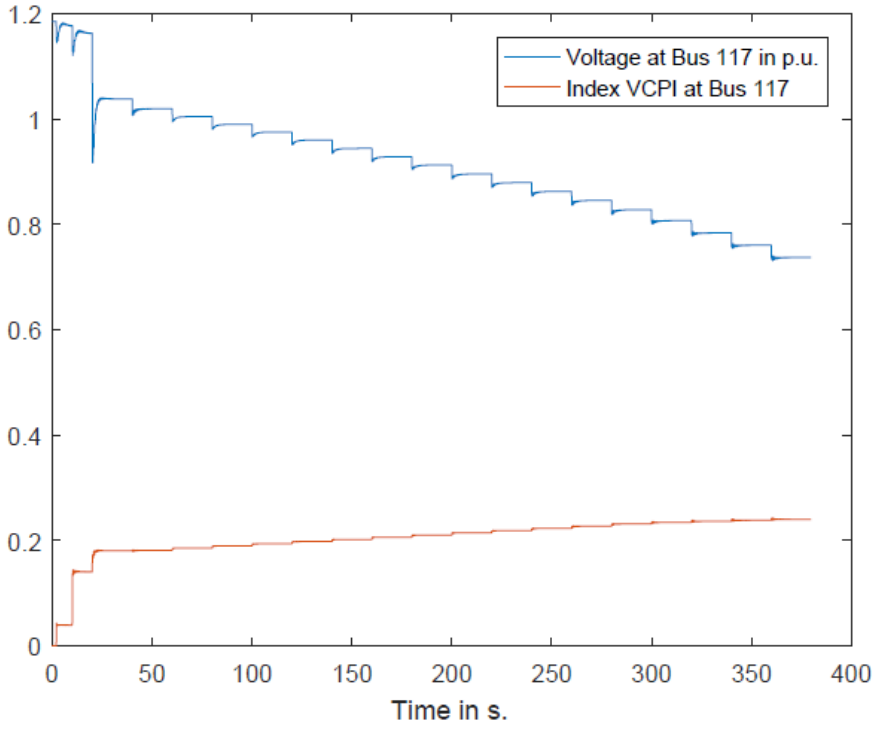

Figure 4.26: VCPI and Voltage (p.u.) plots with respect to Time (s.) at bus 117 with two tripped lines, OLTC and OEL disabled

4.4 Discussion

The conducted dynamic simulations in the simple 10-bus system illustrated how the indicators acted with the constant increase of load, and the OEL and OLTC proved to be essential in reflecting on how the voltage instability and collapse occur in the system. Also, the dynamic and continuous computation of the thevenin impedances during the simulation proved to be very efficient since the real time duration of the simulation was exactly equal to the simulation time that was set in PSS/E. Furthermore, the VCPI was practically constant during the whole simulations due to its dependence on voltages and admittance only. The ISI and VCSIscc proved to be more adaptable in signaling a voltage instability or collapse. Additionally, although the ISI and VCSIscc showed to act in a similar way, the former gave a better indication of voltage collapse when two lines were tripped, whereas the latter gave better indication when one line is tripped instead. This encourages the use of two indicators instead of one when analyzing voltage instability and predicting voltage collapse. However, In the next chapter, the ISI will only be taken into account in order to avoid any computational burden. The other two indicators will be excluded.

On the other hand, the real-time PV-curves were plotted during dynamic simulation. it is shown in Fig. 4.27, 4.28, 4.29 and 4.30 that it is impossible to analyze the power system stability using these curves due to the simple fact that the loads depend on voltages. It is interesting to notice in the same figures how the voltages are high at the beginning of the simulation due to the light loads, but a slight load increase drops the voltage value drastically. The constant increase and decrease in power transfer or voltages are mainly due to the load increase and their dependence on voltage.

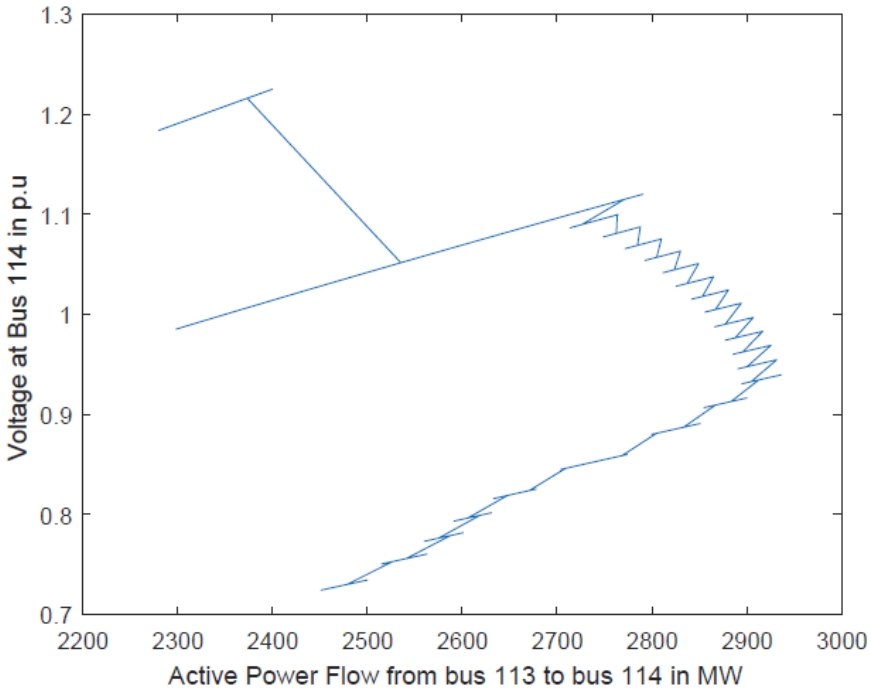

Figure 4.27: PV-curve showing active Power Flow from bus 113 to 114 with respect to voltage at bus 114 in dynamic state when one line is tripped

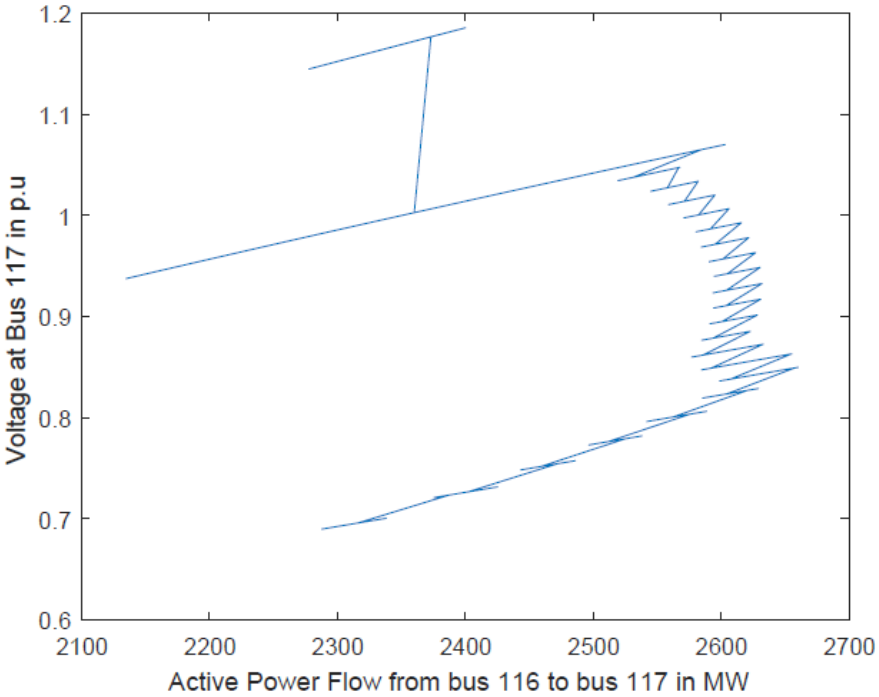

Figure 4.28: PV-curve showing active Power Flow from bus 116 to 117 with respect to voltage at bus 117 in dynamic state when one line is tripped

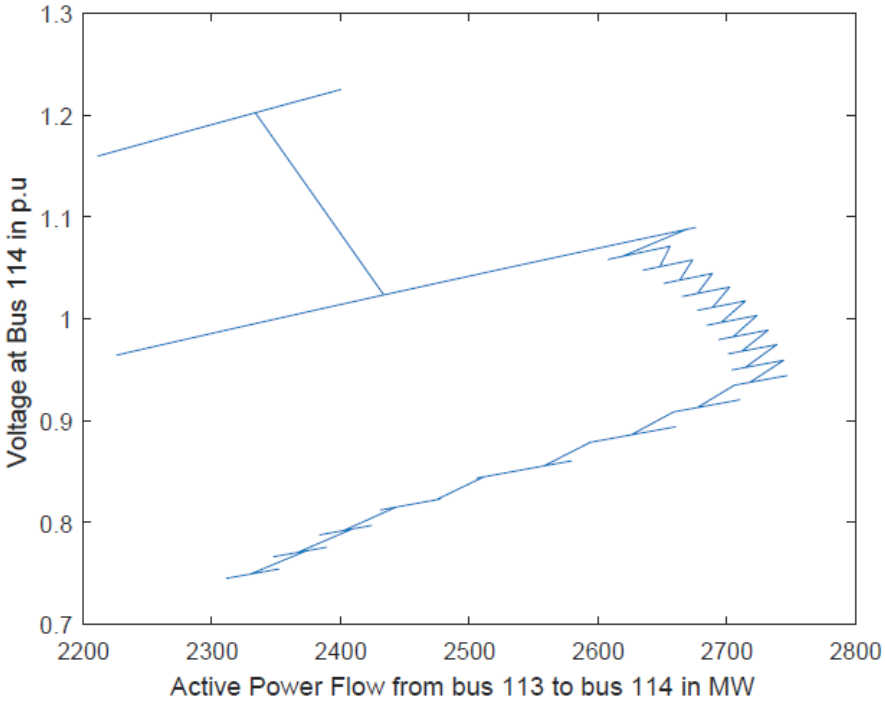

Figure 4.29: PV-curve showing active Power Flow from bus 113 to 114 with respect to voltage at bus 114 in dynamic state when two lines are tripped

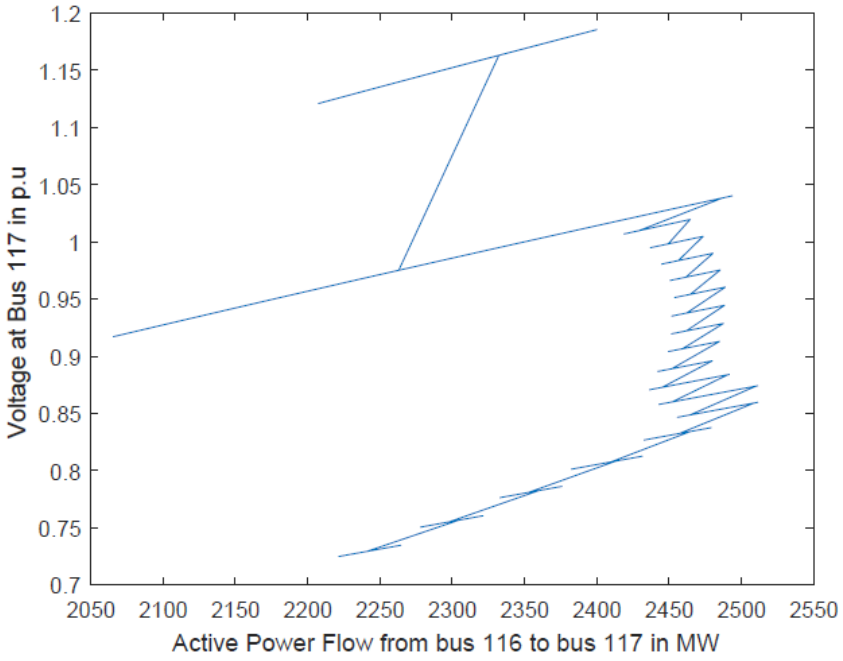

Figure 4.30: PV-curve showing active Power Flow from bus 116 to 117 with respect to voltage at bus 117 in dynamic state when two lines are tripped

5

Evaluation of indicators on the Nordic32 system

In this chapter, the ISI will be evaluated in two different cases and its behavior will be observed. The first case will be by applying a three-phase fault between buses 4032 and 4044, and the second case is to trip a big generator at bus 4042.

5.1 Diagram and Model Setting From CIGRE

The Nordic32 single line diagram is built based on a 1995 CIGRE report [2], as shown in Fig. 5.1. The loads are considered to be moderate and will be completely converted into constant current loads for simplicity.

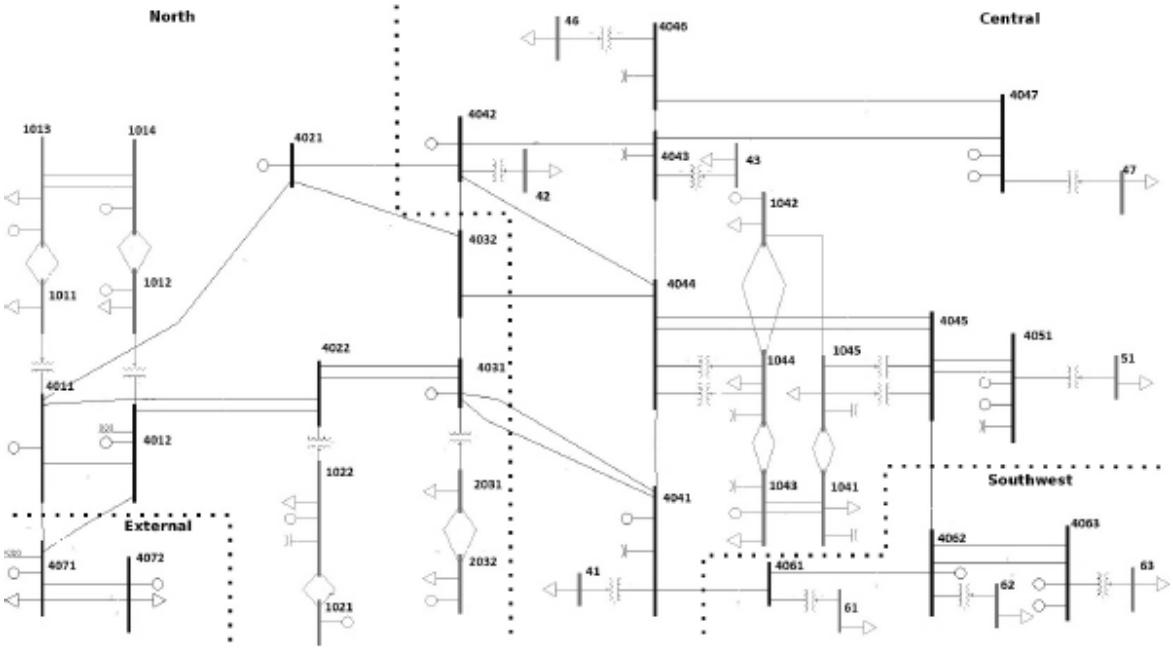

Figure 5.1: Nordic32 system single line diagram

5.2 Indicators Evaluation

In order to evaluate the indicator in the Nordic32 test system, data were obtained from each of the two simulation cases and processed in Matlab to calculate the indicators. The simulations in both cases were run for 20s. and then, the disturbance was applied, leading to the activation of OEL, OLTC,distance relays and under-voltage relays.

5.2.1 Case1:3-Phase Balanced Line Fault

After applying a 3-Phase Balanced Line Fault, the distance relay tripped the faulted line, the OLTC and OEL are activated as in [6], and voltage collapse occurs at 270s. due to the cascaded tripping of the generators by the under-voltage relays.The results were quite unexpected, especially due to the oscillations or transients of the ISI.

The ISI at buses 1041,1044 and 1045 proved to be the most noticeable as shown in Fig. 5.2, 5.3 and 5.4.

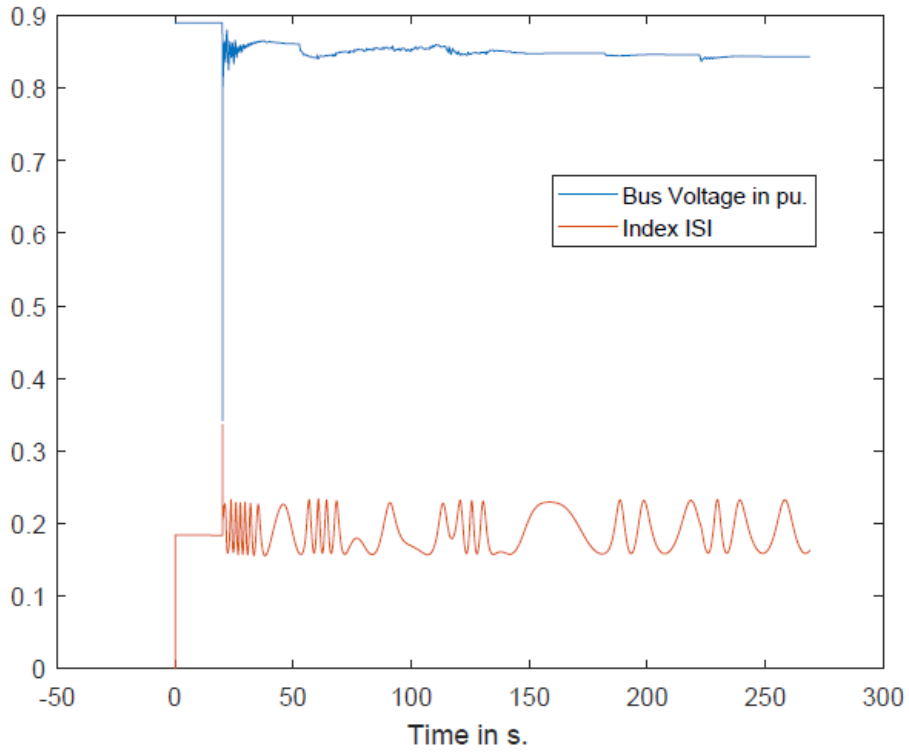

Figure 5.2: ISI and Voltage at bus 1041 for Case 1

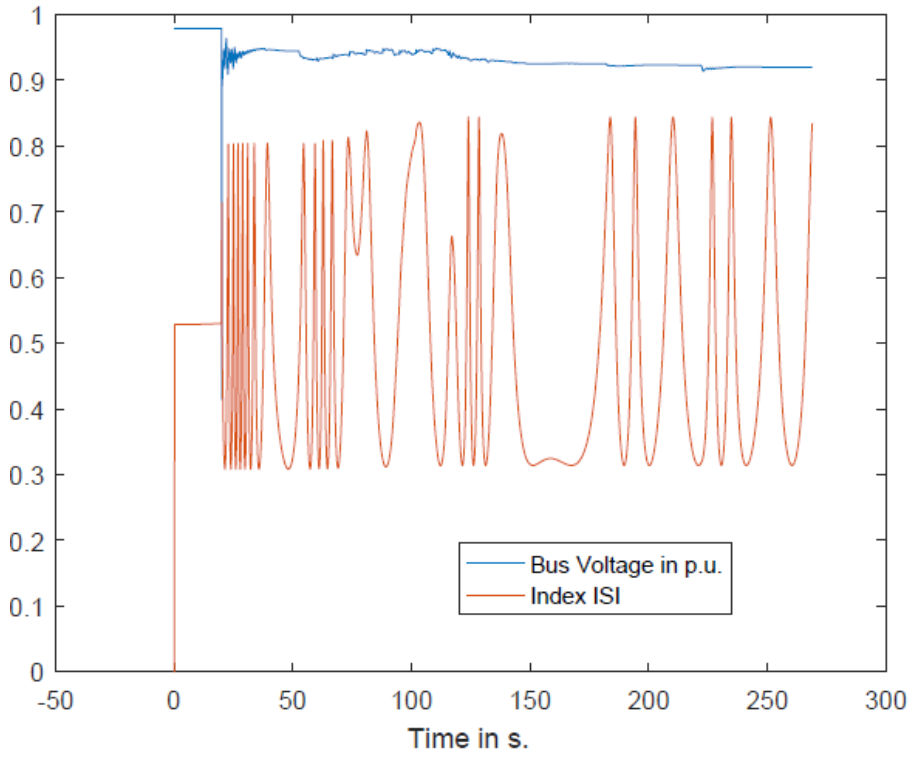

Figure 5.3: ISI and Voltage at bus 1044 for Case 1

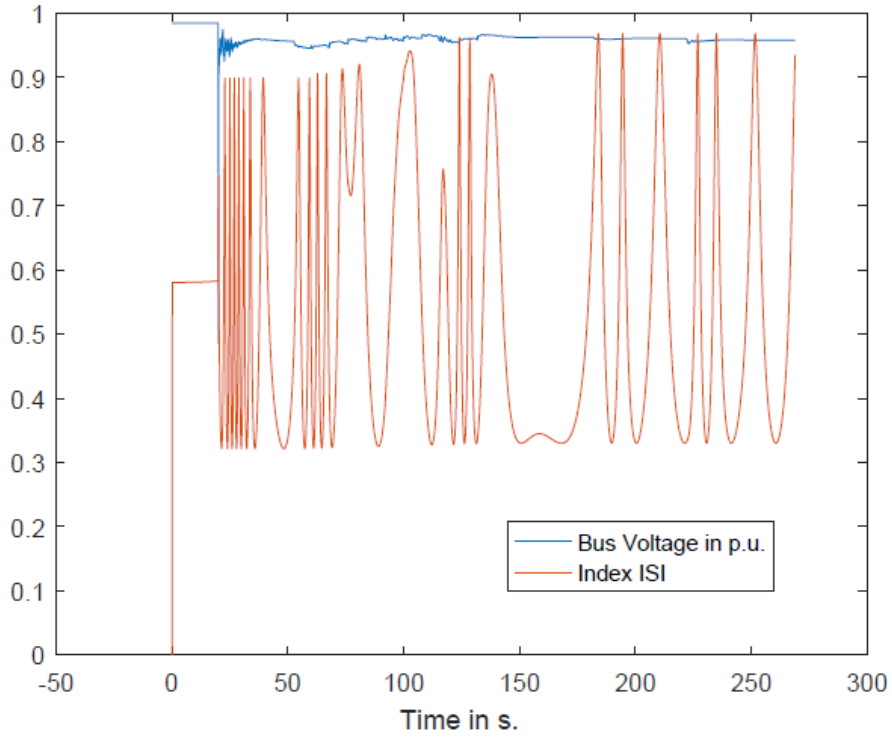

Figure 5.4: ISI and Voltage at bus 1045 for Case 1

5.2.2 Case2:Generator Tripping

Tripping the generator at bus 4042 led to the activation of OELs and OLTCs to bring back the voltages to the acceptable ranges. However, the disturbance is harsher than the 3-phase fault due to the fact that an unbalance between load and generation was created, and the tripped generator was considered to be a big one. The voltage collapse occurs at 115s. and transients are visible starting at 80s.

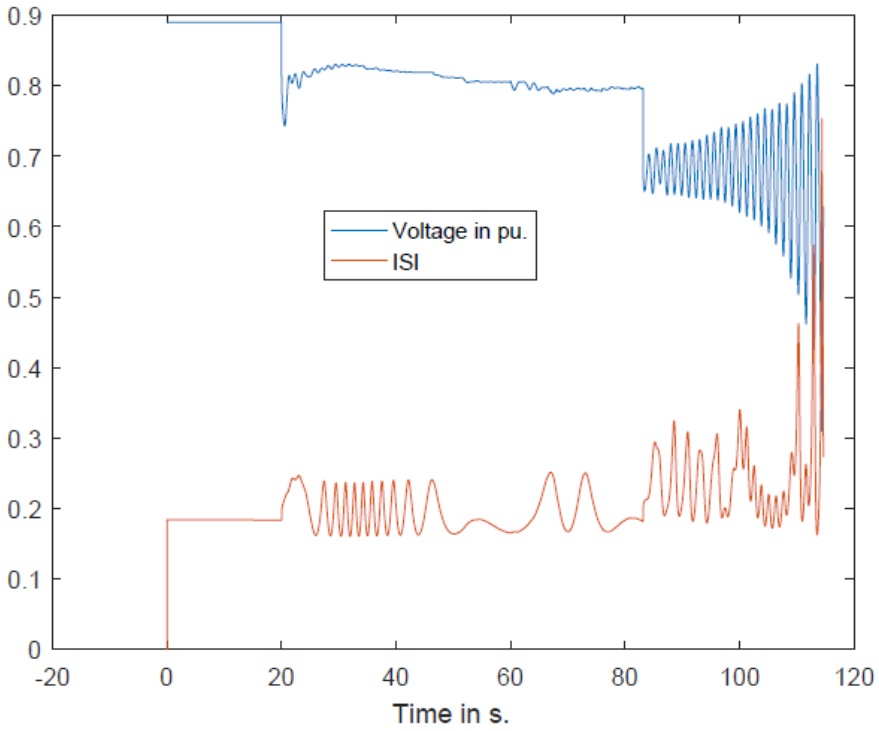

Figure 5.5: ISI and Voltage at bus 1041 for Case 2

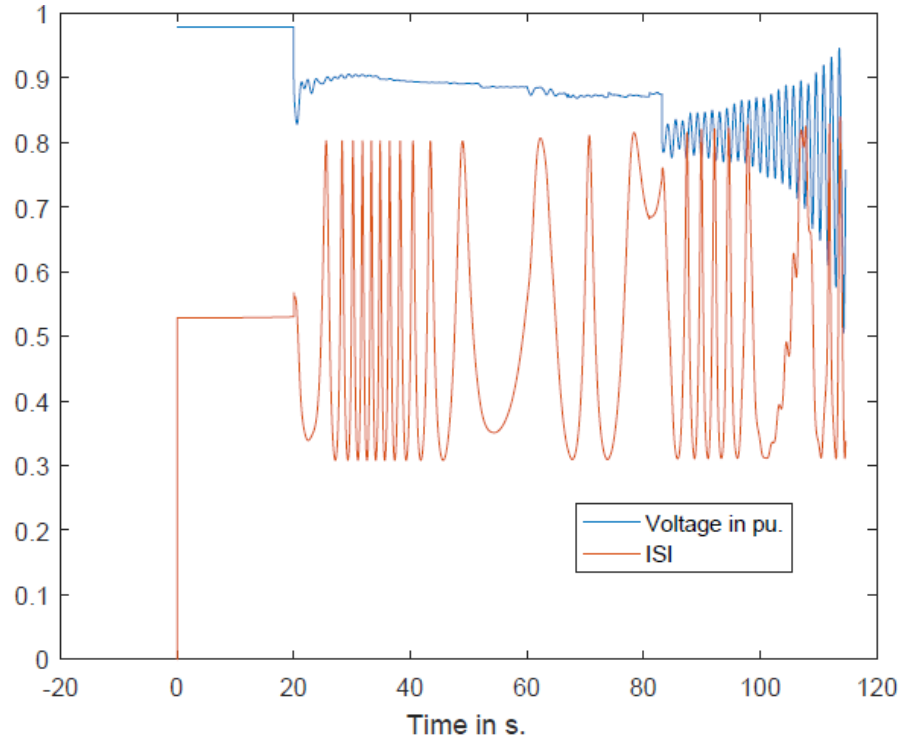

Figure 5.6: ISI and Voltage at bus 1044 for Case 2

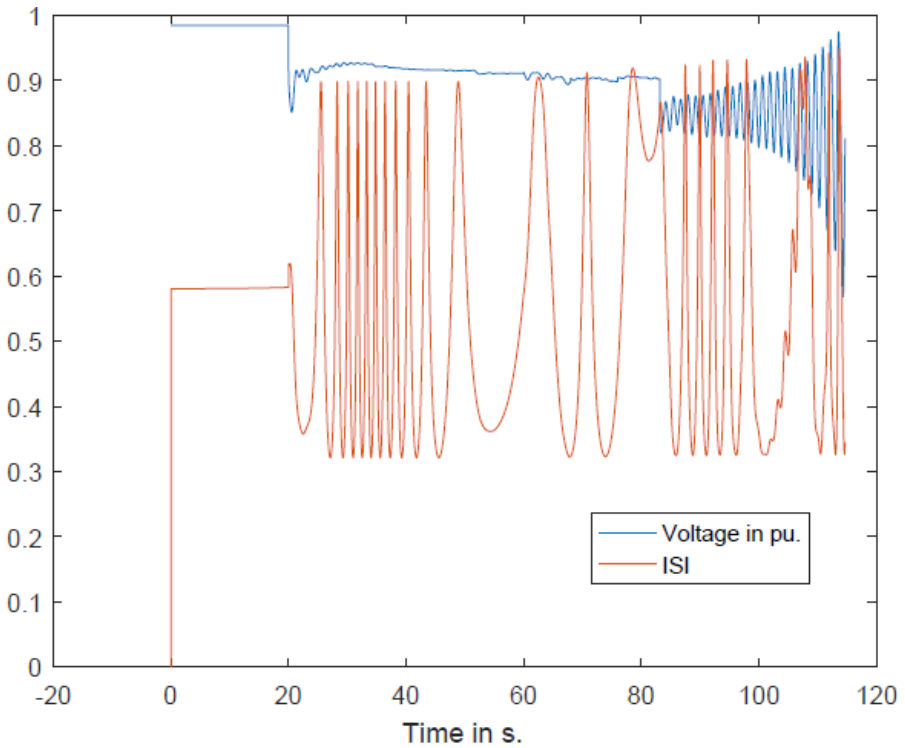

Figure 5.7: ISI and Voltage at bus 1045 for Case 2

5.3 Indicators Analysis and Discussion

The two cases showed an expected performance of the ISI indicators. In both cases, the ISI trends were quite similar and showed that buses 1041,1044 and 1045 are the weakest buses in the system. it can be said that the indicators follow the events occurring the system after disturbance. Additionally,the OLTCs and OELs are taken into account in the computation of the thevenin impedance, including the tripping of the lines, which modify admittance in the matrix. The oscillations can also be explained from the angle oscillations. It is important to mention that the angles are taken into account when computing the indicators, and equivalent loads are computed based on eq. 2.11.

The observed oscillations in the ISI can be due to the angle oscillations, caused by the transient and frequency instabilities in the system after a 3-phase line fault and a generator tripping occur, which are out of scope of work. Also, it is critical to mention that the equivalent loads seen from these buses were calculated following eq.(2.11), which explains the oscillations. Looking at the ISI of buses 41 and 46 in Fig. 5.8 and 5.9, it can be seen that oscillations are practically minimal as opposed to the ISI of buses 1044 and 1045. It can be explained from eq.(2.11) and from Fig. 4.1 that buses 41 and 46 are final-end load buses, whereas the other buses are intermediary ones, meaning that they are connected to several other buses and have loads connected to them.

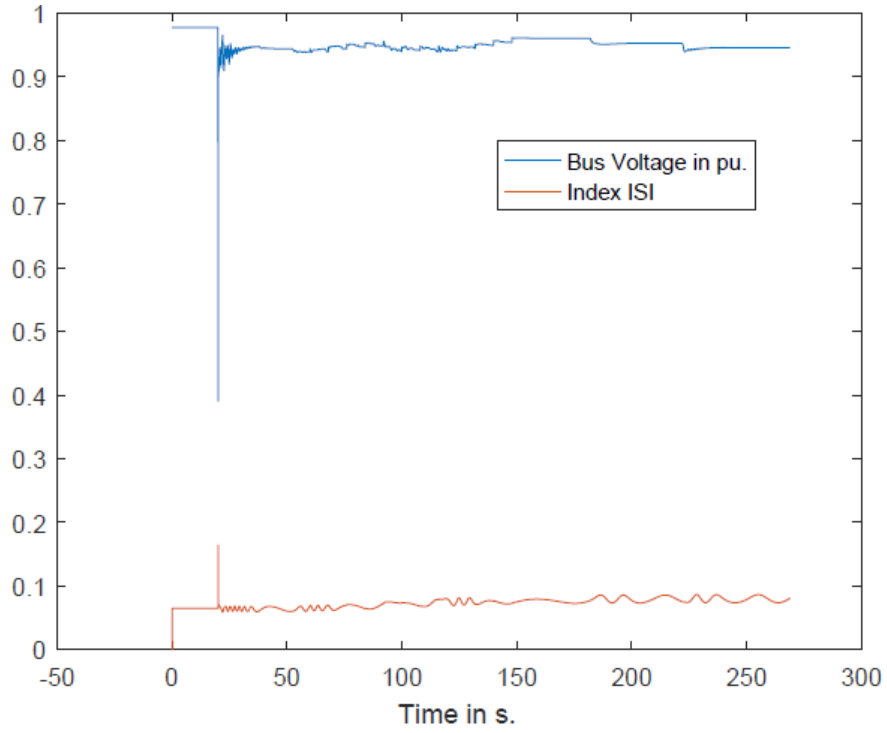

Figure 5.8: Voltage and ISI at bus 41

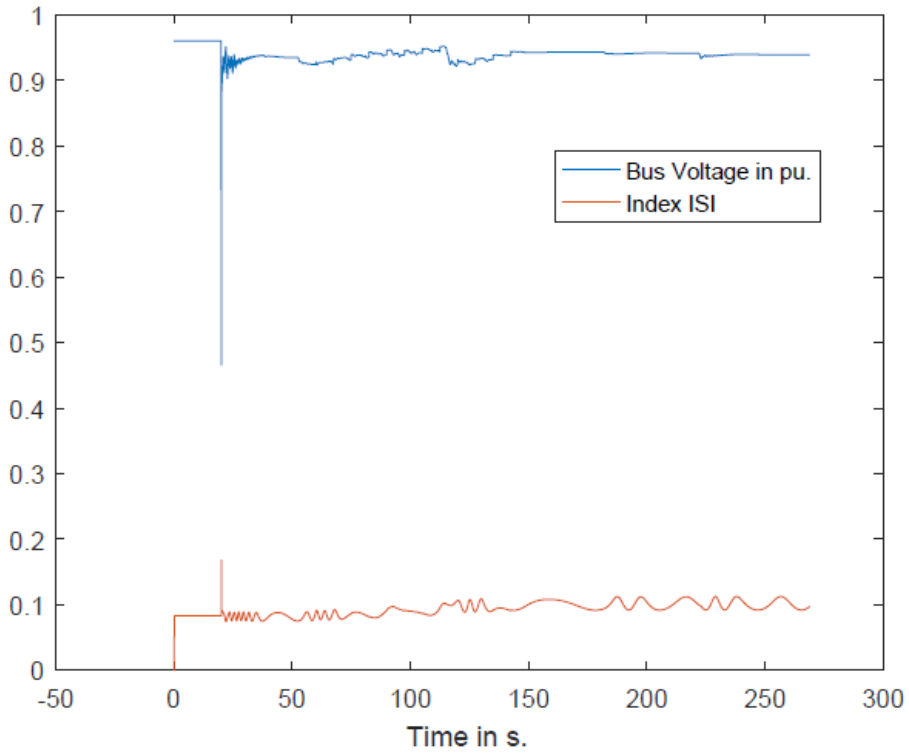

Figure 5.9: Voltage and ISI at bus 46

After observation, it is crucial to find a way to average the ISI, or get rid of the oscillations, so that it can reflect the behavior of the system so that the coordinated control method can be successful. Therefore, it was decided to use a filter with high time constant, and allow the devices to act based on certain ISI values, as already shown in Fig. 3.1. The implementation of the model, with the filtered indicators, will be shown in the next chapter.

6

Voltage Collapse Prevention

This chapter shows how the prevention of voltage collapse occurred with the use of both OEL and AVR signals, and load-shedding based on the filtered ISI. The method was tested in the Nordic32 system.

6.1 Control Method Implementation

The purpose of the method is to monitor the voltage stability of the system during dynamic simulation, which can considered as real-time in order to be able to mitigate voltage instability and prevent voltage collapse. The model was developed based on Fig. 3.1 in the Fortran Code, in which part of it can be found in Appendix B and C. The model is built as a miscellaneous model since it is monitoring the whole system and not controlling components in the system, and is written in Intel Visual Fortran 2005 [22] as an .F90 file and compiled using the PSS/E Environment manager to link it to PSS/E libraries. The model is called from the .dyr file in the interpreter or simulation script written in Python.

6.2 Setting of the Model

As already mentioned in chapter 3, the first step is to measure the voltage magnitudes, voltage angles and the power flow in the OLTC transformers in order to obtain correctly the tap changing position. Since the network admittance matrix is assumed to be know at the beginning of the simulation, it is imperative to monitor if any changes occur in the system, such that tripping of a line, OEL and OLTC. Afterwards, the matrix is inversed to get the thevenin impedances, which are the diagonal elements of the inversed matrix. After computing the ISI, its value is analyzed. If it is greater than 0.4, the AVRs of the closest synchronous generators to the weak bus are activated until OELs are activated. On the other hand, if it is greater than 0.6, the AVRs of the closest synchronous generators to the weak bus with load-shedding are activated. The reason behind these thresholds is due to the selection of the filter, although it is expected to have a threshold of 0.8 as seen in

the 10-bus system. Due to time constraint and limitation in the scope of work, the threshold will be assumed to be correct, but additional studies are needed for future works.

6.3 Evaluation

6.3.1 Case 1: 3-Phase Branch Fault

Starting with case 1, the least severe disturbance, it is noticeable that no voltage collapse occurred at 270s., and AVR set-points increased by 5% at generator buses 1012,1013,4071,4072 and 4011. No load-shedding was needed. Fig. 6.1, 6.2 and 6.3 show that the model is operating correctly. Looking at the filtered ISI, it is noticeable that the oscillations are longer and the voltages are more stable to values a bit lower than the value prior to the fault. The AVR-setpoint increase started with the generators closest to the weakest buses. If the OEL is activated and the ISI is still at an unacceptable level, the AVR setpoints of the next closest available generators are activated. The simple algorithm is based on shortest distance and if-conditions due to the small size of the power system.

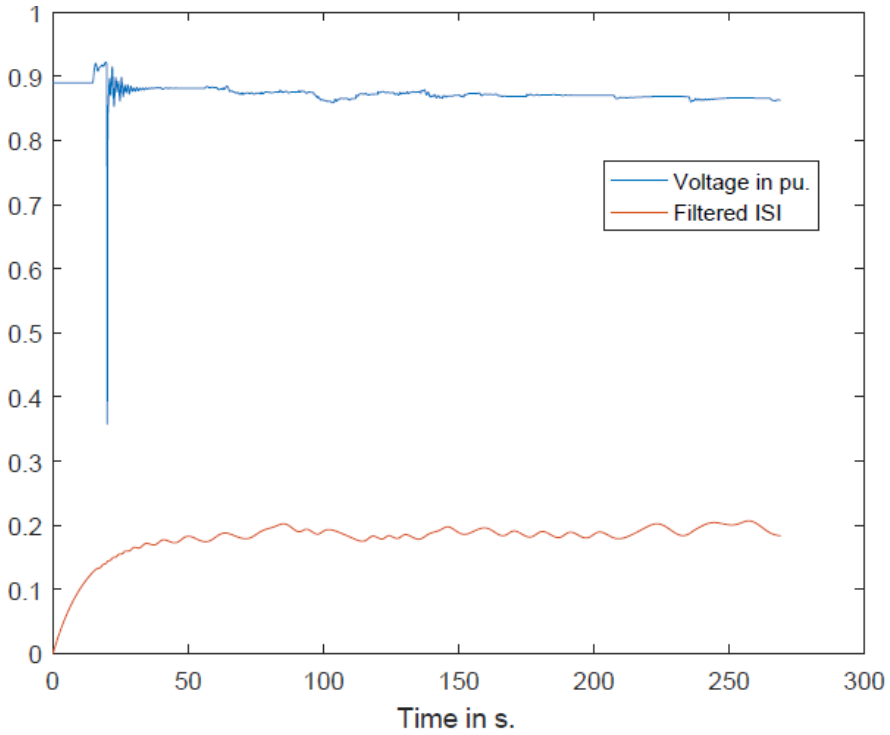

Figure 6.1: Case 1 with control model: Voltage and filtered ISI at bus 1041

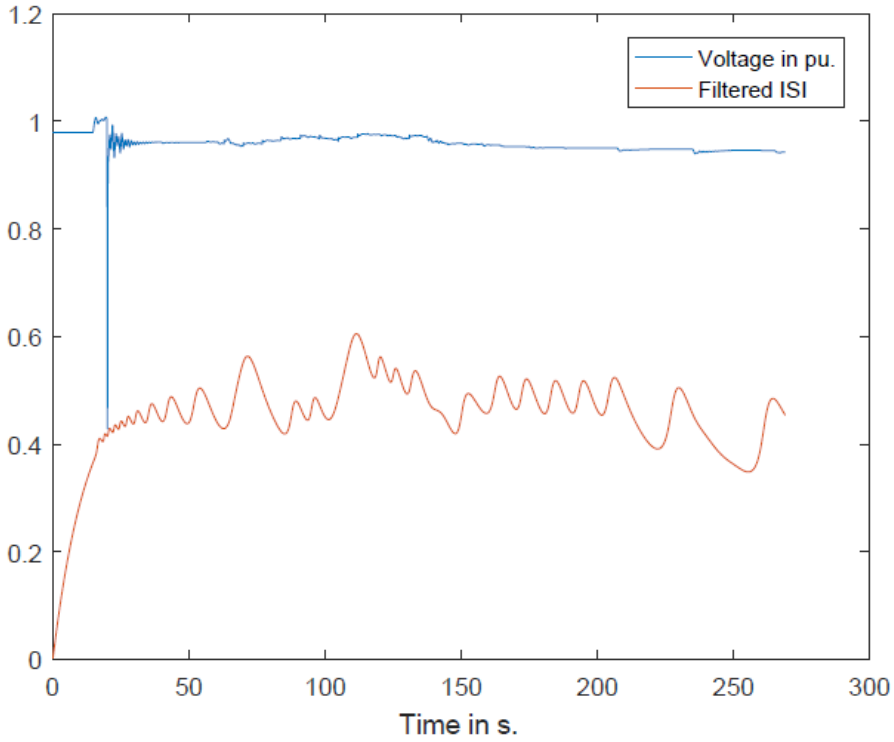

Figure 6.2: Case 1 with control model:Voltage and filtered ISI at bus 1044

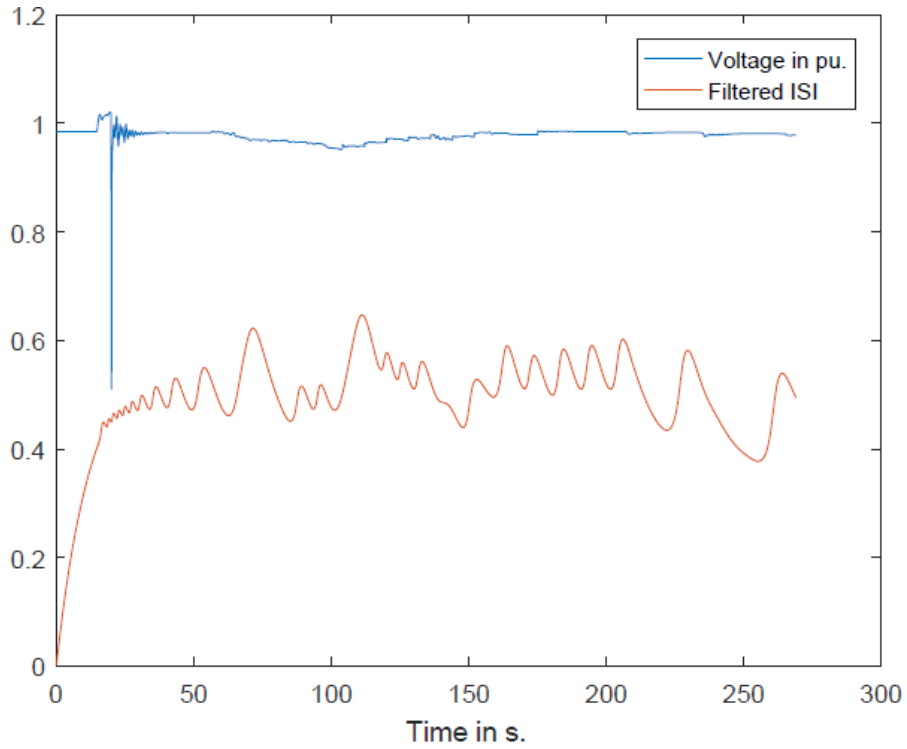

Figure 6.3: Case 1 with control model:Voltage and filtered ISI at bus 1045

Additionally, no major simulation events after 200s. are shown, i.e. no OEL timers

and no OLTC operations are activated. The increase of AVR setpoints is initiated when the ISI is greater than 0.4. This decision is based on pure observation of the oscillations and transients, and can't be considered entirely correct.

6.3.2 Case 2: Generator Tripping

As already mentioned, case 2 is more severe compared to case 1, with a shorter time course until collapse. It was shown that the voltage collapse occurred at around 115s. In this case, the AVR setpoints was not enough to prevent voltage collapse, and load-shedding was used. it can be seen from Fig. 6.4, 6.5 and 6.6 that the ISI indicators are stabilized after 250s. However the voltage levels went close to 1.4p.u, and decreased after reaching at 1.2 p.u and load-shedding was terminated.

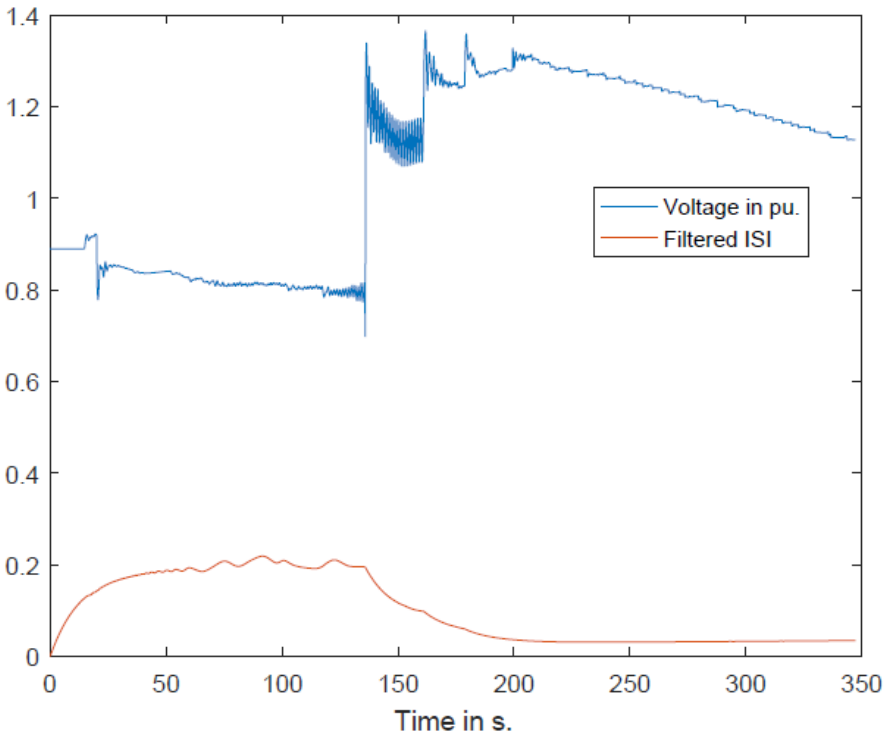

Figure 6.4: Case 2 with control model:Voltage and filtered ISI at bus 1041

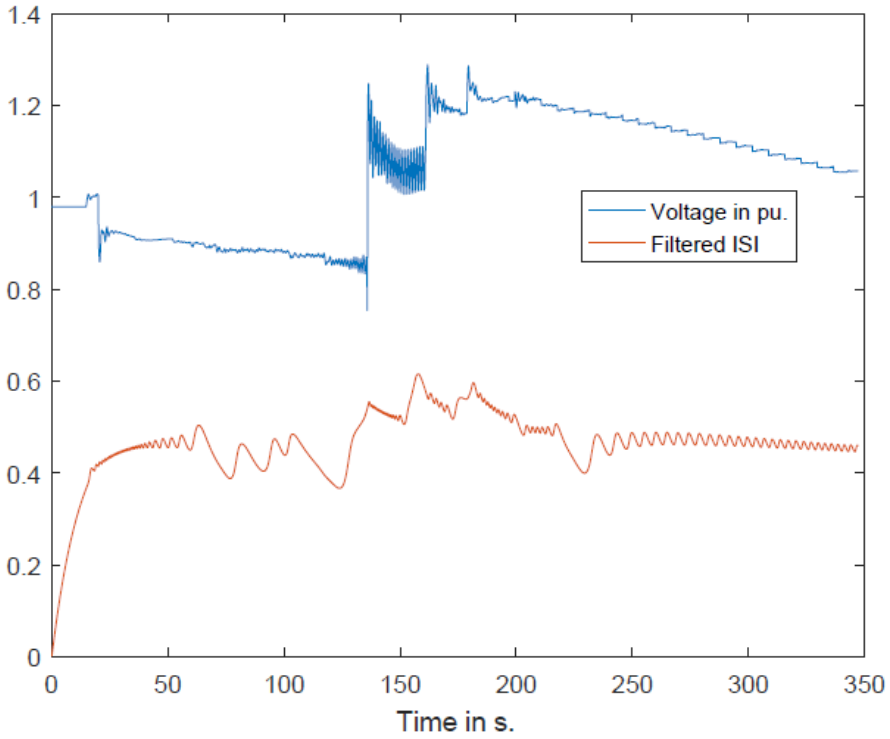

Figure 6.5: Case 2 with control model:Voltage and filtered ISI at bus 1044

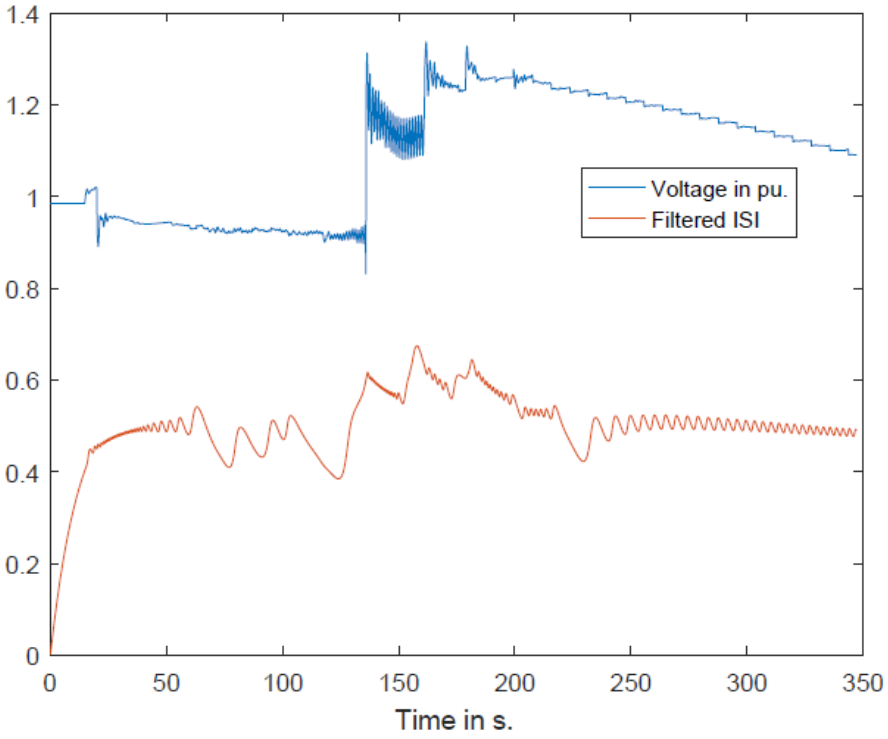

Figure 6.6: Case 2 with control model:Voltage and filtered ISI at bus 1045

Furthermore, the stability can be realized from the angle deceleration compared to

the simulations without the control model. The load-shedding is observable in Fig. 6.7 and 6.8. The loads have been shedded twice, which are located at buses 1044 and 1045. Every time the shedding is activated, 35% of the total loads are shedded. This may seem too severe, but it is important to remember that the tripped generator was producing 630 MW. To bring back the balance between load and generation, loads had to be reduced twice. The percentage value to shed loads with was based on trial and error. A low percentage led to the increase in the loads shedding, i.e. the loads were reduced too many times, and reached a value close to 0 p.u. On the other hand, a percentage higher than 35% tend to extensively reduce a load at one bus, or completely eliminate it. The goal is to shed loads at buses at or closest to the weak bus. Additionally, load-shedding should occur at couple of buses to improve the stability of the system. Therefore, 35% was decided to be the most acceptable value.

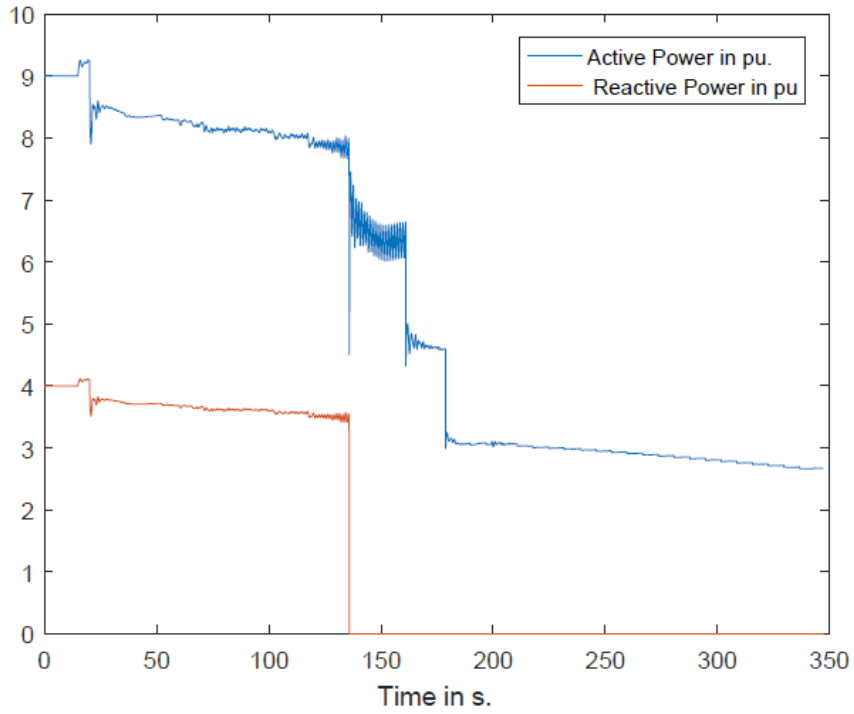

Figure 6.7: Case2 with control model: Active and reactive load power at bus 1044

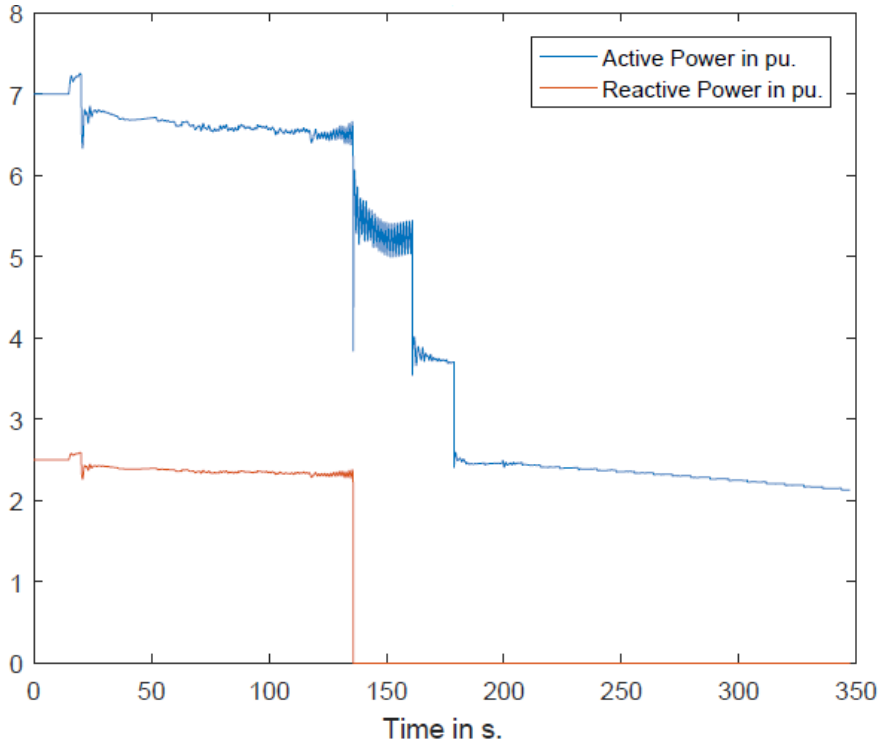

Figure 6.8: Case2 with control model: Active and reactive load power at bus 1045

6.4 Discussion

It was shown that the coordinated control proved to be able to prevent voltage collapse in both cases. In the first case, the increase of the cascaded increase of the AVR-setpoints prove to be enough to avoid voltage collapse, which was predictable because the equivalent transmission impedance from the bus of interest point of view has been increased, reflecting the weakening of the system. Also, the tripping of other generators due to under-voltage relays were avoided and the fixed shunt compensation available in the Nordic32 helped since an increase in voltage allowed a generation of additional reactive power since it is proportional to the square of the voltage. Furthermore, it has to be ideally done such that no over-voltage occurs at any bus and no OEL is activated

In the second case, load-shedding proved to be essential, although it should be considered as a last case scenario. The loads were shedded twice by 35% and located at the weakest buses 1044 and 1045. However, tripping an important generator that was producing 630MW proved to be severe, and load-shedding turned out to be the only solution for the time being. However, although voltage collapse was avoided, the voltage level at both buses 1044 and 1045 overshot and was above 1.2 p.u for a small period of time, which should have been avoided.

The filtered ISI indicator proved to be acceptable in detecting voltage instability,

but it is not enough to show all of the weaknesses in the system. In [6],the TPSI was highest at different buses, and loads were shedded at buses 42 and 46. It is needed to combine different indicators in order to observe all of the weaknesses in the system., and increase the robustness and efficiency of a coordinated control of different generators, which also could lead to an increase in the computational burden.

Finally, PSS/E is limited at some extent, especially that it is not possible to control the OLTC of the transformers from the built model. It was planned that the OLTC could be blocked for a certain period of time , or even reverse its operation.

7

Conclusion and Future Work

7.1 Conclusions

It was focused on using indicators based on the network admittance matrix, and continuous voltage and angle measurements. The motivation is also to compute the thevenin impedances as efficient and as fast as possible. Following the measurements and computations, the model is initiated based on different thresholds mentioned in chapter 3, and the implementation of the model in PSS/E was considered to be successful.

Furthermore, it can be concluded as follows:

- It was shown in the 10-bus system a good illustration of the impact of load increase on the indicators and voltage stability. The ISI and VCSIscc proved to give best result as opposed to the VCPI, which showed no change in case of load increase. However, it was decided that only the ISI will be used for the rest of the thesis.

- After evaluating the ISI in the Nordic32 system, the main observation is the oscillations and transients of the indicator due to angle acceleration from disturbances, like short-circuit fault or generator tripping. To overcome this challenge, a filter was used to dampen the oscillations, which can't be seen as a proper solution, but assumed to be acceptable for this thesis due to time constraint and scope of work limitations.

- The coordinated control method model was developed and implemented in PSS/E with the ISI and OEL signals as inputs. The method is based on first locating the weak buses, and then increasing the AVR set-points of the closest synchronous generators. If the OEL is activated, the AVR set-points of the next closest synchronous generators are increased, and so on. If the ISI is greater than 0.5, the AVR set-points are increased, but load is shedded if it is greater than 0.6. In the two cases that were presented in chapters 5 and 6, the model successfully prevented the voltage collapse, although it cannot be considered as a complete and a perfect system. Furthermore, the detection of voltage instability and actions taken to avoid voltage collapse were done

in real-time, considering that dynamic simulations are equivalent to real-time events. This is a selling point to the TSOs, who need fast actions to avoid blackouts, and reliable indicators that reflect the power system health and behaviour. This work is open to lots of investigations and optimization.

7.2 Future Work

There are different ways to continue and optimize the work. Suggestions are as follows:

- It is interesting to mention that there is a faster way to compute the thevenin impedances. From [8], the network admittance matrix can be re-arranged and only a matrix of non-voltage controllable buses can be inversed instead, i.e. the inverse of 21 by 21 matrix is enough to obtain the thevenin impedances instead of a 41 by 41 matrix. This way, different indicators can be used to optimize the detection and prevention of voltage instability and collapse. However, the matrices are now to become dynamic or varying. In case of an OEL activation, the generator is no more able to control the bus voltage, which consequently becomes a non=controllable bus or load bus. The size of the matrix will therefore decrease or increase depending on the situation. This is a big challenge for future work.

- Optimize the calculation of the ISI and study its oscillations and transients, and find a way to dampen them in a correct way that will reflect correctly the state of the system.

- It is advisable to find ways to control directly the OLTC, since they are catalysts to voltage instability. Additionally, other corrective actions such as series and shut FACTS devices can be implemented in the system to make it more robust.

- The model is designed only for the Nordic32, since it was assumed that the network admittance is known. The model is sought to be universalized and the network admittance should be built based on measurements.

- Instead of using indicators, it was sought to find ways to link PSS/E to optimization programs, such as GAMS. For example, after analyzing the situation in the system, a program can calculate the optimum reactive power dispatch, taking into account all of the limitations available in the system. Unfortunately, the focus was directed to computing the thevenin impedances, which was successful.

Bibliography

[1] P. Kundur. *Power system stability and control*. EPRI Power System Engineering Series, MacGraw-Hill Inc., 1994.

[2] Kenneth Walve. Nordic32a-a cigre test system for simulation of transient stability and long term dynamics. Technical report, Svenska Kraftnat, Rev-1994-03-01, 1993.

[3] L. Huang, J. Xu, Y. Sun, T. Cui, and F. Dai. Online monitoring of wide-area voltage stability based on short circuit capacity. In *2011 Asia-Pacific Power and Energy Engineering Conference*, pages 1–5, March 2011.

[4] P. Kundur, J. Paserba, V. Ajjarapu, G. Andersson, A. Bose, C. Canizares, N. Hatziargyriou, D. Hill, A. Stankovic, C. Taylor, T. Van Cutsem, and V. Vittal. Definition and classification of power system stability ieee/cigre joint task force on stability terms and definitions. *IEEE Transactions on Power Systems*, 19(3):1387–1401, Aug 2004.

[5] M. Begovic, B. Milosevic, and D. Novosel. A novel method for voltage instability protection. In *Proceedings of the 35th Annual Hawaii International Conference on System Sciences*, pages 802–811, Jan 2002.

[6] David Stenberg and Joakim Akesson. Development of a system protection model against voltage collapse in PSS/E. Master's thesis, Chalmers University of Technology, Department of Department of Energy and Environment, Gothenburg, Sweden, 2016.

[7] V. Balamourougan, T. S. Sidhu, and M. S. Sachdev. Technique for online prediction of voltage collapse. *IEE Proceedings - Generation, Transmission and Distribution*, 151(4):453–460, July 2004.

[8] S. Sommer and H. Jóhannsson. Real-time thevenin impedance computation. In *2013 IEEE PES Innovative Smart Grid Technologies Conference (ISGT)*, pages 1–6, Feb 2013.

[9] Siemens Power Technologies. Pss®e 34 application program interface, March 2015.

[10] Siemens Power Technologies. Pss®e 34 program operation manual, March 2015.

[11] Siemens Power Technologies. Pss®e 34 model library, March 2015.

[12] MathWorks. Matlab web page, March 2017.

[13] H. Saadat. *Power System Analysis*. PSA Publishing, 2010.

[14] F. Karbalaei, H. Soleymani, and S. Afsharnia. A comparison of voltage collapse proximity indicators. In *2010 Conference Proceedings IPEC*, pages 429–432, Oct 2010.

[15] V. Storvann, E. Hillberg, and K. Uhlen. Indicating and mitigating voltage collapse comparing voltage stability indicators. In *2012 3rd IEEE PES Innovative Smart Grid Technologies Europe (ISGT Europe)*, pages 1–8, Oct 2012.

[16] V. Storvann. Maintaining voltage stability, an analysis of voltage stability indicators and mitigating actions. diploma thesis, NTNU, Trondheim, June 2012.

[17] J. Zhang, M. Liu, Y. Yin, W. Lin, Q. Wang, L. Liu, and Y. Shao. A transient voltage stability index based on critical equivalent impedance. In *2014 International Conference on Power System Technology*, pages 25–29, Oct 2014.

[18] M. Bahadornejad and N. K. C. Nair. Intelligent control of on-load tap changing transformer. *IEEE Transactions on Smart Grid*, 5(5):2255–2263, Sept 2014.

[19] Narain G. Hingorani; Laszlo Gyugyi. *Understanding FACTS:Concepts and Technology of Flexible AC Transmission Systems*. Wiley-IEEE Press, 2000.

[20] H. Anton. *Elementary Linear Algebra*. John Wiley & Sons, 2010.

[21] Y. He, Y. Song, G. Du, and D. Zhang. Research of matrix inversion acceleration method. In *2009 International Conference on Computational Intelligence and Software Engineering*, pages 1–4, Dec 2009.

[22] Intel. Intel fortran web page, March 2017.

A

10-Bus System Simulation Model

A.1 Steady-state system data

The tested model is an example from [4]. The base frequency is 60Hz and the system base power is 100MVA. The data are follows:

- Transmission Line Data (in p.u on 100 MVA base)

Line	R	X	B
111-112	0.000	0.0040	0.000
112-113(each)	0.0015	0.0288	1.173
115-116	0.0010	0.0030	0.000

- Transformer Data (in p.u on 100 MVA base)

Transformer	R	X	Winding 1 Ratio
T1	0.000	0.0020	0.8857
T2	0.000	0.0045	0.8857
T3	0.000	0.0125	0.9024
T4	0.000	0.0030	1.0664
T5	0.000	0.0026	1.0800
T6	0.000	0.0010	0.9937

- Transformer T6 OLTC parameters

Controlled Bus	Bus 117
Control Mode	Voltage control
Auto adjust taps	Yes
Tap positions	33
R1max(p.u.)	1.1
R1min(p.u.)	0.9
Vmax(p.u.)	1.1
Vmin(p.u.)	0.9

- Shunt capacitors data

Bus	MVAr
113	800
114	600
115	700

- Generation data

Generator Bus and Name	Machine power base(MVA)	Scheduled active power (MW)	X_{source}(p.u.)	$V_{nominal}$(p.u.)
Bus 211 G1	1400	1157	0.215	1.01
Bus 212 G2	2200	1736	0.215	0.9646
Bus 213 G3 (Slack Bus)	6000	-	1	0.98

A.2 Dynamic system data

G1 and G2 GENROU Dynamic Model	'GENROU' 1 4.1 0.03 0.56 0.0620 2.09 0 2.07 1.99 0.28 0.49 0.215 0.155 0.03 0.2 '
G3 GENCLS	'GENCLS' 1 0 0/
G1 SEXS Dynamic Model	'SEXS' 1 0.2 10 50 0 0 4.5/
G2 SEXS Dynamic Model	'SEXS' 1 0.2 10 50 0 0 4.5/
G1 MAXEX2 Dynamic Model	'MAXEX2' 1 4 1.02 60 1.04 40 1.05 10 1 0.002 -1 /
T6 OLTC Dynamic Model	116 'OLTC1T' 117 1 30 0 5/

B

Coordinated control method model

Table B.1: Model ICONs:VOLMAG function

ICONs	Value	Description
F	41	Bus Index for VOLMAG function
F+1	42	Bus Index for VOLMAG function
F+2	43	Bus Index for VOLMAG function
F+3	46	Bus Index for VOLMAG function
F+4	47	Bus Index for VOLMAG function
F+5	51	Bus Index for VOLMAG function
F+6	61	Bus Index for VOLMAG function
F+7	62	Bus Index for VOLMAG function
F+8	63	Bus Index for VOLMAG function
F+9	1011	Bus Index for VOLMAG function
F+10	1041	Bus Index for VOLMAG function
F+11	1044	Bus Index for VOLMAG function
F+12	1045	Bus Index for VOLMAG function
F+13	2031	Bus Index for VOLMAG function
F+14	4022	Bus Index for VOLMAG function
F+15	4032	Bus Index for VOLMAG function
F+16	4043	Bus Index for VOLMAG function
F+17	4044	Bus Index for VOLMAG function
F+18	4045	Bus Index for VOLMAG function
F+19	4046	Bus Index for VOLMAG function
F+20	4061	Bus Index for VOLMAG function
F+21	1012	Bus Index for VOLMAG function
F+22	1013	Bus Index for VOLMAG function
F+23	1014	Bus Index for VOLMAG function
F+24	1021	Bus Index for VOLMAG function
F+25	1022	Bus Index for VOLMAG function
F+26	1042	Bus Index for VOLMAG function
F+27	1043	Bus Index for VOLMAG function

Table B.2: Model ICONs : VOLMAG function (Continued)

ICONs	Value	Description
F+28	2032	Bus Index for VOLMAG function
F+29	4012	Bus Index for VOLMAG function
F+30	4021	Bus Index for VOLMAG function
F+31	4031	Bus Index for VOLMAG function
F+32	4041	Bus Index for VOLMAG function
F+33	4042	Bus Index for VOLMAG function
F+34	4047	Bus Index for VOLMAG function
F+35	4051	Bus Index for VOLMAG function
F+36	4062	Bus Index for VOLMAG function
F+37	4063	Bus Index for VOLMAG function
F+38	4071	Bus Index for VOLMAG function
F+39	4072	Bus Index for VOLMAG function
F+40	4011	Bus Index for VOLMAG function

Table B.3: Model ICONs : FLOW function

ICONs	Value	Description
F+41	1044	Bus Index for FLOW function
F+42	4044	Bus Index for FLOW function
F+43	'1'	Branch Index for FLOW function
F+44	1045	Bus Index for FLOW function
F+45	4045	Bus Index for FLOW function
F+46	'1'	Branch Index for FLOW function
F+47	4041	Bus Index for FLOW function
F+48	41	Bus Index for FLOW function
F+49	'1'	Branch Index for FLOW function
F+50	4042	Bus Index for FLOW function
F+51	42	Bus Index for FLOW function
F+52	'1'	Branch Index for FLOW function
F+53	4043	Bus Index for FLOW function
F+54	43	Bus Index for FLOW function
F+55	'1'	Branch Index for FLOW function
F+56	4046	Bus Index for FLOW function
F+57	46	Bus Index for FLOW function
F+58	'1'	Branch Index for FLOW function
F+59	4047	Bus Index for FLOW function
F+60	47	Bus Index for FLOW function
F+61	'1'	Branch Index for FLOW function
F+62	4051	Bus Index for FLOW function
F+63	51	Bus Index for FLOW function
F+64	'1'	Branch Index for FLOW function
F+65	4061	Bus Index for FLOW function
F+66	61	Bus Index for FLOW function
F+67	'1'	Branch Index for FLOW function
F+68	4062	Bus Index for FLOW function
F+69	62	Bus Index for FLOW function
F+70	'1'	Branch Index for FLOW function
F+71	4063	Bus Index for FLOW function
F+72	63	Bus Index for FLOW function
F+73	'1'	Branch Index for FLOW function

Table B.4: Model CONs

CONs	Value	Description
G	4π	ISIs filter time constant
G+1	5	AVR set-point increase rate (%)
G+2	2.9579	Generator rated field current (p.u.)
G+3	3.6618	Generator rated field current (p.u.)
G+4	1.8991	Generator rated field current (p.u.)
G+5	35	Load shedding step (%)

Table B.5: Model STATEs

STATEs	Value	Description
S		ISI filter STATE for bus 41
S+1		ISI filter STATE for bus 42
S+2		ISI filter STATE for bus 43
S+3		ISI filter STATE for bus 46
S+4		ISI filter STATE for bus 47
S+5		ISI filter STATE for bus 51
S+6		ISI filter STATE for bus 61
S+7		ISI filter STATE for bus 62
S+8		ISI filter STATE for bus 63
S+9		ISI filter STATE for bus 1011
S+10		ISI filter STATE for bus 1041
S+11		ISI filter STATE for bus 1044
S+12		ISI filter STATE for bus 1045
S+13		ISI filter STATE for bus 2031
S+14		ISI filter STATE for bus 4022
S+15		ISI filter STATE for bus 4032
S+16		ISI filter STATE for bus 4043
S+17		ISI filter STATE for bus 4044
S+18		ISI filter STATE for bus 4045
S+19		ISI filter STATE for bus 4046
S+20		ISI filter STATE for bus 4061

Table B.6: Model VARs

VARs	Value	description
D		Internal voltage magnitude variable
D+1		Internal voltage angle variable
D+2		Internal active power variable (MW)
D+3		Internal reactive power variable (MVAr)
D+4		Internal reactive power variable (MVA)
D+5		Filtered ISI for Bus 41
D+6		Filtered ISI for Bus 42
D+7		Filtered ISI for Bus 43
D+8		Filtered ISI for Bus 46
D+9		Filtered ISI for Bus 47
D+10		Filtered ISI for Bus 51
D+11		Filtered ISI for Bus 61
D+12		Filtered ISI for Bus 62
D+13		Filtered ISI for Bus 63
D+14		Filtered ISI for Bus 1011
D+15		Filtered ISI for Bus 1041
D+16		Filtered ISI for Bus 1044
D+17		Filtered ISI for Bus 1045
D+18		Filtered ISI for Bus 2031
D+19		Filtered ISI for Bus 4022
D+20		Filtered ISI for Bus 4032
D+21		Filtered ISI for Bus 4043
D+22		Filtered ISI for Bus 4044
D+23		Filtered ISI for Bus 4045
D+24		Filtered ISI for Bus 4046
D+25		Filtered ISI for Bus 4047
D+27		Bus constant power load (Output Channel)
D+28		Bus constant admittance load (Output Channel)
D+29		Bus constant current load (Output Channel)
D+30		Internal load shed timer
D+31		Internal load shed timer
D+32		Internal load shed timer

In order to include the model in the .dyr file, the following should be written:

1, 'USRMSC', 'CORE',512,0,74,6,21,33,ICON(F)-ICON(F+73),CON(G)-CON(G+5)/

Then, include CORE.dll in simulation. It is important to know that all listed ICONs and CONs are included in the .dyr file. Additionally, the model CORE.dll needs to be imported to PSS/E when running the simulation. Since Python is used, the following command is needed: psspy.addmodellibrary(r"Z:\Pathname \CORE.dll").

C

Coordinated control method model partial Fortran Code

The model was built using Intel Visual Fortran 2005 (Fortran), with the format .f90. It is compile using PSS/E 34 Environment manager.

After writing the the model using Fortran, The output folder and name of the model are chosen, and then the .f90 file is added under 'User Model Fortran Source File'. The compilation is then run by pressing on 'Compile+Create DLL'.

The model is specific to the Nordic32 since the numbers of ICONs must be listed, although it was planned at first to universalize the model. Furthermore, the network admittance matrix is known and written in the model. However, changes can occur in the matrix from a change in the transformers on-load tap-changers or activation of the OEL of generators.

Due to the length of the written code (54 pages), only partial codes will be shown in the next page, related to matrix computation and part of the coordinated control method.

CORE_NORDIC_3.f90Programmer's Notepad - CORE_NORDIC_3.f90

```
1815
1816        subroutine inverse (Y,invY,n)
       !Function to obtain Inverse of any invertible Matrix by factorizing and
       solving
1817              complex,dimension(n,n) :: Y, invY
1818              complex,dimension(n,n) ::L, U
1819              complex,dimension(n) ::b, t, x
1820              complex ::coeff
1821              integer :: n,k,i,j
1822           ! step 1: forward elimination
1823
1824                L=CMPLX(0.0D0,0.0D0)
1825                U=CMPLX(0.0D0,0.0D0)
1826                b=CMPLX(0.0D0,0.0D0)
1827           do k=1, n-1
1828              do i=k+1,n
1829                 coeff=Y(i,k)/Y(k,k)
1830                 L(i,k) = coeff
1831                 do j=k+1,n
1832                    Y(i,j) = Y(i,j)-coeff*Y(k,j)
1833                 end do
1834              end do
1835           end do
1836
1837           ! Step 2: prepare L and U matrices
1838           ! L matrix is a matrix of the elimination coefficient and the diagonal
       elements are 1.0+j0
1839           do i=1,n
1840             L(i,i) = cmplx(1,0)
1841           end do
1842           ! U matrix is the upper triangular part of A
1843           do j=1,n
1844             do i=1,j
1845               U(i,j) = Y(i,j)
1846             end do
1847           end do
1848
1849           ! Step 3: compute columns of the inverse matrix C
1850           do k=1,n
1851             b(k)=cmplx(1,0)
1852             t(1) = b(1)
1853           ! Step 3a: Solve Lt=b using the forward substitution
1854             do i=2,n
1855               t(i)=b(i)
1856               do j=1,i-1
1857                 t(i) = t(i) - L(i,j)*t(j)
1858               end do
1859             end do
1860           ! Step 3b: Solve Ux=t using the back substitution
1861             x(n)=t(n)/U(n,n)
1862             do i = n-1,1,-1
1863               do j=n,i+1,-1
1864                 x(i)=(t(i)-U(i,j)*x(j))/U(i,i)
1865               end do
1866             end do
1867           ! Step 3c: fill the solutions x(n) into column k of C
1868             do i=1,n
1869               invY(i,k) = x(i)
1870             end do
```

CORE_NORDIC_3.f90Page 53, 01-Jun-17 - 3:36:28 PM

Figure C.1: Inverse Matrix Function, part 1

CORE_NORDIC_3.f90Programmer's Notepad - CORE_NORDIC_3.f90

```
1871            b(k)=cmplx(0,0)
1872          end do
1873          end subroutine inverse
1874
1875
1876
1877
1878
1879
1880
1881
1882
1883
1884
1885
1886
1887
1888
1889
1890
1891
1892
1893
1894
1895
1896
1897
1898
1899
1900
```

CORE_NORDIC_3.f90Page 54, 01-Jun-17 - 3:36:28 PM

Figure C.2: Inverse Matrix Function, part 2

CORE_NORDIC_3.f90Programmer's Notepad - CORE_NORDIC_3.f90

```
      GENFIELD(15)<(CON(G+3)*1)).AND.(VREFCHECK(15)==0)))THEN
 861                          VREF(GENINDEXARRAY(15))=GENVREF(15)*((CON(G+1)/100)+1
      )    !AVR set point increase
 862                          VREFCHECK(15)=1
                                                  !Set check so the current
      generator will not increase AVR set point again
 863                          WRITE ( ITERM, * )
 864                          WRITE ( ITERM, * )
 865                          WRITE ( ITERM, * ) 'NORDIC32 SYSTEM COORDINATED
      CONTROL METHOD'
 866                          WRITE ( ITERM, * ) 'VREF INCREASE AT BUS' , GENERATOR
      (15), 'by', CON(G+1), '%', 'IN AREA 8'
 867                          WRITE ( ITERM, * )
 868                          WRITE ( ITERM, * )
 869                        ELSEIF(((GENOEL(16)==0).AND.(GENVREF(16)<1.1).AND.(
      GENFIELD(16)<(CON(G+3)*1)).AND.(VREFCHECK(16)==0)))THEN
 870                          VREF(GENINDEXARRAY(16))=GENVREF(16)*((CON(G+1)/100)+1
      )    !AVR set point increase
 871                          VREFCHECK(16)=1
                                                  !Set check so the current
      generator will not increase AVR set point again
 872                          WRITE ( ITERM, * )
 873                          WRITE ( ITERM, * )
 874                          WRITE ( ITERM, * ) 'NORDIC32 SYSTEM COORDINATED
      CONTROL METHOD'
 875                          WRITE ( ITERM, * ) 'VREF INCREASE AT BUS' , GENERATOR
      (16), 'by', CON(G+1), '%', 'IN AREA 8'
 876                          WRITE ( ITERM, * )
 877                          WRITE ( ITERM, * )
 878                        ELSEIF(((GENOEL(17)==0).AND.(GENVREF(17)<1.1).AND.(
      GENFIELD(17)<(CON(G+3)*1)).AND.(VREFCHECK(17)==0)))THEN
 879                          VREF(GENINDEXARRAY(17))=GENVREF(17)*((CON(G+1)/100)+1
      )    !AVR set point increase
 880                          VREFCHECK(17)=1
                                                  !Set check so the current
      generator will not increase AVR set point again
 881                          WRITE ( ITERM, * )
 882                          WRITE ( ITERM, * )
 883                          WRITE ( ITERM, * ) 'NORDIC32 SYSTEM COORDINATED
      CONTROL METHOD'
 884                          WRITE ( ITERM, * ) 'VREF INCREASE AT BUS' , GENERATOR
      (17), 'by', CON(G+1), '%', 'IN AREA 8'
 885                          WRITE ( ITERM, * )
 886                          WRITE ( ITERM, * )
                                                          !IN AREAS 5 and 8
 887                        ELSE
 888                          write(24,*) 'Cant proceed any longer'
 889                        END IF
 890     END IF               !AREA 1 END
 891
 892
 893              IF (STATE(S+13) .ge. 0.4 .or. STATE(S+15) .eq. 0.4) then
                                                        !AREA 3
 894
                  !Increase AVR set points when an OEL is activated in AREA 8
 895                        IF(((GENOEL(8)==0).AND.(GENVREF(8)<1.1).AND.(GENFIELD(8
      )<(CON(G+4)*1)).AND.(VREFCHECK(8)==0)))THEN
 896                          VREF(GENINDEXARRAY(8))=GENVREF(8)*((CON(G+1)/100)+1)
          !AVR set point increase
```

CORE_NORDIC_3.f90Page 27, 01-Jun-17 - 3:36:28 PM

Figure C.3: Coordinated Control Algorithm first example

CORE_NORDIC_3.f90Programmer's Notepad - CORE_NORDIC_3.f90

```
897                             VREFCHECK(8)=1
                                                    !Set check so the current
      generator will not increase AVR set point again
898                             WRITE ( ITERM, * )
899                             WRITE ( ITERM, * )
900                             WRITE ( ITERM, * ) 'NORDIC32 SYSTEM COORDINATED
      CONTROL METHOD'
901                             WRITE ( ITERM, * ) 'VREF INCREASE AT BUS' , GENERATOR
      (8), 'by', CON(G+1), '%' , 'IN AREA 3'
902                             WRITE ( ITERM, * )
903                             WRITE ( ITERM, * )
904                           ELSEIF(((GENOEL(11)==0).AND.(GENVREF(11)<1.1).AND.(
      GENFIELD(11)<(CON(G+4)*1)).AND.(VREFCHECK(11)==0)))THEN
905                             VREF(GENINDEXARRAY(11))=GENVREF(11)*((CON(G+1)/100)+1
      )    !AVR set point increase
906                             VREFCHECK(11)=1
                                                    !Set check so the current
      generator will not increase AVR set point again
907                             WRITE ( ITERM, * )
908                             WRITE ( ITERM, * )
909                             WRITE ( ITERM, * ) 'NORDIC32 SYSTEM COORDINATED
      CONTROL METHOD'
910                             WRITE ( ITERM, * ) 'VREF INCREASE AT BUS' , GENERATOR
      (11), 'by', CON(G+1), '%', 'IN AREA 3'
911                             WRITE ( ITERM, * )
912                             WRITE ( ITERM, * )
913                           ELSEIF(((GENOEL(4)==0).AND.(GENVREF(4)<1.1).AND.(
      GENFIELD(1)<(CON(G+4)*1)).AND.(VREFCHECK(4)==0)))THEN
914                             VREF(GENINDEXARRAY(4))=GENVREF(4)*((CON(G+1)/100)+1)
          !AVR set point increase
915                             VREFCHECK(4)=1
                                                    !Set check so the current
      generator will not increase AVR set point again
916                             WRITE ( ITERM, * )
917                             WRITE ( ITERM, * )
918                             WRITE ( ITERM, * ) 'NORDIC32 SYSTEM COORDINATED
      CONTROL METHOD'
919                             WRITE ( ITERM, * ) 'VREF INCREASE AT BUS' , GENERATOR
      (4), 'by', CON(G+1), '%' , 'IN AREA 2'
920                             WRITE ( ITERM, * )
921                             WRITE ( ITERM, * )
922                           ELSEIF(((GENOEL(5)==0).AND.(GENVREF(5)<1.1).AND.(
      GENFIELD(5)<(CON(G+3)*1)).AND.(VREFCHECK(5)==0)))THEN
923                             VREF(GENINDEXARRAY(5))=GENVREF(5)*((CON(G+1)/100)+1)
          !AVR set point increase
924                             VREFCHECK(5)=1
                                                    !Set check so the current
      generator will not increase AVR set point again
925                             WRITE ( ITERM, * )
926                             WRITE ( ITERM, * )
927                             WRITE ( ITERM, * ) 'NORDIC32 SYSTEM COORDINATED
      CONTROL METHOD'
928                             WRITE ( ITERM, * ) 'VREF INCREASE AT BUS' , GENERATOR
      (5), 'by', CON(G+1), '%', 'IN AREA 2'
929                             WRITE ( ITERM, * )
930                             WRITE ( ITERM, * )
931                           ELSEIF(((GENOEL(10)==0).AND.(GENVREF(10)<1.1).AND.(
      GENFIELD(10)<(CON(G+4)*1)).AND.(VREFCHECK(10)==0)))THEN
932                             VREF(GENINDEXARRAY(10))=GENVREF(10)*((CON(G+1)/100)+1
```

CORE_NORDIC_3.f90Page 28, 01-Jun-17 - 3:36:28 PM

Figure C.4: Coordinated Control Algorithm second example

D

PSCC 2018 paper

A system protection model against voltage collapse based on real-time impedance stability index

Ahmad Sultan Esreb
Department of Electrical Engineering
Chalmers University of Technology
41296 Gothenburg, Sweden
Email: esreb@student.chalmers.se

Le Anh Tuan
Department of Electrical Engineering
Chalmers University of Technology
41296 Gothenburg, Sweden
Email: tuan.le@chalmers.se

***Abstract*—This paper presents a novel method to prevent voltage collapses in power systems based on real-time calculation of Impedance Stability Index (ISI). In this method, the ISI can be computed very fast by inverting the network admittance matrix through LU-Decomposition. The real-time ISI calculation is implemented in system protection model which is developed as a "users-written model" in PSS/E. The model is able to detect the possibility of a prominent voltage collapse and to perform timely control actions to avoid voltage collapse. The control actions that have been considered include modifications of set-points of automatic voltage regulators (AVRs) of synchronous generators and load shedding. A case study has been carried out using the Nordic-32 test system. The study results have shown that the model performs very well in term of both performance of calculation of ISI and the successful deployment of control measures to prevent voltage collapses.**

***Keywords*—Voltage collapse, System protection model, Impedance Stability Index (ISI), Load-shedding, Over-excitation Limiter (OEL), Automatic voltage regulator (AVR).**

I. Introduction

In power systems of today, more inverter-based renewable generation technologies [1], which own different and faster dynamic responses as compared those of conventional synchronous generators, are being integrated. This leads to a high need to develop new methods to faster and more efficiently assessing system stability which are needed if we are to deliver a secured system operation in the future. Different studies were conducted regarding computation of voltage instability/collapse indicators in both steady-state and real-time [2], [3],[4]. In [3], it was shown how the computation of Impedance Stability Index (ISI) and VSCI (voltage stability index based on short circuit capacity) were used to indicate and mitigate voltage instability. However, the main challenge in the computation of these indicators stem from the heavy demand for computation of the Thevenin impedances. In [4], the Thevenin impedances at only voltage-controllable buses, such as generators, were computed in real-time in an efficient way. This paper aims to develop a system protection scheme against voltage collapse based on the ISI indicator computed in real-time, which represents one main challenge since the thevenin impedances must be computed as fast as possible.

The motivations behind real-time calculation of voltage stability index are to help the system operator to:

- Obtain good information on the power system conditions
- Act as fast as possible to increase the chances to save the system
- Minimize the amount of loads to be shed.

The increased knowledge on real-time assessment of voltage stability and protection will allow the transmission system to be more intelligent, to operate more efficiently and the energy resources in the system can be used in the most economical way.

The principle of the system protection model is that, when the ISI is found to be close to a certain threshold in real-time, i.e. indicating that the system is close to a voltage collapse, the system protection scheme (SPS) will be activated to send the control signals to various control devices in the system, such as synchronous generators reactive power re-dispatch, set-points of On-Load Tap Changer (OLTC) transformers, controls of HVDC/FACTS[5] and power-electronic converters of renewable generation, modification of distance-relay settings, under voltage load shedding, etc. The activation of Over-Excitation Limiters (OELs) of synchronous generators, voltage measurements from OLTC transformers can also be used as input signals in the SPS.

The main challenge is when, from where, and how many changes that should be made to the controllers of the devices that would be sufficient to save the system and drive the system back to the secure condition from collapse. However, the first task is how to identify a voltage collapse, and how to detect if a system is converging towards it.

This paper aims to develop a coordinated control method of different power devices (AVR set-points and Load-shedding) in order to be able to prevent voltage collapse as fast as possible based on Impedance stability index (ISI). It will be assumed that voltages, currents and phases are measured in real-time as fast as possible, and the simulations will be considered accurate enough that the control method can be used in real life projects or power systems. Additionally, it will be assumed that the power systems, including generators, transformers, FACTS devices and loads, are accurately modeled on PSS/E, and study of transients and oscillations are out-of-scope.

The main contributions of the paper can be summarized as follows:

- Development of a method for very fast calculation of impedance stability index based on the LU-decomposition method [6].

- Development of a user-defined model in Power System Simulator for Engineering (PSS/E)[7][8][9] using Fortran [10] for testing of algorithms for voltage collapse prevention methods. This model is able to calculate the ISI in real-time as opposed to the static calculation, and then perform control actions accordingly. The computation of the ISI was tested on the Nordic-32 test system [11]. The results are analyzed using Matlab [12].
- The developed model was tested using the Nordic 32-bus system. The tests have shown that the method works well in term of both performance of calculation of ISI and the successful deployment of control methods to prevent voltage collapses.

The rest of the paper is organized as follows: Section II presents the computation method of ISI and its evaluation. Section III presents the proposed system protection model based on real-time calculation of ISI. Section IV presents the results of a case study using the Nordic-32 test system when applying the system protection model to prevent voltage collapse. Finally, the main conclusions from the study are made in Section V.

II. Computation of Impedance Stability Index (ISI) based on LU decomposition and Its Evaluation

A. Impedance stability index (ISI)

This index is based on the maximum power transfer in a circuit. Fig. 1 shows the thevenin equivalent circuit.

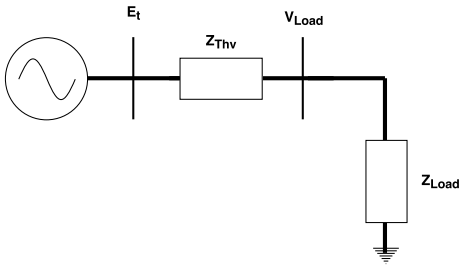

Figure 1: Thevenin equivalent circuit

From Fig.1 and using voltage divider rule and ohm's law, the load voltage and current can be calculated as:

$$V_{Load} = E_t \frac{Z_{Load}}{Z_{Load} + Z_{Thv}} \tag{1}$$

$$I = \frac{E_t}{Z_{Load} + Z_{Thv}} \tag{2}$$

Using eq.(1) and eq.(2), the power dissipated by the load is determined as follows:

$$P_{Load} = V_{Load} I \cos\delta = E_t^2 \frac{Z_{Load}}{(Z_{Load} + Z_{Thv})^2} \cos\delta \tag{3}$$

From eq.(3), the maximum power transfer occurs when $\frac{dP_{Load}}{Z_{Thv}}$ = 0. The solution will be Z_{Load} =Z_{Thv} [13], which implies that voltage instability critical point is reached when ISI=1

$$ISI = \frac{|Z_{Thv}|}{|Z_{Load}|} = 1 \tag{4}$$

If ISI < 1, the voltage is considered stable, and unstable otherwise.

One way to compute the ISI in real time is to invert the network admittance matrix in order to obtain the equivalent thevenin impedance of a bus of interest. To get the equivalent load impedance, the fastest way is to first compute the equivalent load power from eq.(5), then obtain its inverse, which is multiplied by the voltage at the bus.

$$S_k = V_k I_k^* = V_k [\sum_{j=1}^{N} Y_{kj} V_j]^* \tag{5}$$

B. Inversion of Network Admittance Matrix

The presented algorithm to obtain the thevenin impedance is by inverting the admittance matrix. For any n-bus system, the network admittance matrix can be represented by an $n \times n$ matrix as follows:

$$\mathrm{Y} = \begin{bmatrix} y_{11} & y_{12} & y_{13} & \cdots & y_{1n} \\ y_{21} & y_{22} & y_{23} & \cdots & y_{2n} \\ \cdots & \cdots & \cdots & \cdots & \cdots \\ y_{n1} & y_{n2} & y_{n3} & \cdots & y_{nn} \end{bmatrix}$$

The thevenin impedances for all buses are the diagonal elements of the matrix Z = Y^{-1}. it is important to note that the network admittance matrix must be updated based on different changes that occur in a power system, such as adding the impedance of the generator X_d in case an OEL is activated, or the turn ratio of an OLTC transformer changes.

The matrix can be inverted by computing the determinants. If Y is a 2×2 matrix such that

$$\mathrm{Y} = \begin{bmatrix} y_{11} & y_{12} \\ y_{21} & y_{22} \end{bmatrix}$$

$$\text{Then } \mathrm{Z} = \mathrm{Y}^{-1} = \frac{1}{\det(\mathrm{A})} \begin{bmatrix} y_{22} & -y_{12} \\ -y_{21} & y_{11} \end{bmatrix}$$

where A = y_{11} y_{22} - y_{21} y_{12} However, this method becomes too exhaustive as the size of matrix increases. There is a better and much faster way, based on simple 'solving' algorithm and factorization, also called 'LU' decomposition.[6] The motivation behind the factorization is due to the sparsity of the admittance matrix in any power systems , i.e. the matrix will contain many zero elements. Furthermore, for any n-bus system, the matrix will always be a square one with non-zero diagonal elements.

1) LU Decomposition: The first step in obtaining the inverse of the admittance matrix is to decompose into a lower and upper triangular matrix, such that:

[Y]=[L][U], where L is the lower triangular matrix and U is the upper triangular matrix, where:

$$L=\begin{bmatrix} 1 & 0 & 0 & \dots & 0 \\ l_{21} & 1 & 0 & \dots & 0 \\ l_{31} & l_{32} & 1 & \dots & 0 \\ \dots & \dots & \dots & \dots & \dots \\ l_{n1} & l_{n2} & l_{n3} & \dots & 1 \end{bmatrix}$$

$$U=\begin{bmatrix} u_{11} & u_{12} & u_{13} & \dots & u_{1n} \\ 0 & u_{22} & u_{23} & \dots & u_{2n} \\ 0 & 0 & u_{33} & \dots & u_{2n} \\ \dots & \dots & \dots & \dots & \dots \\ 0 & 0 & 0 & \dots & u_{nn} \end{bmatrix}$$

It is important to notice that the diagonal elements of [L] are equal to 1 and the LU decomposition is feasible only for square invertible matrices with non-zero diagonal elements. Fortunately, in any real-life n-bus system, the admittance matrix will always be square, invertible or non-singular, with non-zero diagonal elements.

Since [L][U]=[Y], and using matrix multiplication, it is clear that the first row elements of [U] can be determined straight forwardly, such that: u_{11}=y_{11}, u_{12}=y_{12},..., u_{1n}=y_{1n} because only the first element in the first row of matrix [L] is non-zero and equals to 1. Furthermore, the elements of [L] and [U] can easily be determined using the same concept by iteration and by solving. For example, $l_{21} \times u_{11} = y_{21}$, but $u_{11} = y_{11}$, then $l_{21} = \frac{y_{21}}{y_{11}}$. It is good to notice that the equation has only one unknown in it, and other quantities that were already found in the previous equations. This pattern continues until the last row. Similar factorization techniques exist, but the LU decomposition is acceptable for the thesis.

2) Solve: After obtaining L and U, the next step is to solve the a set of equations [Y][X]=[C], where [X] is the a matrix of unknowns to be determined.

Since [Y] = [L][U], then: [L][U][X]=[C].

Multiplying both sides by $[L]^{-1}$, we get: $[L]^{-1}[L][U][X]=[L]^{-1}[C]$ Since $[L]^{-1}[L]$ = [I], where [I] is the identity matrix or

$$I=\begin{bmatrix} 1 & 0 & 0 & \dots & 0 \\ 0 & 1 & 0 & \dots & 0 \\ 0 & 0 & 1 & \dots & 0 \\ \dots & \dots & \dots & \dots & \dots \\ 0 & 0 & 0 & \dots & 1 \end{bmatrix}$$

then [I][U][X]=$[L]^{-1}$[C] and [U][X]=$[L]^{-1}$[C]. Let $[L]^{-1}$[C]=[T],we get:

$$[L][T] = [C] \tag{6}$$

and

$$[U][X] = [T]. \tag{7}$$

Therefore, we can solve first eq.(6) or [T], and then use eq.(7) to calculate [X].

C. Evaluation of ISI

The algorithm for computing the ISI is evaluated in the Nordic-32 test system. The single line diagram is built based on a 1995 CIGRE report [11] and the loads are considered to be moderate and will be completely converted into constant current loads for simplicity as shown in Fig. 2.

A simulation study is done by tripping a generator at bus 4042. In order to evaluate the indicator in the Nordic32 test system, data were obtained and processed in Matlab to calculate the indicators. The simulation was run for a duration of 500s. At 20s, the disturbance was applied, leading to the activation of OEL, OLTC, distance relays and under-voltage relays during the simulation.

In fact, tripping the generator at bus 4042 led to the activation of OELs and OLTCs to bring back the voltages to the acceptable ranges. However, the disturbance is harsh due to the fact that an unbalance between load and generation was created, and the tripped generator was considered to be a big one. The voltage collapse occurs at 115s. and transients are visible starting at 80s.

The case showed an expected performance of the ISI indicators, and the trends were quite similar and showed that buses 1041,1044 and 1045 are the weakest buses in the system, as shown in Fig. 3 for bus 1044.

The rest of the results will be shown in Section V. It can be said that the indicators follow the events occurring the system after disturbance.

Additionally, the OLTCs and OELs are taken into account in the computation of the thevenin impedance, including the tripping of the lines, which modify admittance in the matrix.

The oscillations can also be explained from the voltage angle oscillations or acceleration at bus 1044 [14]. It is important to mention that the angles are taken into account when computing the indicators, and equivalent loads are computed based on eq. (5).

Furthermore, the angle oscillations can be explained by the transient and frequency instabilities [14] in the system after a generator tripping occurs, which are out of scope of work. Also, it is critical to mention that the equivalent loads seen from these buses were calculated following eq.(5), which can explain the oscillations.

After observation, although the computation was very fast, it is crucial to find a way to average the ISI, or get rid of the oscillations, in order to reflect the behavior of the system so that the coordinated control method can be successful. Therefore, it was decided to use a filter with high time constant, and allow the devices to act based on certain ISI values, as already shown in Fig. 4.

III. System protection model based on ISI

Initially, the network admittance matrix is assumed to be known and updated by monitoring the power system. The voltage magnitudes and angles are measured at all buses, the OELs are being monitored, the OLTC tap-changer positions are observed by measuring the active power flow through the transformers, as shown in eq. (8).

$$P = \frac{V_i V_j sin\delta}{a} y_t \tag{8}$$

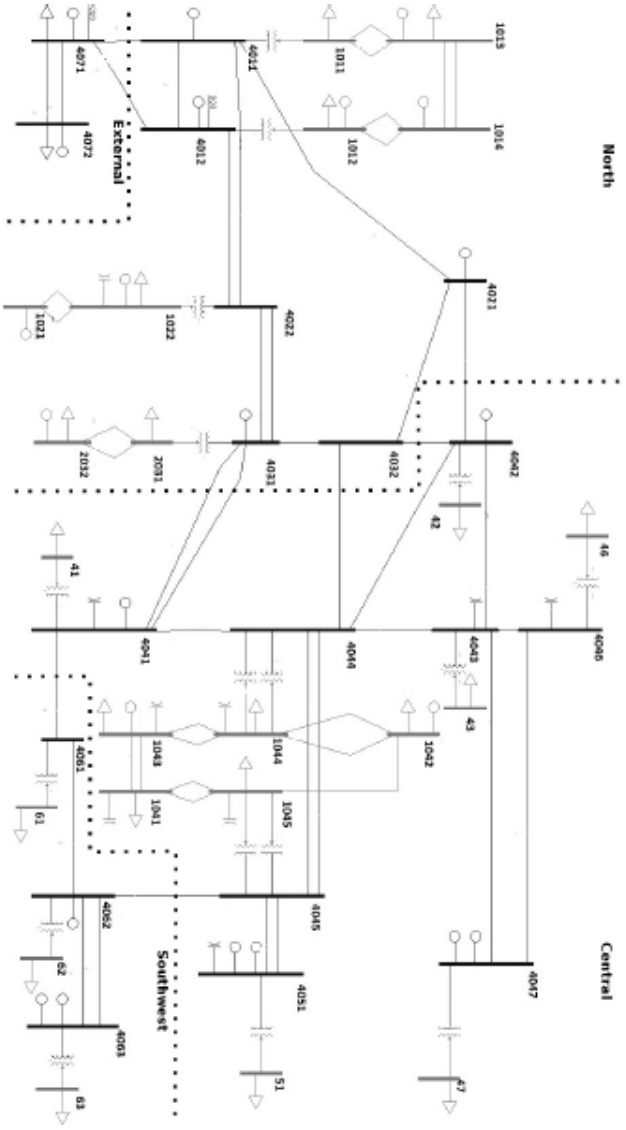

Figure 2: Single line diagram of the Nordic-32 test system

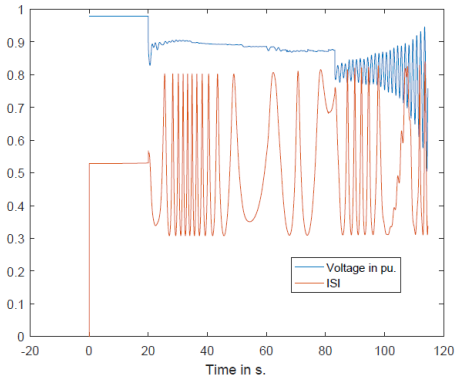

Figure 3: ISI and Voltage at bus 1044

The control method of different devices to prevent voltage collapse can be initiated after determining the indicator at non-voltage controllable buses. With ISI taken into account, if it reaches a certain value signaling voltage instability at any non-controllable voltage bus, the AVR-setpoints are increased. However, if ISI is greater than a value signaling voltage instability close to collapse,and AVR-setpoints are not enough to counter it, load-shedding is then activated at or close to buses of interest. The applied algorithm is summarized in Fig.4 in a simplified way, which indicates that the prevention of voltage collapse is initiated when ISI is greater than 0.5. This value is not random, but is taken into account after analyzing the ISI in the Nordic-32 test system before implementing the model.

A. *Implementation of Protection Model in PSS/E*

The purpose of the method is to monitor the voltage stability of the system during dynamic simulation, which can be considered as real-time in order to be able to mitigate voltage instability and prevent voltage collapse. The model was developed in Fortran based on Fig. 4. The model is built as a miscellaneous model since it is monitoring the whole system and not controlling components in the system, and is written in Intel Visual Fortran 2005 [10] as an .F90 file and compiled using the PSS/E Environment manager to link it to PSS/E libraries. The model is called from the .dyr file in the interpreter or simulation script written in Python.

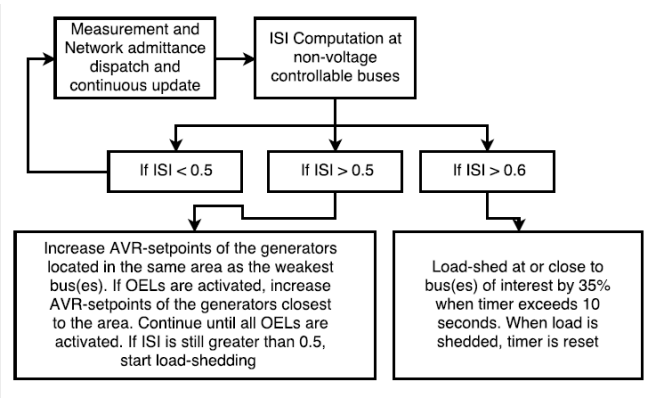

Figure 4: Working Principle of System Protection Model

B. *Setting of the Model*

The first step is to measure the voltage magnitudes and voltage angles of all buses, and the power flow in the OLTC transformers in order to obtain correctly the tap changing position. Since the network admittance matrix is assumed to be know at the beginning of the simulation, it is imperative to monitor if any changes occur in the system, such that tripping of a line, OEL and OLTC. Afterwards, the matrix is inversed to get the thevenin impedances, which are the diagonal elements of the inversed matrix. After computing the ISI, its value is analyzed. If it is greater than 0.5, the AVRs of the closest synchronous generators to the weak bus are activated until OELs are activated. On the other hand, if it is greater than 0.6, the AVRs of the closest synchronous generators to the weak bus with load-shedding are activated. The reason behind

these thresholds is due to the selection of the filter, but due to time constraint and limitation in the scope of work, the threshold will be assumed to be correct, but additional studies are needed for future works.

IV. Case Study: Results and Discussions

A. Description of Study Case

The SPS, described in section III, will be implemented in the Nordic-32 bus system that was used in section II, and the study case will be by tripping a 630MW generator at bus 4042. The dynamic models in the Nordic-32 bus system are taken from [11]. Two simulations have been carried out for the "moderate" loading condition [11]:

- the first one is conducted without implementing the model
- the second one is conducted with the implementation the model

Initially, it will be assumed that the network admittance matrix is available, and being updated and modified during the whole simulation in case there are changes, such as an OLTC action or a line tripping. The voltage magnitude and angle are constantly being monitored and the ISI is being computed in real-time.

B. Results

The simple algorithm of the model is based on shortest distance and if-conditions due to the small size of the power system. After implementation, it is noticeable that no voltage collapse occurred at 115s., and consequently prevented during the whole simulation. The sequence of events that occurred before implementing the model are shown in Table I, whereas the sequence of events after implementing the model are shown in Table II. As can be seen in Table I, the generator at bus 4042 is tripped at 20.00 s. and OEL of generator at bus 4043 is activated at 34.00 s. Different events leading to voltage collapse are observed at different times, such as OLTC actions and undervoltage tripping of generators. In Table II, the generator at bus 4042 is tripped at 20.00 s, but voltage collapse is avoided with the increase of AVR setpoints and load-shedding.

It should be noted that when a generator is tripped, the system will experience the frequency reduction. In the simulations, the system frequency has been controlled and stabilized by governors of the synchronous generators. There was no problem with frequency after the tripping. Since the focus of the paper is on voltage stability, the results on frequency deviations are not presented here.

Table I: SEQUENCE OF EVENTS WITHOUT SYSTEM PROTECTION MODEL

Bus Number	Event	Time (s.)
4042	Generator tripping	20.00
4043	Generator OEL action	34.00
All Transformers buses	OLTC actions	45.00-115.00
2032,4021,4041	Generators OEL actions	110.00
1043,4021,4041	undervoltage tripping of generators	100.00
All buses	Voltage Collapse	115.00

Table II: SEQUENCE OF EVENTS WITH SYSTEM PROTECTION MODEL

Bus Number	Event	Time (s.)
4042	Generator tripping	20.00
4043	Generator OEL action	34.00
1043,4041,4042,4047	AVR-setpoints increase by 5%	40.00-150.00
All Transformers buses	OLTC actions	50.00-150.00
1044,1045	35% Load-Shedding	150.00
1044,1045	35% Load-Shedding	180.00
All Transformers buses	OLTC actions	time $\geqslant$ 190.00
1043,4041,4042,4047	AVR-setpoints increase by 5%	time $\geqslant$ 190.00
All buses	Voltage levels stabilized	time $\geqslant$ 350.00

The AVR set-points increase started with the generators closest to the weakest buses. If the OEL is activated and the ISI is still at an unacceptable level, the AVR setpoints of the next closest available generators are increased. However, they were not enough to prevent voltage collapse, and load-shedding was used. Fig. 5b, 6b and 7b show the voltage and "filtered" ISI levels of the buses 1041, 1044 and 1045 respectively after implementation of the model, and it is observable that the ISI indicators are stabilized after 250s and the voltage levels went close to 1.4 p.u, and decreased after reaching at 1.2 p.u and load-shedding was terminated, as opposed to Fig. 5a, 6a and 7a, which illustrate the voltage and and ISI levels of the same buses 1041, 1044 and 1045 respectively before adding the model. Moreover, the oscillations and transients in the voltages were avoided and it can be seen that the ISIs stabilize after 250s approximately.

The load-shedding is observable in Fig. 8 and 9. The loads have been shedded twice, which are located at buses 1044 and 1045. Every time the shedding is activated, 35% of the total loads are shedded. This may seem too severe, but it is important to remember that the tripped generator was producing 630 MW. To bring back the balance between load and generation, loads had to be reduced twice. The percentage value to shed loads with was based on trial and error. A low percentage, such as 10%, led to the increase in the loads shedding, i.e. the loads were reduced too many times, and reached a value close to 0 p.u. On the other hand, a percentage higher than 40% tend to extensively reduce a load at one bus, or completely eliminate it. However, the main goal is to shed loads at buses at or closest to the weak bus, and load-shedding should occur at couple of buses to improve the stability of the system. Therefore, 35% was decided to be an acceptable value, although a percentage of 25% could have been used.

C. Discussions

It was shown that the coordinated control proved to be able to prevent voltage collapse. The cascaded increase of the AVR-setpoints proved to be insufficient to avoid voltage collapse. Load-shedding proved to be essential, although it should be considered as a last case scenario. However, tripping an important generator that was producing 630 MW proved to be severe, and load-shedding turned out to be the only solution for the time being. Although voltage collapse was avoided, the voltage level at both buses 1044 and 1045 overshot and was above 1.2 p.u for a small period of time, which should have been avoided. The filtered ISI indicator proved to be acceptable in detecting voltage instability, but it is not enough to show all of the weaknesses in the system. It is needed to combine

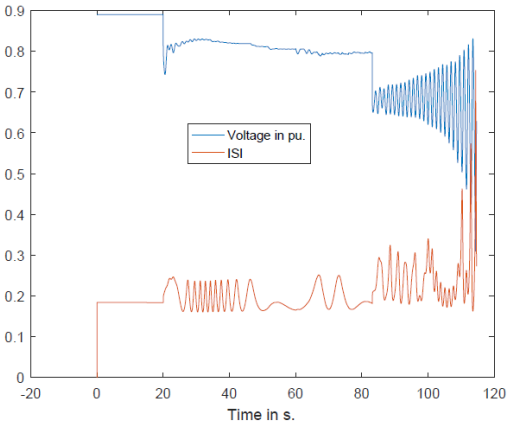

(a)

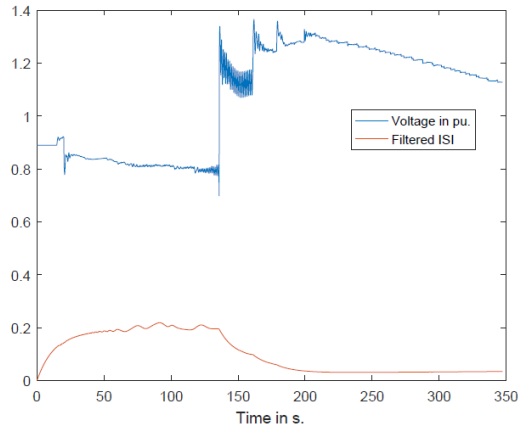

(b)

Figure 5: (a) Voltage and filtered ISI at bus 1041 without SPS. (b) Voltage and filtered ISI at bus 1041 with SPS.

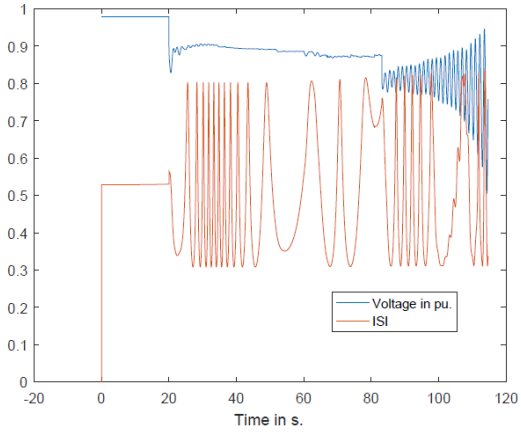

(a)

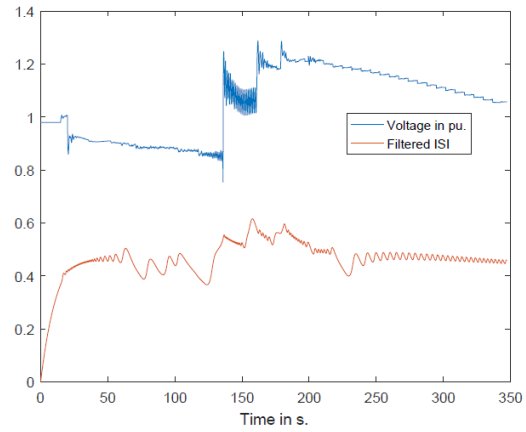

(b)

Figure 6: (a) Voltage and filtered ISI at bus 1044 without SPS. (b) Voltage and filtered ISI at bus 1044 with the SPS.

different indicators in order to observe all of the weaknesses in the system., and increase the robustness and efficiency of a coordinated control of different generators, which also could lead to an increase in the computational burden.

V. Conclusions

This paper has developed a system protection model against voltage collapse using ISI. The ISI has been efficiently computed in real-time based on the network admittance matrix, and continuous voltage and angle measurements. The system protection model as developed in PSS/E with the ISI and OEL signals treated as inputs.

The control measures are changing of AVR setpoints and load shedding which are triggered by threshold of ISI. From the simulation study, it can be concluded that the system protection model performs as expected. However, there are some challenges in applying the model which are related to the oscillations and transients of the indicators as found in the study case with the Nordic-32 test system.

These are mainly due to voltage angle variations caused by disturbances. To overcome this challenge, a filter was used to dampen the oscillation.

This should by no means be seen as the best solution, but rather be an acceptable solution. More work can be further done to improve the design of this filter.

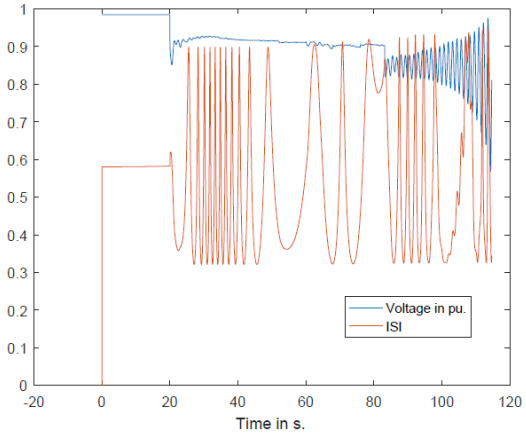

(a)

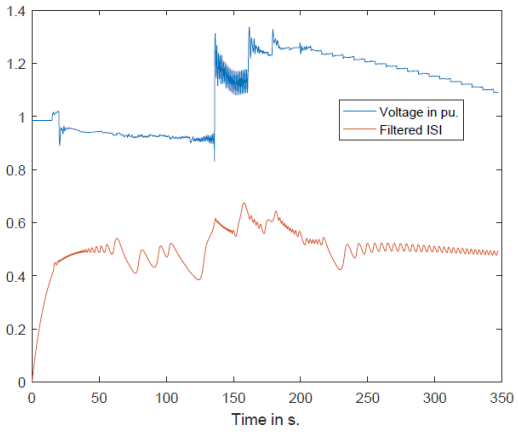

(b)

Figure 7: (a) Voltage and filtered ISI at bus 1045 without SPS. (b) Voltage and filtered ISI at bus 1045 with SPS.

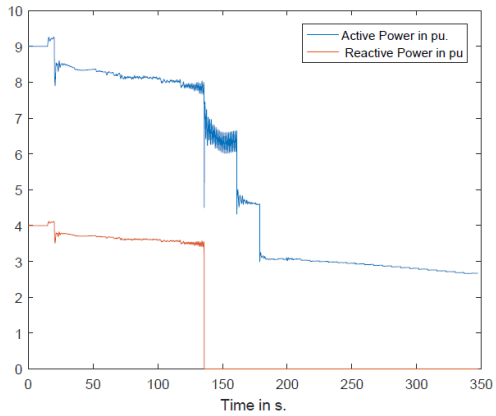

Figure 8: Active and reactive load power at bus 1044 with SPS

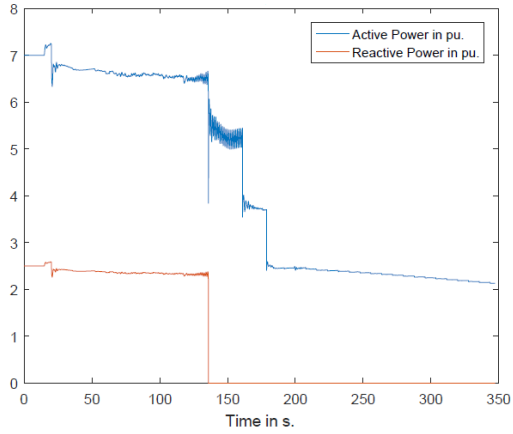

Figure 9: Active and reactive load power at bus 1045 with SPS

ACKNOWLEDGMENT

The authors would like to thank Mattias Persson and Peiyuan Chen from the Department of Electrical Engineering, and Manh Hung Tran from the Department of Mathematical Sciences for their supports.

REFERENCES

[1] M. Begovic, B. Milosevic, and D. Novosel, "A novel method for voltage instability protection," in *Proceedings of the 35th Annual Hawaii International Conference on System Sciences*, Jan 2002, pp. 802–811.

[2] L. Huang, J. Xu, Y. Sun, T. Cui, and F. Dai, "Online monitoring of wide-area voltage stability based on short circuit capacity," in *2011 Asia-Pacific Power and Energy Engineering Conference*, March 2011, pp. 1–5.

[3] V. Balamourougan, T. S. Sidhu, and M. S. Sachdev, "Technique for online prediction of voltage collapse," *IEE Proceedings - Generation, Transmission and Distribution*, vol. 151, no. 4, pp. 453–460, July 2004.

[4] V. Storvann, E. Hillberg, and K. Uhlen, "Indicating and mitigating voltage collapse comparing voltage stability indicators," in *2012 3rd IEEE PES Innovative Smart Grid Technologies Europe (ISGT Europe)*, Oct 2012, pp. 1–8.

[5] N. G. H. L. Gyugyi, *Understanding FACTS:Concepts and Technology of Flexible AC Transmission Systems*. Wiley-IEEE Press, 2000.

[6] Y. He, Y. Song, G. Du, and D. Zhang, "Research of matrix inversion acceleration method," in *2009 International Conference on Computational Intelligence and Software Engineering*, Dec 2009, pp. 1–4.

[7] Siemens Power Technologies, "PSS®E 34 Model Library," March 2015.

[8] ——, "PSS®E 34 Application Program Interface," March 2015.

[9] ——, "PSS®E 34 Program Operation Manual," March 2015.

[10] Intel, "Intel fortran web page," March 2017. [Online]. Available: https://software.intel.com/en-us/fortran-compilers(accessedJune1st2017)

[11] K. Walve, "Nordic32a-a cigre test system for simulation of transient stability and long term dynamics," Svenska Kraftnat, Rev-1994-03-01, Tech. Rep., 1993.

[12] MathWorks, "Matlab web page," March 2017. [Online]. Available: http://se.mathworks.com/(accessedJune1st2017)

[13] T. Cutsem and C. Vournas, *Voltage Stability of Electric Power Systems*. Springer, 1998.

[14] P. Kundur, *Power system stability and control*. MacGraw-Hill Inc.: EPRI Power System Engineering Series, 1994.